ISSN 1512-3936

ISSN 2960-9682(Online)
DOI: : https://doi.org/10.52340/building

Georgian Technical University

BUILDING

#2(72) 2025

SCIENTIFIC-TECHNICAL JOURNAL

Tbilisi - 2025

Responsible secretary Tinatin Magradze (Georgia)
Tel: +995 599 478422
E-mail: t.magradze@gtu.ge
Web-site: https:mshen-journal.ge

indexed in Google Scholar

The magazine is published since 2006

Table of Content

5Human-Centered Urban Design through the rehabilitation of public spaces in Milans historic districts

Nino Imnadze, Mariam Botchorishvili
Georgian Technical University, M.Kostava st 77, Tbilisi 0159, Georgia.
n.imnadze@g tu.ge

DOI: https://doi.org/10.52340/building.2025.72.02.01

Abstract This article analyzes adapted public spaces within the historical districts of Milan—„Vesta"and „Apple Piazza Liberty"—in the context of architectural strategies that transform the city into a human-oriented and healthy urban environment. „Urban Health" has become one of the key priorities of contemporary architectural practice. [2] [1] Growing evidence confirms that the physical structure of buildings and public spaces directly influences human psychological, emotional, and social well-being. In this regard, Milan represents a particularly significant case study. Two distinct yet conceptually interconnected examples—"Apple Piazza Liberty", where a historic square is reinterpreted as a contemporary urban amphitheater (Foster + Partners, 2018) [3], and "Vesta", a semi-public social platform located along the historic Brera street (Belingardi, 2022) —share a common architectural logic, a new architectural paradigm, respect for the cultural-historical context, spatial strategies, and a tangible impact on urban well-being.

A comparative analysis of "Vesta" (designed by Stefano Belingardi) and "Apple Piazza Liberty" (designed by Foster + Partners) reveals their strong conceptual relationship with urban health, specifically within the framework of healthy peacemaking and urban well-being [4] [5]. Both projects exemplify contemporary urban approaches in which architectural concepts actively support social well-being. In both cases, spatial-volumetric structure, transparency, openness, visual and acoustic connections with nature, and location within a dense urban context create intermediate, restful indoor–outdoor spaces—a pause between the "city" and the "human." [1]

Such spaces play a crucial role in mental health by enabling psychological relief from the accelerated rhythm of urban life, fostering a sense of refuge, facilitating informal and spontaneous social interactions, and encouraging exploration and discovery. [5] The analysis demonstrates that despite differing functions (restaurant and store), both spaces are united by shared principles: human-scale design, openness, microclimatic comfort, and the promotion of social interaction. Both projects achieve a balance between history and contemporaneity, prioritizing physical, social, and mental well-being.

Thus, Milan's contemporary urban transformations are not solely the result of large-scale projects but also of the introduction of a new architectural paradigm within historical districts through small-scale public spaces that reinforce the relationship between public space, public life, and urban health (peacemaking / urban well-being). [5]

Key words: Healthy Urbanism, Public space, mental health, Scale, Rehabilitation.

Introduction

Urban Health and Contemporary Challenges. The main challenge for 21st century cities is urban health, or the city's ability to create: a healthy psychological environment, platforms for social interactions, an ecologically sustainable environment, and spaces adapted to the human scale [2]. The World Health Organization (WHO) Healthy Cities Framework emphasizes that the physical characteristics of the urban environment – connection to nature, noise, lighting, accessibility, opportunities for social interaction – determine people's well-being. [5] With the growth of the population of Tbilisi, "urban health" has become one of the most important problems. Despite the fact that

Tbilisi is actively renewing the existing infrastructure (parks, squares, roads), and carrying out rehabilitation and reconstruction works in historical districts, each intervention is fragmentary and lacks systematicity. Accordingly, the issue requires research, sharing of international experience, and a new architectural paradigm in order to achieve a "human-friendly city." [1]

In the context of urban health, "Apple Piazza Liberty" and "Vesta" in the historic center of Milan represent important research objects. Both are conceptually conceived as open-social spaces that create an environment appropriate for urban health in the historic districts of the city. [6].

Main Part

Urban health encompasses three main dimensions — physical, mental, and social well-being, which are directly related to the quality of city planning, the availability of open public spaces, ecology, and architectural solutions [5]. Architecture, as a formative agent of space, shapes the environment in which people conduct their everyday lives. Research in neuroarchitecture confirms that spatial configuration directly affects neural responses, attention restoration, and patterns of social interaction. As architect Steven Holl argues, "contemporary architecture must account for human movement through layered spaces in which light, material, geometry; color; smell, wind, and the sound of water intersect." [7] Consequently, urban infrastructure exerts a profound influence on physical and mental health as well as social well-being. Contributing factors to urban stress include the lack of parks and pedestrian spaces, noisy and chaotic environments, high building density, and traffic congestion. The existence of inclusive, accessible and multifunctional public spaces plays an important role in improving social well-being.

Milan is particularly noteworthy in this regard. This study examines two distinct yet conceptually related examples: Apple Piazza Liberty, where a historic square is reimagined as a contemporary urban amphitheater, and Vesta, a semi-public social platform situated on the historic Brera Street. Both projects share architectural logic, a new paradigm of intervention, respect for cultural-historical context, spatial strategies, and measurable influence on urban well-being. (Foster+Partners, 2018; Belingardi, 2022)

Research Methodology and Objectives: The research methodology includes architectural-typological analysis, spatial and social observation, and comparative analysis. The primary objective is to identify architectural solutions that foster human-oriented environments and respond effectively to urban health strategies.

Apple Piazza Liberty (Figure 1.) represents an architectural paradigm that transforms a historic square into a contemporary socio-cultural amphitheater (Foster + Partners, 2018). Completed in 2018 by Foster + Partners, with design direction by Apple's Chief Design Officer Jonathan Ive, the project is located along the extension of Corso Vittorio Emanuele within Milan's dense cultural and tourist network. The site previously lacked a strong identity, with surrounding development primarily dating to the early 20th century. A rectilinear glass volume bearing the brand's emblem, functioning simultaneously as an entrance portal and a fountain, defines the architectural expression of the Apple Store. Its surface dynamically reflects the historical characteristics of the site while emphasizing the contrast between contemporary structure and historic urban landscape. The visual perception of the structure changes throughout the day. (Figure 2,)

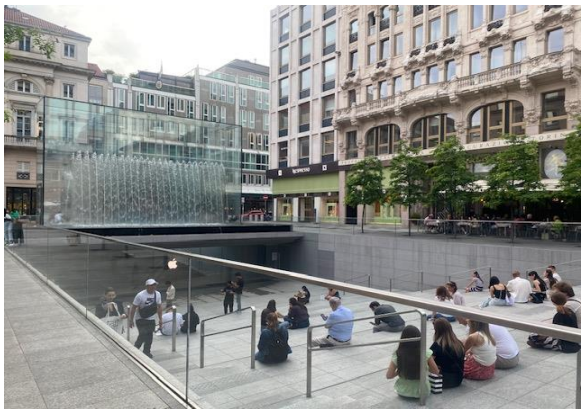

Fig.1

A sensitive and soft microclimate creates around it, contributing to a calm and tranquil atmosphere. Another important element: the effect of the material used - the stone cladding made of traditional Lombard stone Beola Grigia creates a new intervention with the material historical language of Milan. The new square responds to the principles of mental health: water, as an element of nature, reduces stress caused by urban density, regulates the microclimate, and partially suppresses urban noise. (Figure 3, 4) The constant sound of water balances the acoustic environment. The accessible amphitheater supports psychosocial well-being by welcoming users of all social groups.

Fig.2

Fig.3

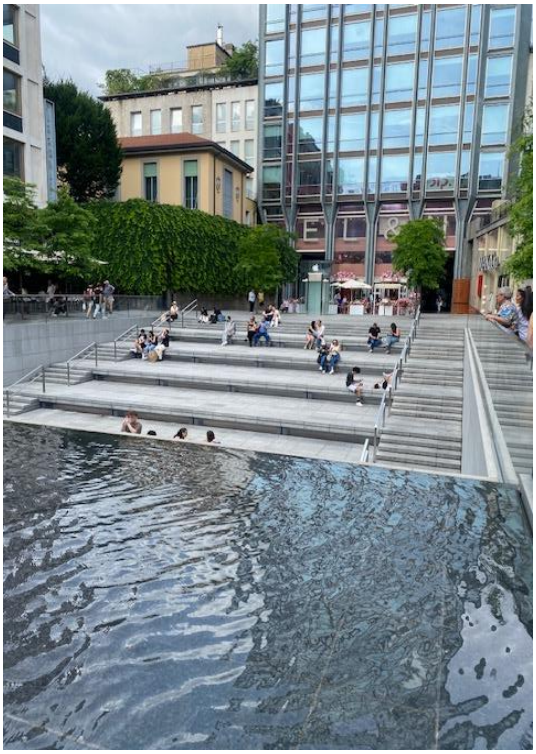

Fig.4

The building does not dominate the development but is of a human-friendly scale, transparent and in delicate dialogue with the environment. However, its architectural forms - strict geometry - contrast with the facade solutions of the buildings surrounding the square. The main space of the building is developed on the lower level of the square. (Figure 5, 6)

Fig. 5

An open, recessed amphitheater connects the upper and lower levels.

Apple Piazza Liberty is a visually stable environment. Minimalist shapes and the sound of water create a psycho-emotionally less stressful environment, which promotes psychological well-being.

Fig. 6

Vesta is a contemporary, multi-level, visually permeable structure located within one of Milan's most historic and rich cultural districts. Its name references the Roman goddess Vesta, while its primary material—travertine—is characteristic of Milanese architecture, firmly anchoring the project within the city's historical memory. (Figure 6, 7) (Belingardi, 2022)

Fig.6

Vesta functions not merely as an architectural object with a defined program but as a social, emotional, and multifunctional space that activates residual urban voids between buildings. (Figure 8) Through architectural means, it establishes a harmonious relationship with the heavily touristic pedestrian Brera Street. The elegant stair-ramp operates simultaneously as an entrance and a social platform—an inclusive, open meeting space. The project represents a delicate dialogue between history and contemporaneity.

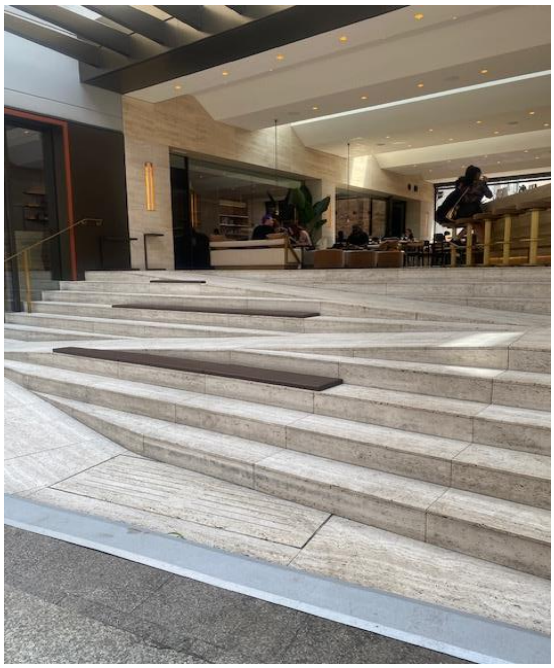

Fig. 7

Fig. 8

The stair-podium is the only visible architectural gesture, acting not as a conventional entrance but as an "urban stage"—a small public space that restores urban atmosphere and merges the rhythm of street life with the intimacy of the restaurant below. By locating primary functions on lower levels, the intervention avoids disrupting the historic street rhythm and instead enhances it. Despite its contemporary structure, the building increases psychological comfort and generates an urban health effect through the activation of social interaction.

Comparative Analysis and Critical Aspects

The comparative analysis of Vesta and Apple Piazza Liberty clearly demonstrates their conceptual alignment with urban health principles, healthy peacemaking and urban well-being (Project for Public Spaces, 2016[4]). Both projects exemplify contemporary urban approaches in which architectural ideas actively contribute to social well-being. In both cases, spatial-volumetric composition, transparency, openness, sensory connection with nature, and integration within dense urban contexts create intermediate, restorative spaces between the city and the individual. However, despite their positive impact, critical aspects must be acknowledged: commercial pressure, gradual loss of spatial neutrality, and issues of equality and accessibility require careful consideration in future development.

Conclusions

Milan's contemporary urban transformations are not solely the result of large-scale projects such as Piazza Gae Aulenti or CityLife Piazza Tre Torri, nor initiatives like Piazza Aperte, which convert car-oriented spaces into pedestrian public areas. Rather, they reflect the introduction of a new architectural paradigm within historic districts through small-scale public spaces that strengthen the relationship between public space, public life, and urban health (placemaking / urban well-being). Projects such as the rehabilitation of the Sant'Ambrogio area—creating a network of cultural, historical, and religious pedestrian streets and the human-scaled green corridor of Porta Magenta — demonstrate how contemporary interventions can preserve historic structures while enhancing urban well-being.

Although Apple Piazza Liberty and Vesta differ in terms of location, conceptual, functional program, architectural approach, and scale, they

share a common urban significance. Each project creates a Human – centered environment in which architecture, landscape, movement, and social activities are integrally and hybrid intertwined. Both interventions play a significant role within the city is established urban structure by contributing to the formation of multifunctional public spaces aligned with the principles of urban health and contemporary peacemaking.

Reference

1.Gehl, J. (2011). Life Between Buildings: Using Public Space. Washington, DC: Island Press.
2.World Health Organization. (2016). Urban green spaces and health: A review of evidence. Copenhagen: WHO Regional Office for Europe.
3. Foster + Partners. (2018). Apple Piazza Liberty, Milan: Project Description and Design Concept. London: Foster + Partners.
4. Project for Public Spaces. (2009). What Makes a Great Place? New York: PPS.
5. World Health Organization. (2010). Healthy Cities Framework. Copenhagen: WHO Regional Office for Europe.
6. Carmona, M. (2019). Public Places, Urban Spaces: The Dimensions of Urban Design. London: Routledge.
7. Holl, S. (2011). Questions of Perception: Phenomenology of Architecture. San Francisco: William Stout Publishers.
8.Gehl, J. (2013). Cities for People. Washington, DC: Island Press.
9.Montgomery, C. (2013). Happy City: Transforming Our Lives Through Urban Design. New York: Farrar, Straus and Giroux.
10.Whyte, W. H. (1980). The Social Life of Small Urban Spaces. New York: Project for Public Spaces.
11.Pallasmaa, J. (2012). The Eyes of the Skin: Architecture and the Senses. Chichester: Wiley.
12.Salingaros, N. A. (2015). Biophilia and Healing Environments: Healthy Principles for Designing the Built World. New York: Terrapin Bright Green.
13.Ellard, C. (2015). Places of the Heart: The Psychogeography of Everyday Life. New York: Bellevue Literary Press.
14.Mehta, V. (2014). The Street: A Quintessential Social Public Space. London: Routledge.
15.Lynch, K. (1960). The Image of the City. Cambridge, MA: MIT Press.
16.CABE. (2009). Future Health: Sustainable Places for Health and Well-being. London: Commission for Architecture and the Built Environment.
17.Comune di Milano. (2018). Piazze Aperte: Tactical Urbanism and Public Space Regeneration Program. Milan: Municipality of Milan.

Overhead Costs in Estimates for Construction, Installation, and Electrical Works

Nikoloz Dadiani
GAC, NNLE; Georgia, Tbilisi, B. Akhospireli Street, 9/2
dadiani.post@gmail.com

DOI: https://doi.org/10.52340/building.2025.72.02.02

Abstract Overhead costs in construction projects can represent up to 35-40% of total costs. Various methodologies exist to calculate these costs, most commonly as a percentage of direct costs or labor expenses. However, some issues related to calculating intrinsic overhead costs remain unresolved, for example: 1) when using price data from comparable projects, and 2) when managing outsourcing work. These and other relevant issues are discussed in this article. Construction, installation, electrical, and commissioning work in Georgia are used as the primary basis for analysis and calculations. Sources of information include relevant literature, the author's own experience, and research in the field of hydrotechnical and energy structure construction. Recommendations for estimating overhead costs are proposed. Some proposals require constructive opposition but must be considered when planning and implementing construction projects. The findings contribute to improving cost management practices in the Georgian construction sector.

Key words: construction, direct costs, estimates, overhead costs, wages, work.

Introduction

Overhead costs represent indirect expenses essential for construction project management, organizing and maintaining, significantly influence overall profitability. Careful assessment and proactive monitoring of these costs not only ensure profitability but also lay the foundation for successful project delivery. In the construction industry, effectively managing indirect costs can be challenging, but technology offers numerous solutions to optimize this process. Integration of modern software tools and data analytics has revolutionized the management of these costs, leading to increased accuracy and efficiency in calculations [1]. While direct costs form the foundation of project budgets, overhead costs ensure operational continuity and effectiveness [2].

The classification of overhead costs typically includes two main categories:

Administrative and business expenses:

- Administrative personnel salaries;
- Employee insurance contributions;
- Postal services and communications;
- Use of computer programs;
- Maintenance of office buildings;
- Business travel;
- Occupational health, safety, ecology.

Production organization costs:

- Temporary (non-titled) facilities and structures;
- Fire safety and security;
- Implementation of new technologies and production methods;
- Innovations and intellectual property management;
- Surveying and supervision;
- Preparation for project delivery.

These costs are an integral part of any construction project. Correctly calculating overhead costs allows you to avoid unlike expenses and complete the project on time and within budget. It should be noted that the actual amount of overhead costs depends on the type of project, its specifics, and complexity. For the same type of work, overhead costs also depend on the quantity (volume) of work, the duration of the project, and the organizational structure of the company.

Direct costs (labor salaries, machine and equipment operation, materials, and products) are relatively easy to calculate in estimates. Overhead costs, however, often remain hidden and undeciphered. Approaches to calculating overhead costs vary slightly across countries. In the United States government contract overhead rates are regulated through agreements between contractors and federal agencies, primary under Department of Labor guidance.

In its "Guide to Determining Indirect Costs," the Department prescribes that, for government contracts, preliminary overhead rates should first

be agreed upon, and then, once the organization's actual costs for the fiscal year are known, adjustments should be made to the corresponding figures. This Guide provides an example for calculating overhead costs ranging from 28.2% to 39.8% of direct costs [3]. For procurement for public sector needs in the United States, overhead costs are also regulated by the Federal Acquisition Regulations [4].

Generally, in the U.S., overhead costs in construction typically range between 10-40% of direct costs. This system of calculation is not without flaws; for example, when an investor is working on several different types of projects, it is quite difficult to allocate overhead costs across projects. If in such a case one of the projects is financed from the state or equivalent budget, how can overhead costs be proven for this specific project? Will the arguments be relevant?

In European countries, the principles for calculating overhead costs are the same. The overhead percentage is calculated as the ratio of overhead costs to various bases: direct costs or the wage fund for production personnel. Sometimes direct material costs, man-hours, and machine-hours are used as calculation bases.

Table 1

No	Work description	% of Direct costs	% of Workers' basic Salary
1	Equipment and Installations	-	68
2	Radio, TV, Video Surveillance, and Electronic Devices	-	72
3	Low-Current Lines	-	65
4	Electrical Installation	-	75
5	Internal Plumbing	12	-
6	Metal Structure Installation	8	-
7	Drilling and Blasting	14.5	-

Analyzing the logic of accruing overhead costs in estimates for construction, special, and electrical work shown in Table 1, we can identify several weaknesses of this division, in particular:

Construction budget planning is one of the most important and complex components of a project. Even a professionally prepared plan can lose its relevance under the influence of various factors. The same applies to overhead costs. At the project estimate stage, it is quite difficult to account for possible changes and risks, such as changes in Average market prices for materials and labor resources. Consequently, overhead costs may change. Therefore, calculating estimated overhead costs is an important step in any large project.

Main Part. Georgian Context and Current Practice

In Georgia, estimates of overhead costs typically rely on two main approaches depending on the type of work, for example:

a) For construction and installation work, overhead costs as a percentage of direct costs;
b) Electrical work and equipment installation: overhead costs calculated as a percentage of the salaries of primary production workers.

In accordance with Resolution of the Government of Georgia provides for various maximum overhead cost percentages for public procurement, as shown in Table 1 [5].

1) Accruing overhead costs on direct costs cannot be considered an objective approach to solving the problem under consideration.

2) The accrual rate of overhead costs for construction, installation, and electrical work should be revised (explained below).

3) When work is performed by a outsourcing (counterparty/contractor), the estimate must include the amount of in-house overhead costs. The counterparty typically provides the Client with only its final prices, without breaking down individual cost items or highlighting its profit margins—this is the counterparty's right. The issue of in-house overhead costs for contractors has been virtually ignored in specialized literature (no data available) and requires study and appropriate accounting in estimates.

Let's consider each point separately.

First. Adding overhead costs to direct costs is a rather biased method of calculating indirect costs. For example, all other things being equal, the use of unreasonably expensive materials or prohibitively expensive equipment leads to an inflated cost of direct costs and, consequently, an

unjustified increase in overhead costs. In other words, overhead costs should not depend on the use of expensive materials, products, and construction equipment. This is especially important for companies that are natural monopolies in their field of activity, particularly those involved in the transmission and distribution of electricity, gas supply to large (or numerous) consumers, municipal water supply, etc. For large enterprises, whose costs are ultimately passed on to tariffs for providing services to consumers (subscribers), the use of expensive raw material resources is not always the highest priority for monopolistic companies. For this reason, these enterprises may not pay due attention to reducing the permissible prices of material resources.

Based on the above, the calculation of overhead costs as a percentage of direct costs requires revision. From this perspective, when performing construction work, it is more reasonable to calculate overhead costs as a percentage of the cost of workers' wages, as shown for some other types of work listed in points 1...4 of Table 1.

For overhead costs in construction estimates, we propose using the same principles and calculation scheme, i.e., also performing calculations as a percentage of the workers' wage fund.

For electrical installation work (which includes commissioning), the overhead costs in Table 1 are calculated based on the workers' salaries. It's worth noting that commissioning work in electrical engineering is sometimes performed without the participation of workers, solely by engineers and technicians, whose salaries are considered overhead costs. To avoid confusion and double counting, during commissioning work, overhead costs should be calculated on the salaries of contractors, regardless of the category of workers performing the work (this should be recorded in the relevant standards and regulations).

Second. If we take the requirements of the previous paragraph as a basis, the question arises: when calculating estimated overhead costs for construction work, what percentage of workers' salaries should be calculated?

As already noted, most Western countries use two stages of overhead cost calculation: a preliminary calculation based on actual costs from previous years, or similar to other projects, and an adjusted calculation based on the actual results of the financial year. In Georgia, however, fixed standard indicators for these costs are currently in effect. Therefore, to answer this question, let's first consider similar overhead cost indicators adopted, for example, in the Russian Federation, as recommended by [6]. In Methodology [6], overhead costs for all types of work are calculated as a percentage of the workers' wage fund. As an example, several positions for different types of work can be given (Table 2).

Table 2

No	Work description	Overhead costs, as a % of workers' wages
1	Mechanized earthworks	92
2	Manual earthworks	89
3	Monolithic concrete and reinforced concrete structures	102
4	Brick and block structures	110
5	Floors	112
6	Roofs	109
7	Finishing work	100
8	Water supply, sewerage, and gas pipeline networks	117
9	Highways	147
10	Bridges and pipes	140
11	Power lines	103
12	Electrical installations	97
13	Commissioning	74
14	Transportation of workers by road	100

Note. In all cases, when calculating overhead costs, the wages of machine and mechanism operators are also included in workers' salaries.t should be noted that the overhead indicator for almost all items (except one) significantly exceeds the standard value of 75% adopted in Georgia.

The current lack of appropriate computer programs for generating automated electronic estimates in Georgia makes it difficult to account for such a wide range of overhead cost indicators for their application in construction practice. Furthermore, the composition of overhead costs in construction and tax payments differ slightly in the Russian Federation and Georgia. For this reason, we propose, instead of the differentiated indicators for detailed types of work from the Russian Methodology, adopting for Georgia the overhead cost indicators as a percentage of workers' salaries for the sections listed in Table 2, with a correction factor (except for commissioning work) that takes into account the specifics of overhead costs and taxation in the Russian Federation. This means applying K = 0.95 to the data from the Russian Methodology. In this case, the results of comparing certain values will look as follows (Table 3).

Table 3

No	Types of work	Russian Standard (%)	Proposed for Georgia (%)
1	Construction work	105	100
2	Equipment installation	92	87
3	Commissioning	74	75
4	Repair construction	91	86
5	Electrical installation	91	86

Third. Particular attention should be paid to the amount of in-house overhead costs when a third-party contractor performs part or all of the work, when their price is not broken down by cost item. The contractor typically offers prices that include (but do not break down by cost item) all of their costs. In such cases, when working with the contractor (this is always the case in practice), the client can use the contractor's final price as the base price for calculating their overhead costs. This approach is new, systematic, and subject to constructive discussion.

Our task is to understand the following question: what amount of in-house overhead costs should be accrued when the work is performed by the intended contractor?

For the analysis, we adopt the following preliminary conditions with indicative indicators:

1. Labor salaries, machine operation, and material costs in both parties' calculations are market-based and approximately the same. For ease of calculation, direct costs in both cases are assumed to be equal to 100 GEL.

2. When work is performed entirely or partially by the Contractor, overhead costs must be added to the Client's own expenses. In this case, the Client's own expenses primarily include the salaries of its employees and its own overhead costs. The Client's overhead costs must be calculated based on these salaries.

3. We are considering three types of work: construction and installation, electrical work (including commissioning), and commissioning alone. A significant difference between these options is that in commissioning work, the share of contractors' salaries is 3-4 times higher than in construction and installation or electrical work.

4. For all options at this stage, the Client accrues the standard overhead costs specified in

Annexes 1, 2, and 3.

5. Profit in the estimates for an individual Client is calculated at 11.5% of the cost of work, while for the Contractor, it is approximately 35% (based on conservative estimates), although the estimates show approximately 10%.

For the situation considered for the hypothetical Client, the following expertly assessed ratio between the salaries of the Client/General Contractor and the Contractor's workers has been found to be justified in Appendices 1, 2, and 3:

- for construction and installation work - approximately 33%;
- for electrical installation work (including commissioning) - approximately 35%;
- for purely commissioning work - approximately 40% (including on-site training).

This cost distribution is not a stable calculation matrix and requires a differentiated approach for different companies and for different types of work. For this reason, to avoid a distorted understanding of overhead cost standards, this issue should be periodically clarified based on actual data across construction industries.

Therefore, taking into account the current scale of overhead cost standards in Georgia, we propose the following:

When preparing project resource estimates, overhead costs for Client are calculated depending on the type and method of work, namely:

1. When performing work using in-house resources, overhead costs are accrued at the following rates:

1.1. For construction and installation work, including repair work – at a rate of 14% of direct costs (i.e., the total wages of workers, plus the cost of operating machinery and mechanisms, plus the cost of materials and products).

1.2. For electrical work, including electrical work. commissioning works - in the amount of 75% of the payroll for workers and operators of machines and mechanisms (drivers, excavator operators, bulldozer operators, crane operators, etc.). In the case of commissioning work, the initial payroll also includes the salaries of engineers and technicians involved in this work.

2. When performing work in-house, using prices for similar objects, i.e., at costs from third-party sources without breakdown by cost items, overhead costs are not accrued to the Client's costs.

3. When performing work by the Contractor (outsourcing), the following overhead costs are accrued to the Client's costs, depending on the type of work:

3.1. For construction and construction and installation work, including repair work - in the amount of 4.5% of the cost of the Contractor's work (Annex 1).

3.2. For electrical work, including commissioning works - 6.4% of the Contractor's cost of work (Annex 2).

1.3. For commissioning work - 12.3% of the Contractor's cost of work (Annex 3).

4. When preparing a combined project estimate for work performed by the Client and the Contractor, overhead costs are calculated for each job and contractor separately.

Another question: how to reduce overhead costs in construction?

The standards for calculating overhead costs for different participants in the construction business may be acceptable to varying degrees, but always require a commitment to optimization. To achieve consensus between the parties, the estimated overhead costs should be minimal for the investor, and as high as possible for the contractor, but within the limits of reputational safety. The following general guidelines can be considered for a systematic approach to optimizing overhead costs:

- Optimization of administrative and accounting processes, for example, by implementing appropriate computer programs.
- Comparison with industry overhead cost indicators, analysis to identify bottlenecks.

- Reduction of unnecessary utility costs for own needs (electricity, heating, water).
- Optimizing the organization and technology of work production, etc.

Since construction projects often vary in scale, duration, and complexity, companies need to employ strategic methods to fairly allocate overhead costs across projects. The following methods provide a thoughtful and consistent approach to allocating indirect costs [7]:

• Competitive bidding: Helps establish realistic contract prices;

• Financial transparency: Ensures proper reporting and profit assessment;

• Effective resource management: Guided by cost-saving decisions;

• Regulatory compliance and tax aspects: Proper allocation facilitates financial audits.

Conclusion

1. In construction, project estimates should include commissioning work depending on the type and type of work, as well as the planned execution: in-house, with partial involvement of a third party, or through outsourcing of the project.

2. For the construction and electrical work discussed in this article, a new approach to calculating indirect overhead costs is proposed, taking into account the various performers specified in the previous paragraph. The calculations are presented as a systematic approach and should be refined in each organization to improve their validity.

3. For the main types of construction in Georgia, when calculating overhead costs, the need for a gradual transition to a calculation basis based on a percentage of the payroll of workers, drivers, and equipment operators should be taken into account. This new proposal also requires discussion among specialists.

References

1. J. Primsky and T. Riso, Indirect Costs in Construction: An Essential Guide, Procore, 2025, USA. Available: https://www.procore.com/library/indirect-costs-in-construction.

2. FasterCapital, Project Cost Estimator Tool^ How to Estimate the Cost of any Project, Dubai, 2025. Available: https://fastercapital.com/content/Project-Cost-Estimator-Tool--How-to-Estimate-the-Cost-of-Any-Project.html.

3. A Guide for Indirect Cost Rate Determination. U.S. Department of Labor, 2025, p. 39.

4. Federal Acquisition Regulation; Subpart 42/7 – Indirect Cost Rates. Available: https://www.acquisition.gov/far/subpart-42.7.

5. Resolution of the Government of Georgia No. 55, January 14, 2014, Tbilisi.

6. "Methodology for the development and application of overhead cost standards in determining the estimated cost of construction, reconstruction, major repairs, and demolition of capital construction projects" as amended by the Ministry of Construction of Russia dated July 26, 2022.

7. Dannible and McKee, LLP, Certified Public Accountants and Consultants, 2025. Available: https://www.dmcpas.com/article/managing-indirect-costs-in-the-construction-industry/

Unique skyscrapers currently under construction in the world

Irakli Kvaraia, Sophio Gelashvili, Lasha Bochorishvili
Georgian Technical University M.Kostava st 77, Tbilisi 0159, Georgia.
i.kvaraia@gtu.ge, gelashvilisopo1998@mail.ru, lashabochorishvili12@gmail.com

DOI: https://doi.org/10.52340/building.2025.72.02.03

Abstract In recent years, there have been very big changes in the construction industry. It is especially noteworthy that the construction of unique buildings, which is mainly associated with the construction of skyscrapers, has shifted from the USA to Asia. This is primarily due to the versatile possibilities of using monolithic reinforced concrete as the main material in high-rise construction, along with metal structures. In the oil-rich Middle Eastern countries, which are dependent on natural energy resources, the use of other areas for the development of the country's economy is being carried out with great success. First of all, this is tourism, which is especially associated with the construction of new, completely different types of buildings and structures, which in turn contributes to the development of this industry. The best example of this is the "Burj Khalifa", the tallest building built on Earth, which attracts a lot of tourists from all over the world, and their number will increase even more after the construction of buildings taller than it. In order to achieve more impressive results in this direction, a lot of buildings are currently being built worldwide, among which several can be singled out.

Keywords: building, project, innovation concrete, steel, skyscraper

1. Introduction

The construction of any skyscraper is a very important event. In addition to the fact that they are distinguished by their individuality, new materials, technologies and mechanisms are necessarily used. At the same time, world construction practice has shown that the construction of buildings higher than 500 meters is associated with a number of unjustified costs. The main reason for this is the disproportionate increase in the cost of engineering communications and elevators with the increase in the height of the building above this. This was the reason why a few years ago, the Chinese government, one of the most developed countries in the field of construction, banned the construction of buildings higher than 500 meters on its territory. Perhaps this decision was made based on the rich experience that China has. For this, it is enough to note that out of the 12 buildings in the world that are over 500 meters tall, 6 are in China, and 6 are in the United Arab Emirates, Saudi Arabia, Malaysia, the USA, South Korea and Taiwan, that is, there is only one such building in these countries. If earlier countries competed with each other only in the construction of tall buildings, now more and more attention is paid to the creation of new architectural and structural forms, increasing the environmental friendliness and energy efficiency of buildings.

2. Main part

Dubai, in the United Arab Emirates, has already become widely known for its unique buildings in the world. One of these in the near future will definitely become Ciel Dubay Marina. This is the tallest hotel in the world under construction, which is scheduled for completion by the end of 2025. The construction of the 377-meter-high, 82-story and 1,042-room hotel began in 2018.

And the height of its monolithic reinforced concrete structure will be 364 meters. 12,000 m3 of concrete and 2,700 tons of steel reinforcement were spent on its foundation alone. The building is distinguished by many innovative solutions, among which it is necessary to highlight the 300-meter-high atrium inside the building, 12 vertically located gardens, the height of which reaches eight floors; the arrangement of a park and an infinity open pool on the roof; The large, curved, lightweight concrete enclosing elements and glazing were constructed using high-quality steelstructures, giving the building a high truncated cone shape. the hotel is equipped with the most modern energy-efficient systems. Figure 1 shows the construction process, which was halted for a long time during the pandemic. The building is now fully glazed and all major works are complete.

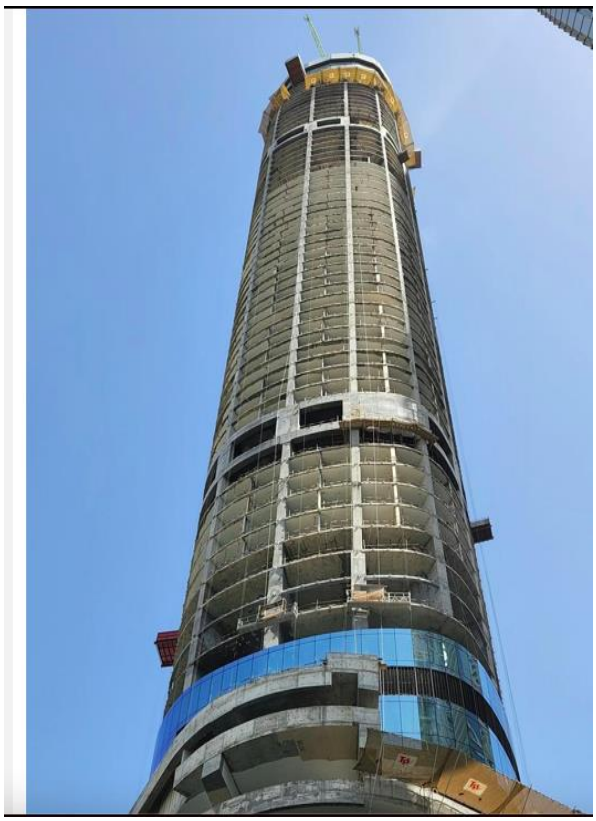

Fig. 1. Construction process

This year, the construction of the Azrieli Spiral Tower, the tallest building in Israel, is also scheduled to be completed in Tel Aviv. Its total height is 255 meters, seven floors, with an underground parking lot for 1,600 cars. The 64-story building is 238.5 meters high from ground level and has a total usable area of 55,000 m2. The originality of the building lies in its shape, which resembles a vertically rolled-up sheet of paper. Two vertical reinforced concrete frames, trapezoidal in plan, are wrapped around a rectangular load-bearing part made of monolithic reinforced concrete. As they approach the upper floors, the outline of the trapezoids changes counterclockwise. During the construction process, this arrangement of the frames gave the impression of a tilt similar to the Leaning Tower of Pisa (Fig.2). The foundation and initial facade of the building are located parallel to the existing streets, and as the height increases, it gradually turns towards the sea. The perception of such a curvature of the frame parts is especially evident

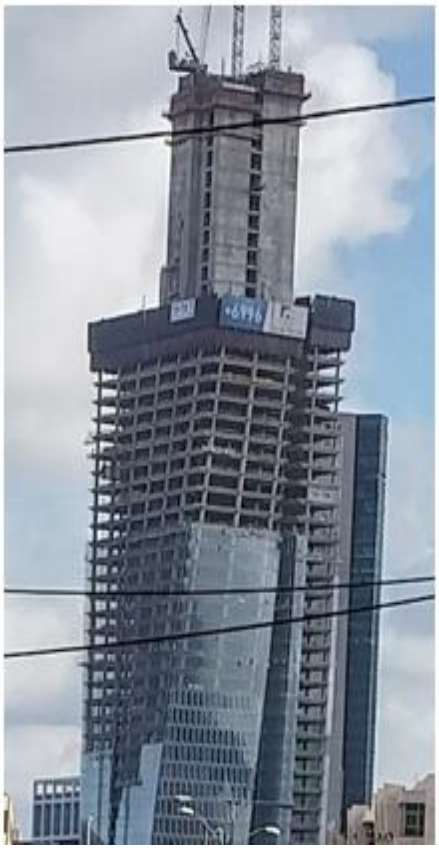

after the

Fig. 2. Construction process

glazing of the building, which is made of aluminum frames (Fig. 3).

Fig.3. Azrieli Spiral Tower

In Saudi Arabia, in the city of Riyadh, the construction of a completely different from other skyscrapers, the largest in the world by volume, a cube-shaped building with sides of 400 m long, began in 2024. Its name is "Muqaab", which means cube in Arabic. Its grandeur is also evidenced by the fact that, taking into account the overlap, it is possible to virtually place 20 Empire State Buildings inside it, which is clearly visible in the picture below (Fig. 4).

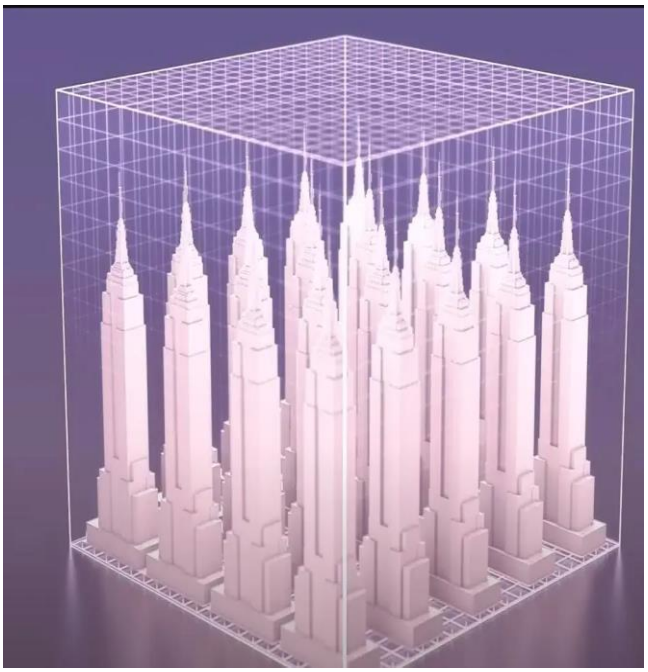

Fig.4. Interior Space

As a supertall (over 350 meters high) building, the Mukaab will be among the top 50 tallest buildings in the world, and for the first time in the world, a skyscraper in the form of a spiral tower will be built inside it. The tower is planned to house a hotel and shopping facilities. Holographic landscapes will be projected from the tower onto the inner walls of the cube, which will create an imitation of an even greater expansion of the internal space. All this will allow an independent mini-city with its own skyscraper to be organized in this huge enclosed space. In a multifaceted green city, in which there will be no shortage of fountains and waterfalls, the problem of protection from the heat has been successfully solved. Despite this, the mentioned building has many opponents due to its similarity to the Masjid al-Haram, the main shrine of Islam in Mecca. The project is financed by the State Investment Fund, which was created to improve the economy separate from oil extraction, where one of the leading places belongs to the development of high-rise

construction. This, along with increasing the country's tourism potential, will also create many jobs for the population (Fig.5).

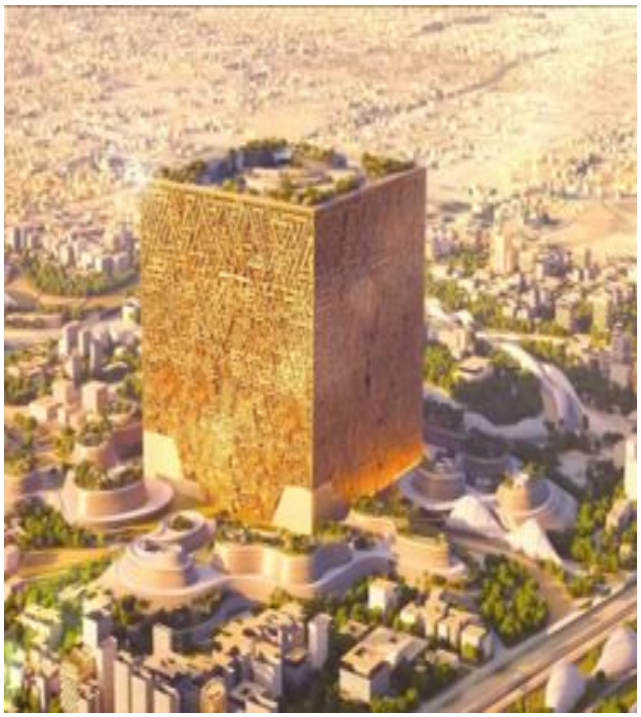

Fig.5. Makaab

Since the start of construction, more than 10 million m3 of soil has been processed, 250 powerful excavators and more than 400 units of various types of heavy equipment, several thousand people are working at the construction site. The arrangement of reinforced concrete piers has begun. The construction of the walls will continue with monolithic reinforced concrete, and their exterior will be covered with clay panels, which will be painted with ornaments characteristic of Saudi Arabia. Its completion is scheduled for 2030, before the World Exhibition opens in Erbil, and its goal is to amaze the world with this incomparable skyscraper-cube.

Another fantastic project has begun in Saudi Arabia, called The Line, which is a 500-meter-high "city wall" stretching 170 km from the Red Sea in the desert, with a population of 5 million (Fig. 6).

Fig.6. The Line

Many people had great doubts about its implementation. It is especially striking that the desert is divided into two parts and the animal world is facing difficulties. Despite this, earthworks are already underway along its entire length at such a pace that an average of 200,000 m3 of soil is being processed and 60 trenches are being constructed per day. According to the latest data, only a 5-km section of the wall will be completed in 2030, and its full completion is expected by 2045 (Fig. 7).

Fig.7. Earthworks

The building consists of two parallel, monolithic reinforced concrete skyscrapers located in a mirror image of each other. According to the project, a total of 135 modules

with the same infrastructure will be created, each 800 meters long. The width is unchanged along the entire length of the wall and is 200 meters. The "wall-city" will be completely glazed using modern energy-efficient materials. Inside, the buildings will be connected to each other by bridges, and the remaining space between them will be three levels. Transport will operate on the first level, which is mainly underground, for example, according to current calculations, the train should take only 20 minutes to get from start to finish. The second level will be arranged in the form of ordinary streets and squares so that all necessary institutions are within a 5-minute walk. The third level, together with the roof, will be a green area for recreation and entertainment. The arrangement of vertical farms for growing food products is envisaged. Interestingly, it is already planned to arrange a large football stadium at a height of 300 meters in the city center (Fig. 8). In addition to the fact that the city will be the most ecological in the world, that is, it will consume renewable energy resources, its management at all levels is envisaged using artificial intelligence.

Fig..8.Stadium in the wall

Also in Saudi Arabia, on the Red Sea coast, the construction of the Jeddah Tower, the world's tallest building and structure, is underway. Its projected height is more than 1 km, but the exact height, like the construction of the Burj Khalifa, has not yet been made public. It is noteworthy that its preliminary cost is 1.23 billion US dollars less than the Burj Khalifa. Initially, the project envisaged the construction of a building one mile (1.6 km) high, but after a more accurate, detailed analysis of the existing soil, it was decided to reduce the height by 1/3. Construction began in 2013 and was planned to be completed by 2020, but was suspended in 2018 due to financing problems. Construction has continued since September 2023 and is scheduled for completion in 2028. The number of floors of the building should be 167, but as a result of the final stage of the project, the number of floors may increase even more. Currently, the total area is 530,000 m2. The three-story glass building, built of reinforced concrete and steel, has a pointed shape that significantly reduces wind load. On the 157th floor, a 30 m diameter cantilevered metal structure is to be built. A viewing platform, which will provide an opportunity to view the surroundings within a radius of 113 km (Fig. 9).

Fig.9. Jeddah Tower

The main architect of the project is the American Adrian Smith, who also supervised the construction of the Burj Khalifa, and the experience gained there is of great help in the construction of the Jeddah Tower. This especially applies to the execution of the engineering part, which has been much improved, but still creates many difficulties. For example, the building will be served by a total of 12 escalators and 59 Kone elevators, 5 of which are two-story. In order for the elevator ropes and other parts not to be unrealistically heavy, the building is planned to have a vestibule for the elevators on three different levels. The speed of the elevators is 10 m/s. For this period, it was planned to build 100 floors, but only 80 floors of the monolithic reinforced concrete frame of the building have been built, which makes its completion within the specified time frame somewhat doubtful.

The history of the construction of the "Dubai Creck Tower", is very interesting. The author of the very original project is the Spanish architect Santiago Calatrava. The monolithic reinforced concrete structure in the shape of an elongated and pointed cylinder is fastened with steel cables at the top of the building (Fig. 10).

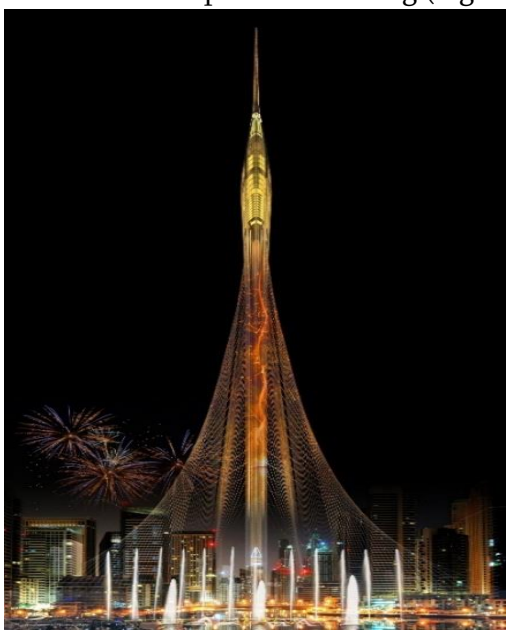

Fig.10. Dubai Creck Tower

The architect was inspired by the gardens of Semiramis, the Eiffel Tower and the traditional element of Islamic architecture - the minaret, which he really implemented in the form of a project. The slightly expanded 20 floors at the top of the tower are especially interesting. Where there will be a hotel, a restaurant, a peripheral observation deck. According to many, this tower can become a symbol of Dubai, just as the Eiffel Tower became a symbol of Paris. Construction began in 2016, and in March 2018 its huge circular foundation was completed. At the end of 2020, construction was suspended due to the pandemic, construction resumed only in March 2024, but the design height was reduced from 1345 meters to 928 meters. The number of floors is 200. The main goal is to build a building taller than the Burj Khalifa before anyone else and maintain the world championship.

Alongside these world-class projects, we should definitely mention the 42-story Citizen skyscraper under construction in Tbilisi, the capital of Georgia, designed by Zaha Hadid's architectural firm. The project will be the first skyscraper built by the world-famous company in the Caucasus region, with cascading green terraces. Its construction began this year and is scheduled to be completed in 2028. Although it is not distinguished by its height (160-170 m), its architectural solution has already attracted the attention of the world community (Fig. 11).

Fig.11. Citizen skyscraper

3. Conclusion

1. The three most ambitious projects currently underway in the world are being implemented in Saudi Arabia. There, as in many Middle Eastern countries, the economy based on oil reserves is being successfully replaced by tourism, which is primarily reflected in the construction of unique buildings;

2. China, which is the leader in skyscraper construction, has banned the construction of buildings higher than 500 meters on its territory since 2021. This is due to the unjustified increase in the cost of engineering communications and elevators when building buildings higher than 500 meters. Despite this, in Saudi Arabia and the United Arab Emirates, a real marathon is being held to attract even more world attention regarding the construction of a skyscraper taller than the Burj Khalifa.

3. The practice of constructing buildings over 100 meters high has existed in Georgia for only two decades, but by 2028, the first skyscraper in the Caucasus, designed by Zaha Hadid's famous architectural company, is planned to be built, which will become the tallest in Tbilisi and will probably stand out worldwide with its original architecture.

References

1. I. Kvaraia, S. Gelahvili Projects of Incredibly High Skyscrapers and Their Implementation Possibilities. BUILDING. Sientific-Technical Journal N1(71), 2025. P. 108-114

2. I. Kvaraia, S. Gelahvili. The Use of Concrete in The Construction of Skyscrapers. BUILDING. Sientific-Technical Journal N1(69), 2024

3. Amelia Khatri. Skyscrapers World Wide.2024. 102 p.;

4. I.Kvaraia., S.Gelashvili. The Tallest Buildings in The Word, Bult in Different Times. BUILDING. Sientific-Technical Journal N1(69), 2024. P.91-95;

4. I.Kvaraia. Longevity of skyscrapers and some cases of their dismantling. BUILDING. Scientific-technical Magazine "Construction" 4(60). 2021. P.112-116;

6. I.Kvaraia. Innovative technologies in construction. Technical University. Tbilisi. 2020. 184 p.;

7. John Hill. How a Skyscraper is Built. Firefly Books. 2017. 192 p

Modular Prefabricated Building Load-Bearing Structures, Integrated observation of the condition, Diagnostics and Monitoring

Giorgi Kaladze
Georgian Technical University, M.Kostava st 77, Tbilisi 0159, Georgia.
Kaladze.giorgi22@gtu.ge

DOI: https://doi.org/10.52340/building.2025.72.02.04

Abstract The article presents an integrated observation, diagnostics, and monitoring system for the condition of load-bearing structures of modular prefabricated buildings. A mobile diagnostic complex for monitoring has been developed, using non-destructive control methods and tools. The main advantages of the complex technology for monitoring construction structures have been identified: integration into a single complex technology - a combination of information modeling, finite element models and experimental data; Swift creation of a reporting SE model of building structures; Complex Technology is a platform for designing buildings and structures monitoring systems; The information modeling process involves the use of specialized software that allows the construction of three-dimensional dynamically changing information models. Information modeling technology is also very effective when monitoring the construction of buildings and structures. The advantages of using this technology are: high speed of model creation according to the results of working drawings or measurements on the object; The information model can include all information about the state of the of the model, starting from the properties of the construction materials to the defects that appear during operation; An informational model is created once, and if necessary,
computational models can be created from this model for the analysis of various systems, as well as models for experimental investigation.

Keywords: Modular, Prefabricated, Building, Load-bearing Structure, Diagnostics, Monitoring.

1. Introduction

Structure of the monitoring system

The monitoring system should have a multi-level hierarchical structure:

Level 1. Structured information cable system;
Level 2. primary transformers;
Level3. Controllers of information collection;
Level 4. Input/output servers;
Level 5. Automated dispatch workstations.

The lower level of the monitoring system is formed by a structured information cable system through a connected connection. The power of the monitoring system elements of construction sites, as a rule, is carried out by linear cable systems.

[1] *Investigation* - This is a set of measures for the examination and evaluation of controlled

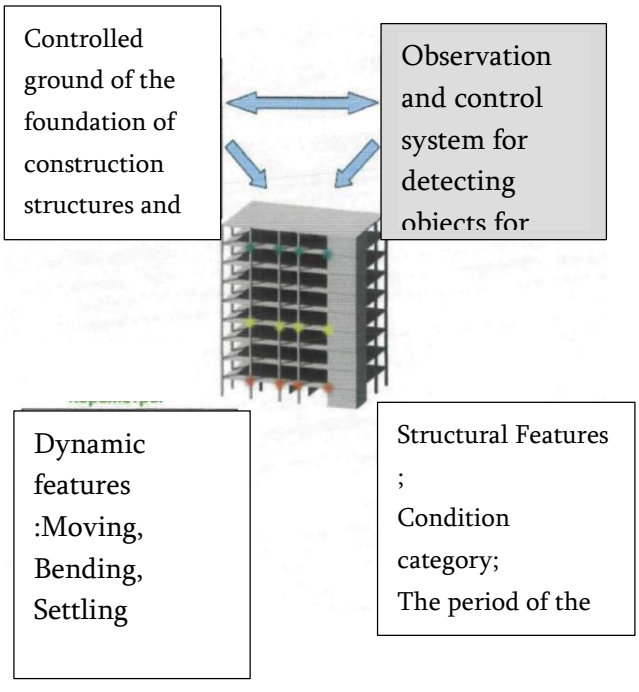

Fig. Structural Investigation and

parameters of actual importance, which characterize the operating condition, usability and labor ability of the objects to be investigated and to determine their suitability for further exploitation. Or the need to restore and

strengthen them. The examination is of a periodic nature. Unlike examination, monitoring is stationary. 2] *Monitoring* is a system for detecting objects of observation and control, on which there have been significant changes in the tense-deformed state and for which it is necessary to investigate the technical condition. So, investigation and monitoring - These are two parallel mutually beneficial processes that ensure safe operation (Fig.1)

Monitoring, like surveying, offers the definition and evaluation of controllable parameters, which include:

1. Static Characteristics:
   - Properties of materials
   - Deformation
   - Displacement (lowering, bending, tilting, etc.)
2. Dynamic Features:
   - Frequency
   - deformation coefficient

The monitoring system should have an open architecture that should allow for further expansion, both in terms of the number of monitoring objects and the number of functions of the systems, as well as allow integration with other monitoring and management systems.

Monitoring Paradigm

Among the controlled parameters may be the load that we assign to the construction, thus causing the internal force to be exerted in the construction. Often, monitoring is used only to control the properties of the structure itself, and therefore the monitoring process is equated with the process of damage detection of structural damages, in which several levels are involved:

Level 1. Finding out the presence of damage in the construction

Level 2. Damage Localization

Level 3. Damage Hazard Assessment

Level 4. Safety forecast for post-construction operation

Here, damage refers to a change in the condition of the structure caused by a change in the properties of the material, which is caused by fatigue deformation, as well as due to the conception and development of micro and macro cracks.

The solution of monitoring tasks by a team of scientists from the laboratory Los Alamos (http://mstitute.lanl.gov/ei/, USA) at all levels is proposed to be considered in the context of the paradigm of static face recognition [3]. This paradigm implies that the monitoring process includes several parts:

1. Evaluation of the tasks of the monitoring system;
2. The process of measuring data;
3. Calculation of materials features;
4. Development of statistical models.

During the evaluation of monitoring tasks, a set of measurement parameters (statistical, dynamic) is determined in the weakest and potentially dangerous areas of the construction.

In the process of data measurements, the selection of transmitters, the determination of their number and the determination of their location, as well as the selection of secondary mark converters are involved.

A feature means a result, a direct or indirect measurement of any of the characteristics of an object. The sign has a sharp physical basis, for example, the frequency of its own oscillations, the shapes of the oscillations, the tensile force. Also, the signs can be heuristic, that is, they may not have a physical dimension, but at the same time give an acceptable result. In fact, signs are parameters of mathematical models that describe physical processes.

Static models are developed to determine the meaning of signs that belong to different states of structures. The processes for calculating signs and developing static models are based on several axioms. Two axioms are more important for this work (given as an indication of the level of monitoring):

Damage assessment requires a comparison of

the two bitterness of the monitoring facility: basic (normal) and continuous (potentially hazardous);

Determination of the presence of damage (level 1) and location (level 2). Damage can be assessed relative to baseline (baseline) condition, injury hazard assessment (level 3) and prognosis (level 4)

We have developed a mobile diagnostic complex for monitoring, using unbreakable control methods and tools given below.

Based on the construction and operation methods of the modular buildings, we distinguish the following types of monitoring:

Dynamic-when the basis for expertise is the data collection on the modular building development. This is the easiest way and can be used to evaluate relatively basic structural elements. In this case, the monitoring objectives are primarily to warn of possible dangers, and to find out the causes is of a secondary nature, because the causes could be directly observed by the engineer.

Competitive- when the results of the identical examination of other building systems are chosen as the basis for examination. In this case, monitoring becomes an analogue of a multi-series exam plan. The study of two or more subsystems of a larger system is carried out in parallel, with the same equipment, at the same time, which provides the basis for making a conclusion about the magnitude of the effect. In addition, such an approach allows to evaluate the magnitude of the hazard, its criticality.

Monitoring during construction and operation allows timely detection of operational problems and structural defects , such as:

1.Bending of horizontal load-bearing structures as a result of the effects of permanent and temporary loads, with an accuracy of up to 0.01 mm;

2. Horizontal displacements in supporting constructions. with an accuracy of up to 0.025%;

3. Displacements in deformational joints, with parallel temperature measurement;

4. Determination of compressive and tensile stresses in the sections of the load-bearing constructions of frame type buildings;

5. Deviations from structural design of beam, diaphragms or supporting walls ;

6. Control of the geotechnical condition of the foundations by

ground water level measurement;

7. Determination of vertical and horizontal displacements of the ground;

8. Ground (lateral) pressure measurement on reinforced concrete structures;

To do listed above measurements are used various sensors(tensiometers, pressure sensors, acceleration sensors). All collected data must be processed by the software.

Methodology

We have developed a mobile diagnostic complex for monitoring, using non-destructive control methods and tools, which are given below.

Non-Destructive Tools

Pic. Moister tester

Pic. Thermal camera

Paint thickness tester

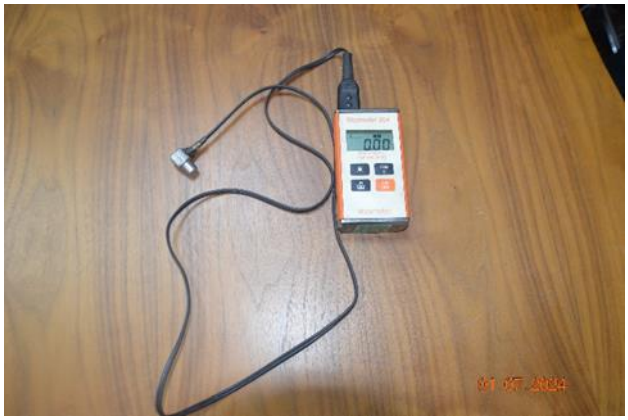

Picture Concrete thickness and Rebar locatorPicture Rebar locator

Concrete crack thickness tester

Picture Weld ultrasonic testing equipmentPicture Weld testing penetrate spray

Picture Distance Measurer

Picture Drone with camera

Non-destructive testing (NDT) is directed to evaluate properties of the material, component or system without causing damage.

Evaluation is conducted in to four phases. The

mobile diagnostic complex is used to evaluate modular buildings integrity, to determine the degree of hidden defects, to assess the stability and condition of foundations, collectors, underground utilities, including geo-technical and geophysical studies of the site.

First phase- Information model - this is a model that contains the geometry of the building, the spatial relationships between the construction elements, and contains the properties of the building components.

Second phase-Certified software is used to learn the finite element model of the object using information model data. Various computer reporting programs can be used for this purpose

Third phase- an experimental analysis is carried out using the data of natural measurements of the acceleration of the structure's oscillations. For experimental modal analysis, a software tool is used here as well.

Fourth phase -In the fourth phase, a comparison is made between the calculation data of the finite element model and the experiment (natural measurements) in order to identify (calibrate) the finite element parameters of the second phase model according to the experimental results of the third phase dynamic analysis.

The main advantages of the complex technology for monitoring are:

- Integration into a single complex technology - a combination of information modeling, finite element model and experimental data.
- Quick creation of the reporting model of the buildings structures.
- Complex technology is a platform for designing monitoring systems for buildings and structures.
- The modeling involves use of the software that allows to create a three-dimensional dynamically changing information models.
- High speed of model creation based on working drawings or on-site measurement results.

An information model is created once, and if necessary, reporting models can be generated from existing model for the analysis of different finite elements, as well as models for experimental modeling.

Let's consider an example of a modular building, where mobile diagnostic complex

could be used for monitoring the structural stability and seismic resistance of the building.

Modular building foundation is reinforced concrete (concrete class B -25). For structural modules are used prefabricated containers. It is a two-story building; second level modules are connected with metal staircase.

Non-destructive tools were used to determine construction materials (Picture 1,2,3,4,5,6,7,)

Foundation dimensions are 600x600x750 mm, concrete class B25, rebar 12mm

Metal Piles 140 mm

RHS 100x100x5

I and U metal profiles N16 and N10 Timber 80x160 mm

Picture RHS dimensions

Picture U profile measurement

Picture

Profile dimension measurement

Pic Timber dimensions measurement

Picture Observed deviation

PictureConcrete testing

Picture . Observed welding defect

Picture . Observed welding defect

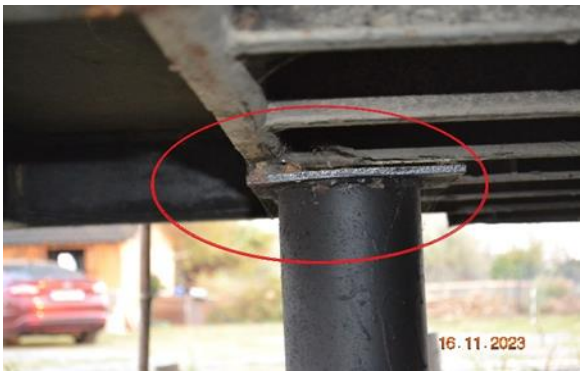

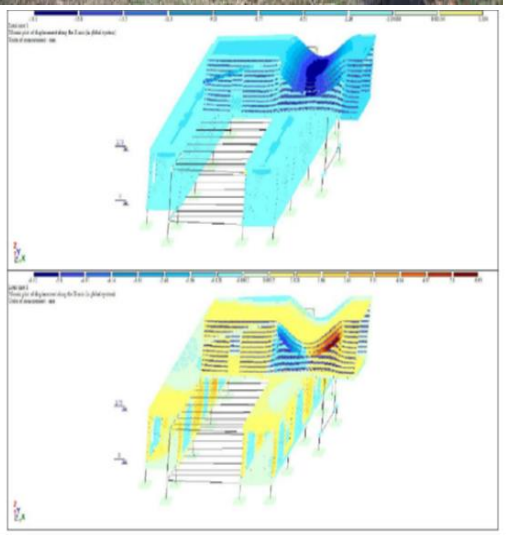

Figure. Screenshots of Structural load distribution Diagram

.Computational Model

According to the data obtained as a result of diagnostics and project documentation, a model of the building is constructed and spatial

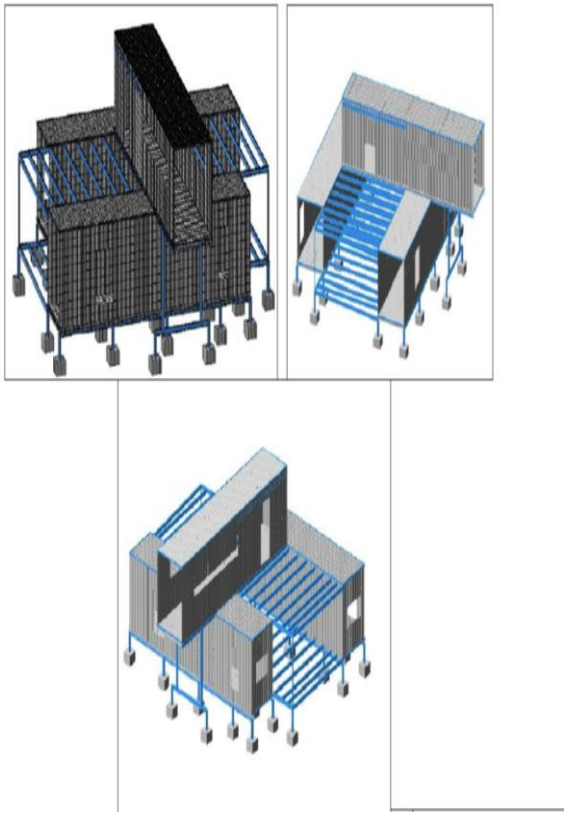

calculation is carried out in "LIRA SAPR 2016 PRO" license N 1/5515. Georgian Construction Code and standard

All on site data measurements were incorporated in a spatial model calculation.

Structural incompliance was not found.

Welding quality was low, but it will not affect structural stability of the building

Although some data were taken from existing on site structural drawings.

Modular buildings digital model was created .

The structure of the mobile complex developed by us makes it possible to obtain objective numerical parameters in the operational monitoring mode, which are related to the total loads on the structure, as well as to determine the stability, seismic resistance and reliability of the modular building, including residual resources. Based on these data obtained, a passport of the technical condition of the building will be developed.

The mobile diagnostics complex includes: a software and technical complex for determining the frequencies of their own oscillations of buildings, structures, technological systems;

Tools for non -destructible control of the strength of structural elements;

Instruments for performing high-precision geodetic measurements;

Tools for conducting geophysical and geological surveys of the construction site;

The mobile diagnostic complex is used to test the strength of buildings, to determine the degree of hidden defects, to assess the sustainability and condition of foundations, collectors, underground and above-ground communications, technological and energy systems, to assess the condition of the fields. Including technological and geophysical surveys.

For the construction of new objects of modular buildings, the following work must be carried out:

Conducting engineering and geological surveys of the construction site, determining the geological structure of the site;

Assessment of the physical, mechanical and load-bearing properties of the soils of the construction site and adjacent territories, detection of hidden cavities;

Identification of a safe distance to the nearest building in terms of the impact of the new construction on the stability of already constructed buildings and structures and on the engineering safety.

Taking into account the identified features of the construction of quickly erected modular buildings during construction, we propose to carry out:

Detection of hidden defects of building structures;

Assessment of the quality of building materials and their compliance with state standards;

Determination of the reliability of the bearing capacity of structural elements;

Conducting high-precision geodetic measurements.

During the reconstruction of the construction of

quickly erected modular buildings in operation, it is advisable to perform:

Assessment of the physical-mechanical and bearing properties of the foundations and the soils of the adjacent areas;

Determination of the technical condition of the foundation;

Conducting high-precision measurements of the geometric parameters of the building and the construction site;

Determination of the bearing capacity of structural elements and the possibility of building additional floors;

Development of specific recommendations for strengthening the structures of buildings and structures;

Secondary examination of buildings and structures in order to verify the effectiveness of the reinforcement works carried out.

The existing methodology of examinations with the help of a mobile diagnostic complex during the construction of fast-moving modular buildings allows for the monitoring of buildings and structures. Based on the data obtained before the exposure to the hazard during the test and its comparison with the data obtained after the impact, a conclusion is made on the degree of damages, as well as the dynamics of the subsequent change in the technical condition of the building are predicted.

Collecting measurement data and analyzing them.

We offer complex monitoring technology, which systematically resolves the issues raised, includes the following stages:

The first stage is informational modeling. Informational model - This is a model that contains the geometry of the building, the spatial connections between the elements of the construction, as well as the properties of the components of the buildings and other information necessary for the future. The information model can be easily changed subsequently based on the results of visual and instrumental examinations or according to the results of the operation of the monitoring system. The second stage, using certified software, is to learn the finite element model of the object using information model data. For this purpose, various computer reporting complex programs can be used, for example, the program ANSYS, Lira sapr, Revi.

The third stage, an experimental analysis is carried out using data from natural measurements of the acceleration of structural oscillations. For experimental modal analysis, a software tool, such as "ARTeMIS Extractor", is also used here.

The fourth stage is to compare the reporting data of the finite element model and the experiment (natural measurements) in order to identify (calibrate) the SE parameters of the second stage model according to the experimental results of the dynamic analysis of the third stage.

The fifth stage, using a calibrated finite element model, is completed by calculating the tense deformed state of the structure and estimating the residual resource.

Conclusion

The main advantages of complex technology for monitoring building structures are:

Integration into a single complex technology (combination of information modeling, finite element modeling and experimental data); Rapid creation of a reporting SE model of building structures; Complex Technology is a platform for designing buildings and structures monitoring system; The information modeling process involves the use of specialized software that allows the construction of three-dimensional dynamically changing information models. Information modeling technology is also very effective when monitoring the construction of buildings and structures. The advantages of using this technology are: high

speed of model creation according to the results of drawings or measurements on the object; The information model can include all the information about the state of the structure of the object, starting from the properties of the construction materials to the defects that appear during operation; An informational model is created once, and if necessary, computational models can be created from this model for the analysis of various systems, as well as models for experimental investigation.

References

1. СП 13-102-2003;
2. ГОСТР53778-2010;
3. M. Tsikarishvili, G. Kaladze K. Tsikarishvili. Development of Algorithm for performing of construction expertise 10th International Conference, New York Interdisciplinary Research and Practices June 1-3, 2024,Manhattan, New York City;pp90-92
4. M. Tsikarishvili, G. Kaladze K. Tsikarishvili. Modular Building Evaluation and Monitoring. 10th International European Conference on Interdisciplinary Scientific Research X-August 27-29, 2024/Zurich, Switzerland, pp. 714-722.
5. M. Tsikarishvili. M. Javakhishvili, T. Magradze K. Tsikarishvili. Automated Building Control and Management Systems - The concept of smart buildings. Scientific-technical journal "Construction" №2 (58), Tbilisi, 2021, pp. 6-12.
6. M. Tsikarishvili, T. Bulia, K. Tsikarishvili. Laying out Models of choice of Manufacturing Expertize and Split Stands edge. The International Scientific and Technical Conference "Problems of Engineering Sciences", Yerevan-Republic of Armenia, may 20-22,2022, Book Abstrcts, pp. 64-65.

AutoCAD File Types and Their Application in Civil Engineering

Manana Dzidziguri, Tinatin Magradze
Georgian Technical University, M.Kostava st 77, Tbilisi 0159, Georgia
mananadzidziguri@gmail.com\

DOI: https://doi.org/10.52340/building.2025.72.02.05

Abstract This article discusses the main AutoCAD file formats and their role in modern engineering, construction and manufacturing processes. There are presented working, standardization, data exchange ,documentation, recovery file formats. Special attention is paid to the discussion of the CAD–CAM–CNC work cycle, which combines computer-aided design and real production into a single technological process.

The purpose of the work is promoting the thoughtful use of AutoCAD files for students and novice engineers and preparing them in accordance with the requirements of the modern professional environment.

Key words: AutoCAD, CAD, CAM, CNC, DWG, DXF, DWS, DWF, PDF, file formats, drawing standards, data exchange.

Introduction

In modern engineering and construction activities, special importance is attached to maximum data accuracy, standardization, and efficient use of time in work processes. Thus, the processes of design, planning, documentation, and production are today closely related to the use of computer programs. In this regard, AutoCAD remains one of the leaders in this direction, both in professional and educational environments.

Such a wide distribution and success of AutoCAD, among other factors, is due to a diverse system of file formats. Different types of files serve different tasks, such as creating working drawings, standardization, quality control, printing and sharing, data recovery. Especially important is the use of AutoCAD files in the integration with the production process, where the AutoCAD file is the first link in the CAD–CAM–CNC technological chain.

Part I. Conditional classification ofAutoCAD file formats

The file types used in AutoCAD are diverse, and each of them performs a specific function at different stages of the workflow For better understand it is possible to conditionally classify files according to their purpose. This will simplify both the learning process and the selection of the right file in professional practice.

1. Working and design files

The purpose of this type of file is to create, edit, update and save a project in the AutoCAD environment.

File tipe - **DWG** file

2.Template and standardization files

This group includes files that ensure a uniform style and compliance with standards for drawings.

File types:

DWT — Template file(purpose-Correct start of the drawing

DWS — Standards File(purpose- control of compliance with established or corporate standards)

3.Sharing and Documentation Files

This category includes files, the purpose of which is the presentation,transmission or archiving drawings, but this file are non-editable

File types:

PDF file-Portable Document Format

DWF -Design Web Format

DWFx-Design Web Format (XPS-based)

DWF, DWFx, and PDF are not working design files, but they play a critical role in engineering communication. These formats provide a secure, standardized, and easily accessible representation of drawings that is an integral part of the modern design process.

4. Data exchange and production files

This file transfer geometry created in a CAD system to CAM programs and CNC machines.

File type: **DXF** (Data exchange and production files)

The main advantages of DXF file are containing clean geometry, maximum compatibility with other systems, possibility of

its use in CAM and CNC environments.
This file is the first and most important link in the CAD-CAD-CAD system.

5. Data protection and recovery files

Files of this category ensure information security and data recovery in case of emergency situations.

BAK — Backup file

SV$ — Autosave file

These files are created automatically and are rarely edited by the user

Used to restore a previous version of a drawing or unsaved data.

Part II. Drawing an standardization file formats(DWG,DWT,DWS)

1)DWG (Drawing) file

DWG (Drawing) is the main file format of AutoCAD, which is used in engineering, architectural and construction design. This format was created by Autodesk and is the environment where the complete technical and graphic information of the drawing is stored.

The drawing is created, edited and updated in the DWG file at all stages of the project.

This filr is widely used in civil engineering.

In particular, for construction plans (floor plans, sections, facades), structural drawings (beams, columns, nodes), engineering networks (water, sewage, electricity) as well as for creating working documentation,

for detailing and processing of nodes and others.

The advantages of the DWG format are high geometric accuracy, the ability to store complete information in one file, integration with BIM and CAM processes, wide support by various CAD systems

It is worth noting that other types of files can be developed around the DWG format

DWG → PDF — documentation and printing

DWG → DWF/DWFx — sharing

DWG → DXF — CAM and CNC production

DWG → DWT/DWS — standardization

Thus, the DWG file is the basis of the AutoCAD workflow

2) DWT (Drawing templates) file.

DWT(Drawing templates) file is a drawing template, a pre-configured DWG file, which is then saved with the .dwt extension. This file is used to start a new drawing in AutoCAD, a prepared workspace; that allows all new drawings to start with a well-defined set of parameters.

A DWT file may contain units, drawing limits, layers, Text and Dimension styles, Page setups, also some geometry in form of Frames, Stamps, Title blocks, Company logos etc.

When a user creates a new drawing using a DWT file, all the necessary settings and basic geometry are already ready.Changes made to the DWT file do not affect existing drawings— they will be applied only to future drawings, which are created using that template.

The DWT file is opened using the New command.

Stages for creatin DWT file:

Stage I – Preparing the Initial DWG File

Open a blank DWG file or an existing DWT template

Stage II – Creating Standard Settings

Create Layers ,Text Styles, Dimension Styles, page settings etc.

Stage III – Adding Geometry (if needed)

Add Frames, Title Blocks, Stamps and Other Standard Elements (company logo etc)

Stage IV – Save as DWT File

Save the file in the template format with (*.dwt) extension.

File → Save As

File Type: *AutoCAD Drawing Template (*.dwt)*

3) DWS (Drawing standards) file.

The DWS file contains a set of standards and styles and is used to verify compliance between the established standards and design drawing settings.

This file uses the check standards tool and controls

a) Layer standards

b) Text styles (font type, text size, title size, etc.)

c) Dimension styles

d) Line types etc.

A certain company may have its own standards (for example, a load-bearing wall on a plan should be made in a red continuous line of 0.5 thickness). The company project manager creates a DWS file, where all the styles are predefined according to the company standards. The user engineer scans the

working drawing during work using the STANDARDS command and compares it with the standards defined by DWS.

Here are the stages for creating a DWS file.

Stage I — Preparing a Standard DWG File

This includes opening a DWG file (empty DWG file or DWT template),

creating Layers, Dimension Text Styles, creating of Standard Hatches and Blocks (if the company uses them).

Stage II Creating a DWS File

Save file in*. dws format

File → *Save As*

File type: *Drawing Standards (*.dws)*

Stage III - Using a DWS File

Open the DWG file to be checked.

Attach an existing standard file to this file.

Manage → CAD Standards → Configure

After that, let's check the compliance of the settings of the file to be checked with the standards of the DWS file

Check Standards

AutoCAD will check: Layer names, colors, Lineweights, Dimension Style, Text Style, and etc..

If something does not match → *it gives us a message.*

The example: Let's we have a layer named DIMLINE in the DWG file, and we do not have such a layer in the DWS file. Then the program will prompt us with a message

! *Non-standard layer detected*

after which it is possible to delete the file or replace it with a standard Layer.

It is important not to be confused with DWT and DWS files. At first we may think that DWT and DWS files are similar to each other, but in fact they have completely different purposes.

The DWT file is used to start a new drawing. Changes to the DWT file do not affect older drawings. It contains certain geometry in the form of frames and stamps. The DWT file is opened using the New command.

The DWS file is used to control standards in an existing drawing,changes to a DWS file may affect an existing drawing (with user approval), it does not contain geometry. The DWS file is opened using the STANDARDS command.

The best option is the combination of **DWS + DWT** both in the professional and learning process, because this provides both a correct start of the drawing and constant control of standards during the work process.

Part III. Data Sharing Files in AutoCAD (PDF, DWF,DWFx)

1)PDF file

PDF (Portable Document Format) is an universal document format that is not tied to a specific CAD system. This file does not require a special viewer . The PDF format is characterized by cross-platform compatibility, high print quality, and the official appearance of the document. Therefore PDF is mainly used for the final, official presentation of drawings.

There are two main ways to convert a drawing to PDF in AutoCAD:

PLOT (by printing to PDF)

EXPORT / PUBLISH PDF (direct export)

Both methods are widely used, and the choice depends on the type and purpose of the drawing.

Creating a PDF using the PLOT command is the most common and controllable method, especially when precise scale is required.

Steps for printing drawing in PDF are following:

Execute the command:*PLOT*

In the Printer/Plotter section, select:

DWG To PDF.pc3

Specify the paper size *(A4, A3, A1, A0, etc.)*

In the Plot Area, select:

Layout (if you are printing from a sheet)

Window (if you only want to move a part)

Specify the scale:

1:100, 1:50, 1:1, etc.

Click *Preview*

If everything is correct — *OK*

Specify the name and location of the PDF file

There are common errors when transferring PDF, such as incorrect scale, too thin or thick lines, Incorrect paper format, poor text readability, print directly from model Space

In professional practice, PDF is almost always created from Layout because the scale is correct, the frame and title block are visible, the printing standard is maintained.

2) DWF file

DWF (Design Web Format) is a compressed

file format created by Autodesk for quick sharing and visual inspection of AutoCAD drawings. DWF files maintain graphical accuracy, but limit editing capabilities, which makes them secure for data transfer.

The advantage of a DWF file is possibility of quickly sharing a drawing with colleagues or a client, very small file size, protected visual information from editing.The disadvantages of a DWF file are the need for a special viewer and the low print quality.

3) DWFx file

DWFx (Design Web Format, XPS-based) is an extended version of the DWF format, based on Microsoft's XPS technology. The main advantage is that DWFx files can be opened using standard Windows tools without installing an additional Viewer.

Part IV.Data exchange and production files(DXF)

DXF (Drawing Exchange Format) is a data exchange format developed by Autodesk, the main purpose of which is transfering geometric information between CAD systems.

DXF is not the main working format of AutoCAD, but it represents a transmission link between different systems and working stages. In modern production, DXF files play an important role in the CAD–CAM–CNC workflow.

Let's recall the meaning of these terms.

CAD (Computer Aided Design) is a set of computer systems and software used for creating, editing and analyzing engineering objects, details and technical drawings. In the CAD environment, geometric models are created, that are the initial data for farther manufacturing processes.

CAM (Computer Aided Manufacturing) is the use of computer systems to plan and control manufacturing processes. CAM programs take the geometry created in a CAD system and convert it into technological instructions that determine the movement of the cutting tool, cutting speed, depth, and sequence of operations.

In other words, CAM is a transitional stage between design and actual manufacturing.

CNC (Computer Numerical Control) is a control system for production machines that operates on the basis of a numerical program. CNC machines receive commands (G-code) generated by a CAM program and automatically perform material processing with high accuracy and repeatability.

In conclusion, CAD–CAM–CNC represents a unified technological chain, where CAD provides the creation of geometry, CAM transforms this geometry into production instructions and CNC performs physical processing. This interconnection is the basis of modern manufacturing systems.

What role does a DXF file play in the CAD–CAM–CNC workflow?

At the CAD stage (for example, in AutoCAD), the exact geometry of the part is created. This geometry is stored in DXF format

In the CAM system, DXF is used to plan cutting paths, while the CNC machine takes the program generated by CAM and performs the actual machining.

In other words, DXF is a bridge between digital design and physical production.

Therefore, a DXF file, as a rule, only requires a geometric description of the drawing. It should include lines and polylines, arcs and circles, closed contours, coordinate data

Thus, the information in the DXF format is represented by a relatively simple structure, which ensures its high level of compatibility with various CAD and CAM systems. DXF can exist in both ASCII and Binary formats, although in manufacturing practice the most common is the DXF R12 ASCII format, which is considered an industry standard.

The DXF format is widely used in manufacturing processes such as laser cutting, plasma cutting, CNC milling, engraving, sheet metal processing, and more. For manufacturing, only the necessary geometry is usually retained in the DXF file, while text, dimensions, blocks, and other auxiliary elements are removed. This reduces the risk of errors and simplifies the work of the CAM program.

When preparing a DXF file for production stage, it is essential to follow the following rules

- ✓ All contours must be closed and continuous
- ✓ All elements must be in the same plane (Z = 0)

- ✓ There should be no duplicated or overlapping lines
- ✓ Simple geometric objects should be used
- ✓ The units (mm)should be defined clearly

Following these rules, the correct reading of the DXF file in CAM and CNC systems will be provided.

Let's consider the simplest example of creating a DXF file

The pict. 1 shows a working drawing of a plate made in dwg format. The drawing is built in compliance with standards, the appropriate layers are created, dimensions, axis lines are indicated.

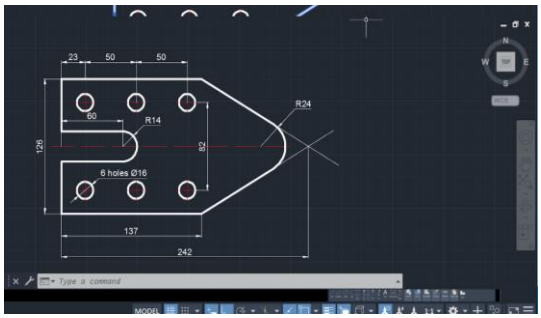

Pic. 1

At the next stage, the drawing should be prepared for conservation to DXF format.

To do this, it is need to clean the drawing from unnecessary information, remove Dimensions Text, Center lines, hatching lines, and so on.

Next stage is executing the commands

OVERKILL (delete double lines)

FLATTEN (Z=0)

PEDIT → JOIN (unite all contours)

The drawing looks like the one in the pic.2.

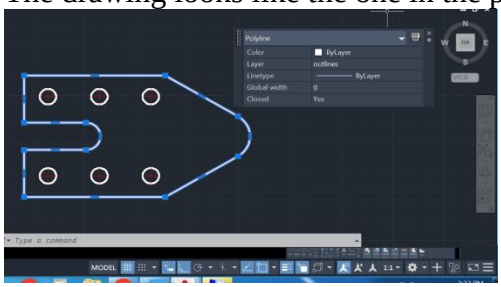

Pic.2

On final stage of creating DXF is

SAVE AS

File type: DXF

Version: AutoCAD R12 ASCII

Part V. Data protection and recovery files (BAK , SV$)

AutoCAD uses two different types of files for data protection: BAK and SV$. Both serve to reduce the risk of drawing loss, but the mechanism and purpose of their creation are different.

1) **BAK file**

BAK file is a backup copy that AutoCAD creates every time you manually save (SAVE). It represents a previous version of a DWG file, automatically updates every time you save and is saved in the same folder as the DWG

This process of restoring working file is performed by renaming the BAK file to DWG format and is an effective data protection mechanism.There are two methods to convert a backup file to a working file.

First method —by renaming the BAK file (the simplest and most effective)

Steps are the followings- open the folder where the working DWG file is saved, find the corresponding file with the .bak extension , suppose *Plan01.bak*

Select the file and rename it to *Plan01.dwg*

In this way we will get the previous version of the DWG file, the state that was before the last SAVE

Second method-Method II — Open from AutoCAD (Open Dialog)

If extensions are not visible in Windows,

Open AutoCAD, click *Open*

In the File type list, select:

All Files (.*)*

Select the .bak file and click Open

After opening the file, *SAVE AS → DWG*

If the BAK file does not exist, this means thatthe file has not been saved yet

or BAK is disabled in AutoCAD settings

To do this, go to

OPTIONS → Open and Save

"Create backup copy with each save" — must be checked by ✓

2) SV$ file

In case of an unexpected shutdown of AutoCAD or the system, it is possible to recover the working drawing using the automatic save file (SV$), which temporarily stores unsaved data.This file is created by the AutoSave mechanism, and is stored in a temporary folder. For restoring of working file the steps are following:

Step I — Finding of the SV$ file

SV$ files are usually not stored in the `

Its most common locations are

Windows:

C:\Users\<UserName>\AppData\Local\Temp

or a folder specified by AutoCAD
From AutoCAD, the address can be accessed in this way

OPTIONS → Files → Automatic Save File Location

Stage II — Identify the corresponding SV$ file
Sort the SV$ files by *Date Modified*
Select the most recent SV$ file
Stage III — *Rename the SV$ file*
Copy the selected .sv$ file to a safe folder
Change the extension:

.sv$ → .dwg

and confirm the extension change
Stage IV — Open the file in AutoCAD

Open the renamed DWG file in AutoCAD if the file opened correctly — save it immediately:

With *SAVE AS*

Conclusion

This article discusses AutoCAD file types and their role in civil engineering design, documentation, and production processes. It shows that in modern engineering practice, each file format has a clear functional purpose and a specific context of use.
The comparative table (pic.3) of AutoCAD files summarizes the material discussed in this article.

File type	Name	Purpose	Edit file	Usage stage	Main feature
DWG	Drawing	Main working file	yes	Design	Stores the complete drawing (geometry, layers, styles)
DWT	Drawing Template	Template	yes	Starting	Standardized drawing source file
DWS	Drawing Standards File	Drawing control	no	Control	Checks Layer, Text, Dim standards
DWF	Design Web Format	Sharing	no	presentation	Lightweight, protected viewing format
DWFx	Design Web Format (XPS-based)	Sharing	no	presentation	Opens in Windows without Viewer
PDF	Portable Document Format	Documentation	no	print/archive	Official, cross-platform format
DXF	Drawing Exchange Format	Data exchange	limited	exchange/manufacture	CAD–CAM–CNC universal format
BAK	Backup File	backup	no	safety	Automatic copy of the previous version of DWG
SV$	AutoSave File	Autosave	no	restoring	Recovery after program shutdown

The comparison presented in the table clearly shows that the correct and targeted selection of file formats is an important component of professional work and a necessary prerequisite for ensuring the quality and efficiency of the project.

Reference

1. Autodesk AutoCAD 2022 Users guide
2. S.Bogoliubov, A.Voinov Engineering Drawing Mir Publisher, Moscow
3. Munir M. Hamad, AutoCAD® 2025 Beginning and Intermediate. ISBN: 978-1-50152-316-8 ;

The Impact of a Debris Flow on Opposing Obstacles

Eduard Kukhalashvili, Shorena Kupreishvili, Nana Beraia, Vakhtang Bogveradze

Technical University of Georgia, M.Kostava st 77, Tbilisi 0159, Georgia.

Sh.kupreishvili@gtu.ge

DOI: https://doi.org/10.52340/building.2025.72.02.06

Annotation: Debris flows are one of the major negative factors affecting the ecological balance of the environment, and various types of measures are used for their regulation. The fluctuations in the transportability and energy characteristics of such anomalies are of such a scale that the ability to mitigate their impact does not align with the potential for maintaining a stable landscape infrastructure environment.

The aim of debris flow regulation in this study is to assess their dynamic impact on structures, evaluate the energy of critical equilibrium, and develop innovative models.

Based on the purpose of regulation, the operational means of both energy and transportability characteristics do not fully meet the high criteria for assessing their impact. Equally relevant is the accuracy of describing the obtained results—such as the flow's adherence to structures, elastic reception, and circumfluence capabilities—using operational means, as well as the complexity of developing innovative solutions. Consequently, refining existing methods of limit equilibrium, wave motion, and impact impulses to assess debris flow energetics and develop innovative flow behavior models through operational means is crucial. Additionally, evaluating the deformation characteristics caused by interactions with opposing obstacles plays a significant role in addressing the challenges of regulating natural anomalies.

Keywords: Debris flows, Ecology, Dynamic impact Assessment, Critical equilibrium, Innovative models, Limit equilibrium, Wave motion, Shock impulses

Main Body

loods are one of the natural disasters in environmental sustainability issues, for which various forms of phytoremediation are used, as well as different regulatory engineering design solutions [1, 2, 3, 7, 11, 13].

The architecture of the proposed structures, structural solutions, and environmental protection objectives are related to the diverse existence of floods, whose transport capacity and energy differ significantly from one another [8, 9].

The scales of fluctuation in the transport capacity and energy characteristics of the presented anomaly are represented by such boundaries that the effect of freeing the environment from them often fails to meet the possibilities of ecological balance.

As determining criteria for the evaluation of energy, when dealing with deformation caused by tension-compression, the possibilities of limit equilibrium and wave motion are often used in engineering practice.

Since the impact of floods on the environment is linked to the complexities of flow-channel interactions, it is essential to consider both the morphometry of the riverbed and the specific characteristics of flow behavior and hydraulics. Due to their anomalous nature, the hydraulics of floods

differ significantly from those of water flows.

Accordingly, establishing a connection between their hydraulics and channel processes represents one of the key challenges in environmental protection [4, 5, 6, 7, 10].

When the channel bed is stable, its diameter varies along the flow direction. It is essential to assess ongoing channel processes and study the energy-defining characteristics of the flow in relation to the parameters determining deformability [12].

The impact of any flow on encountered obstacles depends on pressure changes within its body, disrupting the steadiness of the flow. A similar phenomenon occurs when a debris flow moves through a channel. Pressure changes cause not only the disruption of steadiness but also disturbances during interactions with encountered obstacles.

Due to the complexity of the phenomenon and the multitude of interdependent factors, the scale of deformability and disturbance must be analyzed in relation to elasticity-defining characteristics, while the assessment methodology used in material strength studies should serve as an operational tool.

The disruption of steadiness and the potential for disturbance in a water flow have been established through hydraulic flow observation studies, with a measured value of 0.33. However, this value has not yet been determined for debris flows based on current data, necessitating further research and the development of appropriate theories.

Based on existing statistics on the impact of debris flows on landscape infrastructure, the potential for pressure changes within its body can be represented through rheological principles. When a debris flow encounters obstacles, the formation of a disturbed zone alters its density along with its body.

The expansion of the debris flow body, followed by its replenishment with the next wave within the increased pressure zone, leads to the division of the mass into two parts. The first region, where pressure-driven formation occurs, moves with a velocity V_W. The dynamic impact on velocity within the high-pressure area induces a counterflow movement, which is known as the disturbance velocity V_W.

The stability of debris flows formed in pockets and the potential for equilibrium disruption are associated with the interplay of cause-and-effect factors. Given the complexity of initiation and movement, particular attention must be paid to the proper adaptation of models to the process and the necessity of selecting appropriate geometric shapes for structural forms.

Based on the above, the regulation of such anomalies and the reliability of selecting regulatory measures remain a challenging and unpredictable task for ensuring the stability and decentralization of landscape infrastructure in almost every country. Regulatory measures adapted to incorrect phenomena and the applied operational means often fail to produce the necessary results. Consequently, this leads to cases of overflow in the shoreline zone of the flow, as well as the disruption of settlements, and it is known as a disaster that causes casualties among the residents.

The assessment of the impact potential of debris flows, the refinement of existing calculation models, and their innovative modification in the study are based on the theory of forces.

For the selection of a comprehensive and innovative calculation model and the development of operational computational tools, the following assumptions have been considered and applied:

- During the impact of the debris flow on opposing obstacles, it is assumed that the potential and kinetic energies are equal.

- The relationship between deformation and force is considered linear.
- At the initial stage of tension-compression, the proportionality limit somewhat exceeds that of the process in progress.
- By increasing the number of impact loads on the test sample, no additional deformation occurs.
- After a certain period, the deformation completely disappears, and the relationship between force and deformation becomes linear.
- The threshold for changes in the debris flow mass is a function of its physical and mechanical characteristics.
- When the magnitude of the force acting on the debris mass is equal to the mass's extension, the proportionality coefficient is one. Moreover, an increase in the linear extent of the deformation does not alter this coefficient.

The assessment of the impact of a debris flow on opposing obstacles can be studied based on the scheme presented in Fig. №1.

According to the calculation scheme, the dynamic impact of the linear elongation of the debris mass deformability at section I-I on the vertical axis is represented by Δ_{dyn}, while the static potential of internal friction is denoted by Δ_{st}.

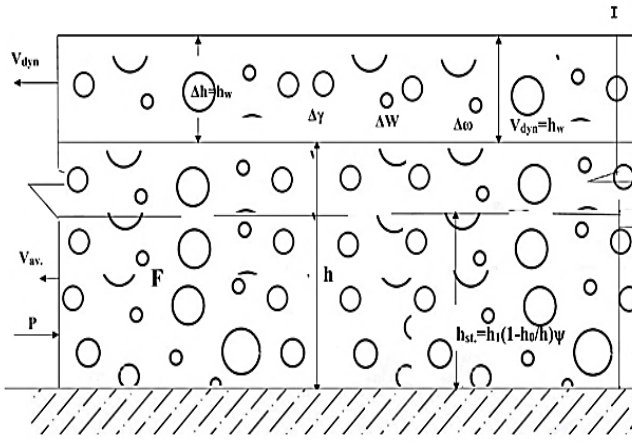

Fig. 1. Calculation scheme of debris flow deformations.

Based on linear deformations, the magnitude of kinetic energy in the case of debris flow mass deformability

$$T=Ph_1=P(h+\Delta_{dyn}) \quad (1)$$

Based on the theory of tension-compression, within the limits of proportionality and considering the internal potential, in the case of a debris flow with a depth of **h,** taking into account the force magnitude $P=K\Delta st$, the magnitude of kinetic energy is

$$T = K\Delta_{st}(h + \Delta_{st}) \quad (2)$$

The magnitude of the energy expended by external forces, according to the calculation scheme, i.e., the work performed, is

$$A = \frac{P\Delta_{dyn}}{2} = \frac{K}{2}\Delta_{dyn}^2 \quad (3)$$

Based on the energy equivalence and the conservation of a continuous medium:

$$\frac{K}{2}\Delta_{dyn}^2 = K\Delta_{st}\left(h + \Delta_{dyn}\right) \quad (4)$$

Equation 4 with respect to Δ_dyn is a quadratic equation, the solution of which is:

$$\Delta_{dyn} = \frac{2hg}{\Delta_{st}} \quad (5)$$

Based on the elastic-deformability of the debris flow, the linear elongation caused by deformation, when the modulus of elasticity is $E=\rho V^2 w$, represented by the density ρ\rhoρ and wave velocity V_w, is given by:

$$\Delta_{st} = \frac{Ph}{EF} = \frac{\gamma h^2}{2}\frac{\left(1-\frac{h_0}{h}\right)^2\psi^2 h}{\rho V_w^2 h\left(1-\frac{h_0}{h}\right)\psi} = h(1-\frac{h_0}{h})\psi$$

(6)

The impact of debris flow on opposing obstacles, considering the deformability of its mass and the effect of the impact, gradually transitions from one established motion to another. The deformation of the debris flow body is characterized by a gradual change in discharge between cross-sections without dynamic effects, which could be caused by inertia and impulses. In this case, the phenomenon is considered quasi-stationary, and gravitational forces are balanced by resistance forces. Under such conditions,

within the limits of proportionality, deformability is stabilized by the gradual change in discharge. The motion parameters transition gradually, and the cross-sectional elements change without dynamic effects. The change in discharge is situated between the depths h gand $h_1 h\_{1} h_1$ of a continuous wave. Accordingly, the computational model can be represented by the continuity equation:

$$Q - \omega V_{\text{w}} = Q + \Delta Q - V_{\text{w}}(\delta\omega + \omega) \qquad (7)$$

In the case of wave generation, since the wave thickness is related to the discharge Q and the live cross-sectional area ω\omegaω, we have: V_w=∂Q/∂ω, For the initial discharge Q, this results in:

$$V_{\text{w}} = \frac{\partial(\omega V)}{\partial\omega} = \omega\frac{\partial V}{\partial\omega} + V\frac{\partial\omega}{\partial\omega} = V + \omega\frac{\partial V}{\partial\omega} \qquad (8)$$

The average velocity of the flow ω with a live cross-section and discharge Q, when the specific discharge is $q=V_{st}h$, $f(\beta) = \frac{\beta}{2(\beta^2-1)} + 1/3(1-\beta^2)$ and $\beta=h_0/h$, the average velocity is given by $Vst=h^2\nu t(\beta)$, and the wave propagation velocity is Vw=3Vst.

In the 6th relation, when $h_0=0$ and Ψ=1, $D_{st}=h$, and when $h_0=h$ and Ψ=1, $D_{st}=0.1$.

Taking the 6th relation into account, in the 5th we obtain:

$$\Delta_{dyn} = h(1 - h_0/_h)\psi\left(1 + \sqrt{1 + \frac{4}{(1-h_0/h)\Psi}}\right) \qquad (9)$$

Based on the linear elongation model, the magnitudes of static and dynamic loads can be expressed by the following relationships:

$$P_{st} = K\Delta_{st}$$
$$P_{dyn} = K\Delta_{dyn} \qquad (10)$$

From the magnitudes of the 10 th forces:

$$P_{dyn} = 4{,}5\left(1 + \sqrt{1 + \frac{4}{\left(1-\frac{h_0}{h}\right)\psi}}\right)\frac{\alpha\omega V_{st}^2}{g} \qquad (11)$$

In the 11th assumption, when $K = 4{,}5\,(1 + \sqrt{1 + \frac{4}{\left(1-\frac{h_0}{h}\right)\psi}})$, the magnitude of the dynamic force is $P_{dyn} = K^* \frac{\gamma\omega V_{st}^2}{g}$.

In order to easily determine the impact capacity of mudflows on buildings, the value of the K* coefficient for various types of mudflows, namely, for the equivalent bond depth h_0 and the internal friction coefficient ψ, is given in the form of Table 1.

Design Values of the Coefficient K*
Table N 1

Ψ \ h_0/h	0	0.2	0.4	0.6	0.8	10
0.1	33.2	30.77	28.90	27.44	26.17	25.09
0.2	25.09	23.32	22.05	20.97	20.09	19.40
0.4	19.4	23.03	17.24	16.56	15.97	15.48
0.6	16.95	15.97	14.89	14.70	14.20	13.82
0.8	15.48	11.47	14.11	13.62	13.32	12.84
1.0	14.50	13.81	13.32	12.92	12.54	12.25

Based on the data presented in the table, it is possible to select appropriate measures according to the magnitude of the corrective coefficient K*, in relation to the characteristics of the mudflow

.**Conclusion**

Mudflows are among the most prominent natural disasters, characterized by their destructive impact. In order to manage and mitigate their effects, various types of structures have been employed, each designed to serve specific regulatory and protective functions. Taking into account both the transport capacity of mudflows and the diversity of structural types used for their regulation, predictive indicators have been established for potential disruption to landscape infrastructure stability. These indicators are based not only on the impact potential of the mudflows but also on the changes in their physical and mechanical properties.

The study proposes scenarios for the disruption of the limiting equilibrium stability of mudflows and their potential impact on encountered resistances.

The applicability limits of rapid assessment tools have been clarified, and innovative models for evaluating the energy behavior of the flow have been developed using the theories of limiting equilibrium, wave motion, and impact impulses.

References

1. G. Gavardashvili, E. Kukhalashvili, T. Supatashvili, G. Natroshvili, K. Bziava, I. Quparashvili. The Research of Water levels in the zhinvali Water Reservoir and Results of Field Resarch on the Debris low tributaries of the River Tetri Aragvi Flowing in it. Conference Proceeding, Rome, Italy, Ian. 17-18, 2019, Part V.;
2. Vynogradov Yu.B. Studies on Mudflows. A.A. Gidrometeoizdat, 1980, 144 p.;
3. Gagoshidze M.S. "Mudflow Phenomena and Control Over Them". Sabchota Sakartvelo Publishing House, Tbilisi, 1970, 386 p.;
4. Natishvili O.G., Tevzadze V.I. Fundamentals of Mudflow Dynamics. Tbilisi, 2007, p.;
5. Natishvili O.G., Tevzadze V.I. Waves in Mudflows. Nauchmekhizdat Publishing House, Moscow, 2011, p. 160.;
6. I.G. Kruashvili, E.G. Kukhalashvili, I.D. Inashvili, D.G. Lortkipanidze, K.G. Bziava. Establishing Hydraulic Parameters of Mudflow Channels, Ecological Systems and Instruments, No. 11, 2011, pp. 9-14;
7. Yano.K., Daido A. Fundamental Studies of Mudflows, Proceedings of the Institute for Disaster Protection, vol. 14, part 2, Kyoto, 1985, pp. 69-93.G. Gavardashvili, E. Kukhalashvili, I. Kvirkvelia. Mudslide Hazards in Stepantsminda (Kazbegi) District and Ways to Regulate the Disaster. "Modern Problems of Water Management, Environmental Protection, Architecture and Construction". 2016. VI Edition, Tbilisi
8. Kruashvili I., Kukhalashvili E., Inashvili I., Bzaiva K. Mudflow events, risk, forecast, protection. GTU, Tbilisi, 2017, 250 p.;
9. I.G. Kruashvili, E.G. Kukhalashvili, I.D. Inashvili, K.G. Bziava, I.L. Klimiashvili. Mathematical model of uneven movement of a connected mudflow. GTU, Journal of Hydroengineering 1-2, (17-18), Tvilisi, 2014, pp. 24-45;
10. Kukhalashvili E., Inashvili I., Bziava K., Kruashvili K., Lortkipanidze D. Determination of the characteristics of the wavy moving link mud in the mudflow channel. GTU, J., "Hydroengineering" #1–2 (19–20), 2015. pp. 70–75;
11. Kukhalashvili E., Kruashvili K., Khutsishvili B. Possible forms of failure of mud-forming soil stability. Problems of agricultural science. Collection of scientific works. Tbilisi 2001. pp. 80–84;
12. Natishvili O.G., Tevzadze V.I. Waves in mudflows. OOO Publishing House "Nauchmekhizdat", M. 2011, p.156;
13. Natishvili O., Kruashvili K., Gavardashvili G., Inashvili I. Methodological recommendations for the design of landslide protection structures (hydraulic calculation). Georgian National Academy of Sciences, Tbilisi, 2016, p.48.

Floating Solar Stations - World Experience for Georgia

Giorgi Kapanadze
Technical University of Georgia, M.Kostava st 77, Tbilisi 0159, Georgia
Email: giorgi.kapanadze@gtu.ge
DOI: https://doi.org/10.52340/building.2025.72.02.07

Abstract: Electricity is a vital resource for a developing country, and its shortage negatively affects all sectors. The utilization of **renewable energy sources** is particularly important.
This paper discusses the construction of **floating solar power stations** equipped with solar panels, a relatively new approach to utilizing solar energy. Floating solar panels can be deployed in seas, lakes, and reservoirs. The paper also reviews the global experience in this field and the potential for its implementation in Georgia
Key Words: Renewable energy, Solar energy, Floating solar panels, Hybrid hydro-power plants.

Introduction

Today, **energy** is a crucial element for the sustainable development and well-being of society [1]. In fact, energy sources are divided into two main groups: **non-renewable resources**, which we use and cannot recreate, and **renewable resources**, which can be easily replenished. Furthermore, renewable energy sources include: **solar energy**, which can be converted into electricity and heat, **wind energy**, **geothermal energy** from the Earth's heat, **biomass** from plants, and **hydro-power** from dams.

Electricity is a vital resource for a developing country, and its shortage negatively affects all sectors. Currently, consumption in Georgia has increased, and the electricity generated by local stations cannot meet the demand, leaving the country dependent on imports. Lately, large waves of public protest have emerged against the construction of hydroelectric power plants (HPPs), resulting in the **stoppage of new power station construction**. **Solar energy**, which can be utilized without major issues, is being gradually adopted by large institutions, factories, and universities. Furthermore, many countries around the world share their experience in this area.

Hybrid Hydro-Power Plants

The utilization of hydropower facilities for tourism and alternative electricity generation is becoming increasingly popular in the 21st century. Placing solar panels in such locations would be a very interesting and important solution for a country like Georgia due to its **limited territory**. Furthermore, it is possible to convert existing stations to a **hybrid regime** (Figure 1) [5].

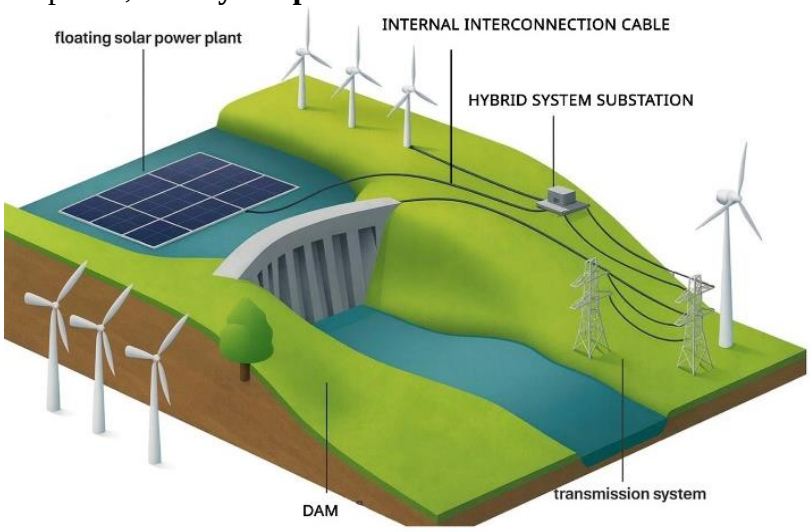

Figure 1: Integration of Floating Solar Stations with Hydroelectric Power Plants.

Tourism is one element at the power station for additional revenue, and the placement of solar panels—both on the reservoir and on the dam body—should be done in a way that does not impede this sector.

Utilization of Floating Solar Panels

Floating panels originated in Asia and Europe, with the first such model installed in Japan in 2007-2008. The largest projects in this area have been completed in China and India, as well as in Brazil, Portugal, and Singapore. They are deployed in seas, lakes, and reservoirs [6].

The electricity generated by a floating solar power station is typically fed into the grid and sold. Additionally, on a seasonal basis, it supplies resources to the pumps of the storage system, protects the water from evaporation, and the panels are cooled, allowing them to operate optimally in this scenario.

Figure 2: Floating Solar Power Station in Georgia and the Netherlands (Beilen)

Covering Canals with Floating Solar Panels

For years, interest and focus were directed solely toward supplying residential facilities—houses, cottages, etc.—with solar electricity, and placing panels on the roof is still considered the most profitable method today.

In 2012, the world's first 1-megawatt pilot project was set up on a canal in India (Gujarat, India) using an appropriate structure [7]. The 750-meter-long power station essentially gave

rise to the idea of utilizing other canals in this manner (Figure 3).

Figure 3: Solar Power Plant Project Located on a Canal (Gujarat), India

Canals in Georgia are of various types. Primarily, they are utilized for irrigation or energy purposes. In order to distinguish where panels can be deployed using a constructive approach, certain details must be taken into account: the geographical area, the type of canal, whether the main part has a concrete lining, its length, and so on. To search for the most optimal canals among the **over 700** based on **bed width** and **location**, GIS technologies offer an excellent solution. **Drone aerial photography** and subsequent calculation of **incoming radiation** create a good foundation for project development.

Figure 4: Georgia, city of Kutaisi, one of the canals with a concrete lining

Solar Power Plants on Dams

This floating solar plant of 218 kWp is installed on a hydroelectric dam, located in Montalegre, Portugal.

The Hydrelio® floating solar system supports 840 panels (260 Wp REC modules), and covers about 0.01 % of the water surface (0.26 out of 2212 ha).

Figure 5: Alto Rabagao. Montalegre, Portugal

.We also have various types of reservoirs in Georgia where they can be utilized in a similar manner. This could involve vertical deployment on dams, or floating panels in the reservoir itself. It is necessary to consider the hydrological regime of the river, the conditions for reservoir filling, and other nuances that allow for the installation of an additional power station.

Figure 6: Georgia, Enguri DAM. Floating Solar Photovoltaic Station Model

GIS Modeling

The appropriate location for the construction of a solar power plant must be selected in advance, based on various types of analysis. **GIS technology** allows us to determine and evaluate several details, for example:

- Meteorological and hydrological conditions,
- Observation of direct solar radiation, both with appropriate instruments and modeling on the relief,
- Determination of relief slope, exposure, and so on.

Conclusion

Georgia has great potential to utilize solar energy in all directions:

- Building rooftops (private/public sector),
- Canals, lakes, and reservoirs,
- Dams and barrages.

The lakes and reservoirs of Georgia are particularly noteworthy. There are around **860 lakes** in Georgia. Most are very small. Therefore, the total lake surface does not exceed 170 km^2. However, floating solar panels can be constructed on the majority of them. Solar panels can also be deployed on most of Georgia's reservoirs, such as the Enguri and Zhinvali reservoirs, which would provide a certain **economic effect**.

GIS technologies can easily identify suitable locations, and electronic modeling can determine the appropriate modifications and parameters for the power plant. It would be beneficial to **restore direct solar radiation measuring stations** nationwide, as multi-year data would strengthen the development of this direction.

Reference

1. Amer, M., Daim, T. U. Selection of renewable energy technologies for a developing county: a case of Pakistan. Energy for Sustainable Development, 15(4), 2011. Pp. 420-435.

2. Wee, H.-M., Yang, W.-H., Chou, C.-W., & Padilan, M. V. Renewable energy supply chains, performance, application barriers, and strategies for further development. Renewable and Sustainable Energy Reviews, 16(8). 2012. Pp. 5451-5465.

3. Van Sark W, Reinders A, Verlinden P, Freundlich A. Photovoltaic solar energy from fundamentals to applications. Willey. 2017. Pp. 720

4. Kumar H., U. Arora, R. Rajasthan Solar Park – An Initiative Towards Empowering Nation. Jain Current Trends in Technology and Science. Volume : II, Issue : I. 2012. Pp. 1-5.

5. Solomin E., E. Sirotkin, E. Cuce, Sh. P. Selvanathan. Hybrid Floating Solar Plant Designs: A Review. Energies 14(10):2751 2021 Pp. 23-48.

6. Kim, S.M.; Oh, M.; Park, H.D. Analysis and Prioritization of the Floating Photovoltaic System Potential for Reservoirs in Korea. Appl. Sci 9. 2019. P.p. 395.

7. Kumar J. C. Rajesh, M. A. Majid. Floating solar photovoltaic plants in India – A rapid transition to a green energy market and sustainable future. Energy & Environment. 2021. P.p. 1-55.

8. Hermanu C., B. Santoso, F.X. Suyinto, R. Wicakson. Design of 1 MWp floating solar photovoltaic (FSPV) power plant in Indonesia. ResearchGate. 2019. Pp. 13-22.

9. Alto Rabagao, Montalegre, Portugal, Photovoltaic solar https://www.frenchrenewableenergy.com/project-details/alto-rabagao-59

10. The First Floating Solar Photovoltaic Power Plant on Water in Georgia https://sunhouse.ge/ka/2024/04/17/motivtive-sadguri/

Timber and Architecture (Part III — The Future)

Guram Svanadze
Georgian Technical University, M.Kostava st 77, Tbilisi 0159, Georgia.
guramsvanadze@gmail.com

DOI: https://doi.org/10.52340/building.2025.72.02.08

Abstract Until the late twentieth century, engineers believed that constructing timber buildings taller than six stories was structurally impossible. Traditional sawn timber offered sufficient strength when forces acted parallel to its grain, yet it remained vulnerable to loads applied perpendicularly. As a result, wood lacked both the tensile capacity of steel and the compressive strength of reinforced concrete—qualities essential for building tall structures and resisting lateral forces such as wind.

Today, however, timber architecture has undergone a radical transformation. Buildings exceeding 80 meters in height have been completed or are currently under construction in Europe, North America, and Australia. Entire "timber districts" are emerging in several cities, and architects are now designing large-scale facilities—airports, railway stations, pedestrian bridges, schools, hospitals, and even stadiums—using engineered mass timber. Research increasingly confirms the positive psychological and physiological benefits of biophilic materials within educational and healthcare spaces. Notably, in 2024 the world's first fully timber stadium opened,

Fig. 1. W350 Project, Tokyo.

signaling a paradigm shift in large-scale structural design.

Fig. 2. Eco Park Stadium, Stround, UK. Zaha Hadid Architects.

This article examines how engineered timber technologies such as CLT, LVL, and Glulam are reshaping contemporary construction, and it analyzes their potential impact on the global building industry in the coming decades.

Introduction

Historically, preparing raw timber for construction required labor-intensive manual work. In contrast, the modern timber industry operates through automated manufacturing systems that process wood with extraordinary speed and precision. Today, engineered components can be fabricated in almost any size or geometric configuration. Large building sections—entire wall panels, floor plates, and even multi-bay structural modules—are assembled in controlled factory environments before being transported to site.

Fig. 3. Illustration showing the process of manufacturing architectural parts in a factory.

This shift has fundamentally changed the nature of construction. Off-site fabrication reduces noise, dust, and on-site labor risks; it accelerates project timelines; and it minimizes weather-related delays. Contemporary engineered wood products—most notably cross-laminated timber (CLT), laminated veneer lumber (LVL), and glued laminated timber (Glulam)—allow entire buildings to be constructed from wood, from primary load-bearing columns to structural walls and diaphragms.

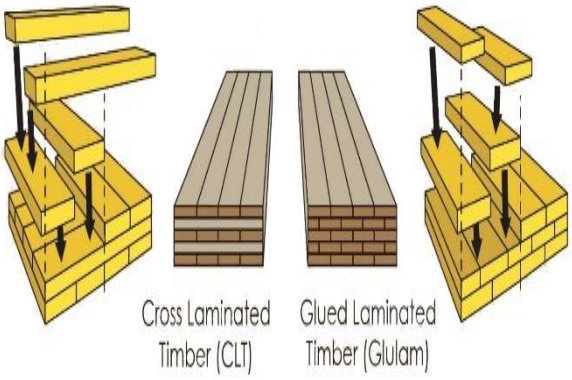

Fig. 5. The illustration depicts the process of transporting an architectural detail made in a factory.

Fig. 6. The illustration shows a plan for making cross-laminated and glued laminated timber.

Moreover, mass timber's favorable strength-to-weight ratio enables the creation of components that, relative to their weight, are stronger than steel. CLT, in particular, exhibits remarkable seismic resilience due to its ability to undergo controlled deformation without catastrophic failure. These *Fig. 4. The illustration depicts the installation process of a factory-made architectural detail.*

innovations challenge long-held assumptions about the limitations of wood, opening new possibilities for tall, large-span, and complex architectural forms.

Main Discussion — How Timber Will Shape the Construction Sector in the Coming Years

Cross-laminated timber represents one of the most transformative developments in architectural materials. Produced by bonding layers of solid-sawn boards in alternating grain orientations, CLT forms robust, dimensionally stable panels that resist loads in multiple directions. Because of this multi-axial strength, CLT performs differently from traditional materials such as reinforced concrete, which tends to crack and fail more abruptly. Timber's elastic behavior allows significant deformation before structural
failure, providing inherent resilience.

Fig. 7. Forte Tower, Melbourne, Australia. 2012

Although first developed in Europe during the early 1990s, CLT entered the International Building Code only in 2015, enabling mass-timber structures up to 18 stories. Since then, the global expansion of tall-timber construction has accelerated dramatically. LVL—created by laminating thin veneers under high pressure—and Glulam—constructed from bonded dimensional timber—further expand design flexibility, allowing architects to create long-span beams, curved elements, and expressive structural forms that would be difficult or inefficient to produce in steel or concrete.

One of the most compelling advancements is the emergence of mass-timber high-rises. Over the last decade, timber buildings have progressively climbed higher: from Melbourne's 32-meter, ten-story Forté Tower in 2012 to the current record-holder, the 25-story, 88-meter **Ascent MKE** mixed-use tower in Milwaukee, USA. Built with Glulam columns and massive CLT floor plates, Ascent demonstrates the viability of timber skyscrapers. Despite its height, the building weighs only one-fifth as much as a comparable reinforced concrete structure.

Fig. 8. Ascent MKE, Milwaukee, USA. 2022.

Even more ambitious proposals are advancing:

- a 21-story residential tower in Amsterdam,

- a 40-story timber skyscraper in Stockholm,
- an 80-story conceptual mass-timber tower at London's Barbican,
- and a 70-story project envisioned in Japan.

These proposals underscore the architectural community's willingness to redefine material hierarchies and challenge the steel-and-concrete paradigm that has dominated since the early twentieth century.

Fig. 9. Ascent MKE, Milwaukee, USA. 2022.

Conclusions

Mass timber—and engineered wood more broadly—constitutes one of the most significant innovations in recent construction history. These materials enable architects to build taller, lighter, and more sustainably than ever before. Global timber consumption continues to rise, surpassing even cement—the closest competitor in volume—whose production currently exceeds 1.3 billion cubic meters per year. Yet this rapid growth also brings new pressures. Only about 40% of the world's harvested wood is used for non-fuel purposes, raising concerns about long-term forestry management and ecological balance.

Here, scientific research and technological innovation play a crucial role. Engineered wood products have the potential to replace energy-intensive materials such as steel and concrete. Glulam and CLT structures are up to five times lighter than reinforced concrete buildings, reducing foundation requirements and minimizing embodied energy. Considering that concrete accounts for roughly 5% of global carbon emissions and steel for approximately 3%, the transition to timber-based construction represents a meaningful pathway toward climate-neutral development.

Recent laboratory breakthroughs further expand wood's relevance in future material science. At the University of Maryland, Professor Liangbing Hu demonstrated that wood's inherent mechanical limitations can be overcome by partial lignin removal followed by high-temperature densification. The resulting material is not only twelve times stronger than natural wood but also three times more durable, positioning it as a viable substitute for metals such as aluminum and steel.

Researchers at the Wallenberg Wood Science Center have even developed transparent wood by removing lignin entirely and infusing the cellular structure with a resin that matches its refractive index—creating a material that could one day replace glass. Meanwhile, Finnish laboratories are advancing methods for producing biodegradable plastics from wood fibers, introducing new possibilities for carbon-neutral consumer products.

Together, these developments point toward a future in which timber is not merely a traditional building material but a foundation for a **post-carbon architectural economy**. Engineered wood could transform everything from

skyscrapers to everyday objects, offering a renewable alternative to some of the most environmentally costly materials of the industrial age. The path ahead suggests not only the rise of taller timber buildings but the emergence of a new material culture—one in which wood, reimagined through science and technology, becomes central to sustainable architectural practice.

Reference

1. *A Handbook for the Sustainable use of Timber in Construction (2021)* – Jim Coulson;
2. *The Age of Wood (2020)* – Roland Ennos;
3. *Design of timber structures (Volume 1/2/3)* – Swedish Wood;
4. *Manual of Multi-Storey Timber Construction* – Hermann Kaufmann, Stefan Krotsch, Stefan Winter;
5. *Rethinking Wood – Future Dimentions of Timber Assembly* – Markus Hudert, Sven Pfeiffer;
6. *Tall Wood Buildings – Design, Construction and Performance* – Michael Green, Jim Taggart;
7. *Cross-Laminated Timber: An overview and development (2016)* - Brandner, R. et al.;
8. *Cross-Laminated Timber for Building Construction: A Life-Cycle Assessment Overview (2022)* - Younis, A. & Dodoo, A.;
9. Structural Design of Tall Mass Timber Buildings (2024) - Kılınç, G.A..

ON THE ANALYSIS OF A TUNNEL LINING OF OVAL CROSS-SECTION BY THE VARIATION METHOD

Demuri Tabatadze , Tebrole Kipiani, Kote Iashvili, Gela Macharashvili
Technical University of Georgia, M.Kostava st 77, Tbilisi 0175, Georgia
d.tabatadze@gtu.ge

DOI: https://doi.org/10.52340/building.2025.72.02.09

Summary A tunnel support (cylindrical shell) of oval cross-section, whose thickness and radius vary stepwise, is analyzed using the variational method.
A discontinuous solution of the governing differential equation is constructed based on the theory developed by Sh. E. Mikeladze.

Keywords: cylindrical shell, spherical shell, differential equation, variational method, discontinuous solution

Introduction

The development of engineering technology has consistently created the need for lightweight structures with high strength and stiffness. One such class of structures is **cylindrical shells**. Owing to geometric diversity and the nature of applied loads, displacements and deformations in these shells are proportional to the shell thickness. This necessitates the use of nonlinear relationships between deformations and displacements, the calculation of which relies on various assumptions and simplifications.
The efficiency of thin-walled shells is associated with the development of improved computational models and refinements of existing analytical methods. In the design of cylindrical shells, anchoring systems composed of rigidly interconnected circular rings are often used. In such cases, the engineer faces the problem of analyzing a shell composed of rigidly connected rings with different cross-sections. Similar difficulties arise when the rings are made of different materials and the internal force distribution must be investigated.

The direct calculation of such structures using classical coupling techniques is difficult and, in many cases, practically impossible. The problem becomes significantly simpler when one applies the general theory for constructing **discontinuous solutions of ordinary differential equations**, developed by **Sh. E. Mikeladze**.

Main Part

In this paper, based on the theories of Sh. E. Mikeladze, a discontinuous solution of the governing differential equation is constructed. This approach makes it possible to conveniently account for abrupt changes in individual geometric, kinematic, and static characteristics of shells.
We consider a tunnel lining modeled as an open cylindrical shell with stepwise changes in the radius of curvature R and thickness h. The structure is subjected to distributed vertical load p and horizontal load q. The load p acts over the entire span, while q is applied at a certain height, beginning from a specified point $s = s_1$ (see Figure 1).

In addition to external loads, the shell is influenced by the reaction of an elastic medium, which acts only in regions where radial displacements are positive (i.e., directed outward along the shell normal). The shell edges at the beginning of this region are assumed to be elastically clamped. Of the curved edges, one is free while the other is hinged.

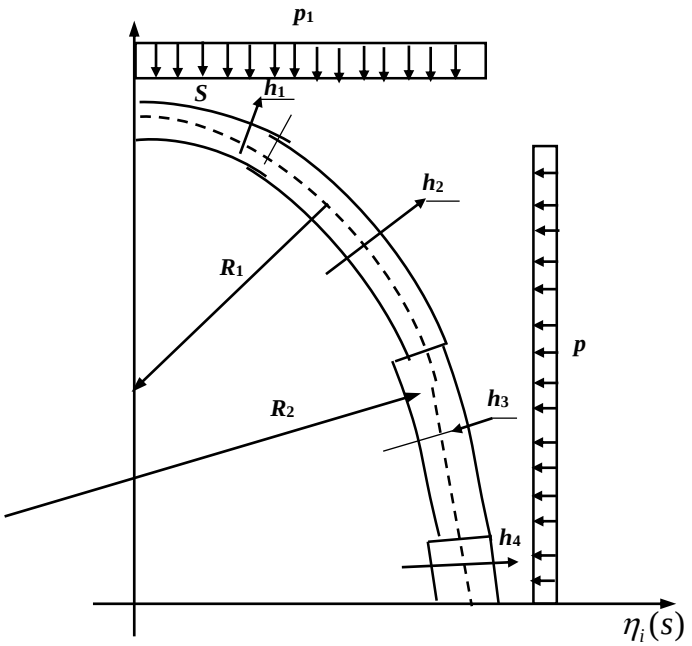

Fig. 1

The calculation of the cylindrical shell is performed using the variational method [1, 2]. The resulting system of governing equations, expressed in the form proposed by V. Z. Vlasov, has the form:

$$\sum_{i=1}^{n_1} a_{ij} F_i^{(4)}(x) + \sum_{i=1}^{n_1} b_{ij} F_i(x) + c_j = 0,\ j = 1,2,3,\dots n_1 \qquad (1)$$

$$a_{ij} = E\int h\eta_i(s)\eta_i(s)ds\,, \qquad 12b_{ij} = E\int R^2 h^3 \eta_i^{(4)}(s)\eta_j^{(4)}(s)ds\,,$$
$$c_j = -\int q_\theta \eta_j'(s)ds + \int R q_n \eta_j^{(2)}(s)ds$$

Where*:*

- *E* denotes the modulus of elasticity,
- the normal and tangential components of external loads are q_n and q_θ
- the functions $F_i(x)$ and $\eta_i(s)$ form a displacement function

The displacement function is represented as:

$$\Phi(x,s) = \sum_{i=1}^{n_1} F_i(x)\eta_i(s)\,,$$

This function satisfies the prescribed boundary conditions. The assumed functions are chosen to be linearly independent and may be interpreted as admissible displacement modes, such as the deflection function of a curved beam of unit width corresponding to a transverse strip of the shell.

Assuming:

$n_1 = 1$, equation (1) can be rewritten as

$$F^{(4)}(x) + b_0 F(x) = c_0 \qquad (2)$$

Where:

$$b_0 = b_{11}/a_{11}\,, \quad c_0 = -c_1/a_{11}\,.$$

the boundary conditions are written as follows:

- at the free edge:

$$F^{(2)}(o) = F^{(3)}(o) = 0\,, \qquad (3)$$

- at the fixed edge:

$$F(l) = F'(l) = 0 \qquad (4)$$

The solution of equation (2), subject to boundary conditions (3) and (4), has the form:

$$F(x) = c_0[1-(\cos\alpha sh\alpha - \sin\alpha ch\alpha)(\sin\beta x ch\beta x + \cos\beta x sh\beta x/\gamma + \\ +2\cos\alpha ch\alpha \cos\beta x ch\beta x/\gamma\,]/b_0 .$$

Where

$$\alpha = \beta l\ ,\ \beta = \sqrt[4]{b_0/4}\ ,\ \gamma = \cos^2\alpha sh^2\alpha - \sin^2\alpha ch^2\alpha - 2\cos^2\alpha ch^2\alpha .$$

Thus, the remaining task is to select an appropriate displacement function $\eta_1(s)$. To accomplish this, we examine the bending of a curved beam with piecewise-constant thickness and radius of curvature.

Governing Equation of the Curved Beam

The elastic equilibrium equation is written as:

$$w^{(5)}(s) + Aw^{(3)}(s) + Bw'(s) = f(s), \qquad (5)$$

Where:

$$A = 2/R^2\ ,\ \ B = 12K/Eh^3 + 1/R^4\ ,$$
$$f(s) = 24[p\sin(s/R + \sum\varphi_i) + p_1\cos(s/R + \sum\varphi_i)/ERh^3\ ,$$
$$\varphi_i = 0 \ \text{ at } s \le s_i \ \text{ and } \ \varphi_l = s_i\left(1/R_i - 1/R_{i+1}\right) \ \text{ at } \ s_l < s < s_{i+1} .$$

- w denotes the deflection of the curved beam w denotes the deflection of the curved beam
- $s_l -$ is the ordinate of the point at which the radius changes abruptly, and K- is the coefficient of the Winkler elastic medium.

The annular strain is assumed to be zero, leading to the differential equation governing the tangential displacement v:

$v'(s) + w/R = 0$.

The boundary conditions are as follows:

- at the axis of symmetry (s = 0): $w' = w^{(3)} = v = 0$;
- at the supports $(s = s_0): w = v = 0$ $w' = E\cdot w^{(2)}/K$.

The stepwise variation of radius of curvature, thickness, load intensity, and the foundation coefficient K leads to jumps of the first kind in the derivatives of the deflection function w. Consequently, it is necessary to construct discontinuous solutions of equation (5). Following Sh. E. Mikeladze, the solution is represented in the form of a generalized w:

$$w(s) = w(0) + \sum_{k=1}^{n}\left\{\left[w'(0)d^{(k)} + w^{(3)}(0)b^{(k)}\right]\sin\left(\frac{k\pi}{2}\right) + \left[w^{(2)}(0)d^{(k)} + w^{(4)}(0)b^{k}\right]cos\frac{k\pi}{2}\right\}\frac{s^k}{k!} + \\ \sum_{i=1}^{m}\sum_{k=0}^{n}\delta_{ik}\frac{(s-s_i)^k}{k!}H(s-s_i) \qquad (6)$$

Where:

$$\mathrm{H}(\xi)=0 \text{ for } \xi \le 0 \text{ and } \mathrm{H}(\xi)=1\ \xi > 0$$

$$b^{(k)} = -A(0)b^{(k-2)} - B(0)b^{(k-4)}, \quad d^{(k)} = -A(0)d^{(k-2)} - B(0)d^{(k-4)},$$
$$c^{(k)} = -A(0)c^{(k-2)} - B(0)c^{(k-4)} + f^{(k-5)}(0) \ \text{ for } k \ge 5,$$
$$\text{and } \ b^{(1)} = b^{(2)} = d^{(3)} = d^{(4)} = 0\ ,\ b^{(3)} = b^{(4)} = d^{(1)} = d^{(2)} = 1 \ \text{ and } \ c^{(1)} = c^{(2)} = c^{(3)} = c^{(4)} = 0$$

.

and the jump magnitudes at points of discontinuity are determined from continuity conditions on deflection, rotation angle, bending moment, shear force, and normal force.

The jumps δ_{ik} at $k \le 4$ are determined from the condition of continuity of the deflection, angle of rotation, bending moment, shear force and normal force, and at $k \ge 5-$ according to the relation obtained by differentiating (5) the appropriate number of times.

Determination of Initial Parameters

To determine the initial parameters $w^{(k)}(0)$ (k = 0, 1, 2, 3, 4), the method of successive approximations is used. The essence of this method is as follows: in the zeroth approximation, δ_{ik} is assumed to be zero; based on the boundary conditions, the parameters $w^{(k)}(0)$ are determined, and then δ_{ik} in subsequent approximations, the procedure is repeated with new values (δ_{ik} And so on, until the required accuracy is achieved.)

After constructing solution (6), we return to selecting the function $\eta_1(s)$.

In accordance with the variational method, we assume that:

$\eta_1^{(2)}(s) = w/R$. Then $\eta_1'(s) = \int_0^s (w/R)ds + \zeta_1$

and

$$\eta_1(s) = \int_0^s (s-t)(w/R)dt + \zeta_1 s + \zeta_2 .$$

The constants ζ_1 and are ζ_2 determined from the boundary conditions on the straight edges.

Reference

A detailed analysis is carried out for the case where the beam thickness changes abruptly at three points: $(s = s_1,\ s_3,\ s_4)$

In this case, the point of load discontinuity p_1 coincides with s_1, and the point of curvature radius discontinuity coincides with s_3.

Example parameters:

uniform vertical load p = 25 *t/m*^{2}, additional distributed load $p_1 = 1{,}5$ *t/m*^{2}, elastic modulus $E = 3{,}21 \cdot 10^6$ *t/m*^{2}. The shell thicknesses were taken as $h_1 = 0{,}7$ *m*, $h_2 = 0{,}8$ *m*, $h_3 = 0{,}95$ *m*, $h_4 = 1{,}1$ *m*, The characteristic arc-length coordinates of thickness discontinuities are: $s_1 = 2$ *m*, $s_3 = 5{,}5$ *m*, $s_4 = 7$ *m*, $s_0 = 8$ *m*, with the total span length *l* = 8 *m*, The radii of curvature were assumed as R_1 = 5,81 *m*, R_2 = 8, 5 *m*, The Winkler elastic foundation coefficient was taken as $K = 16 \cdot 10^3$ *t/m*^{2}.

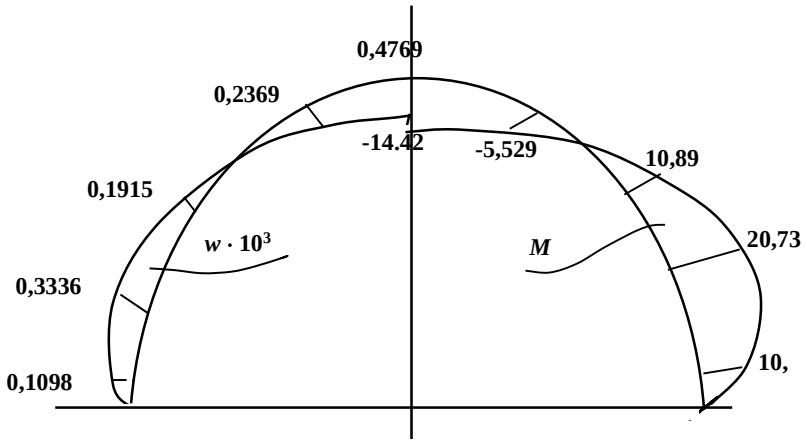

Fig. 2

Figure 2 illustrates the deflection and bending-moment diagrams for the free curved edge of the shell.

Conclusion

In this study, a tunnel lining of oval cross-section with stepwise variations in thickness and radius of curvature was analyzed using the variational method. The governing differential equation of the shell was solved by constructing a discontinuous solution based on the theory developed by Sh. E. Mikeladze, which makes it possible to explicitly account for abrupt changes in geometric and mechanical parameters.

The proposed approach allows the effects of discontinuities in thickness, curvature, loading intensity, and elastic foundation stiffness to be incorporated into the analytical solution without introducing artificial compatibility conditions or complex coupling procedures. The method ensures continuity of displacement, rotation, bending moment, shear force, and normal force at the points of parameter variation, thereby preserving the mechanical consistency of the model.

A numerical example was presented to illustrate the applicability of the method. The obtained deflection and bending-moment diagrams for the free curved edge demonstrate the influence of stepwise parameter changes on the stress–strain state of the tunnel lining. The results confirm that local stiffness variations significantly affect the internal force distribution and deformation pattern of the shell.

The developed analytical framework provides a practical and efficient tool for the calculation of tunnel linings and similar shell structures with piecewise-constant properties. It can be extended to the analysis of shells composed of different materials or resting on nonuniform elastic foundations, and it may serve as a basis for further refinements in the analytical design of underground structures.

Reference

1. Vlasov, V. Z. General Theory of Shells and Its Applications in Engineering. Moscow, 1949.
2. L'Hernite. Resistance of Materials. Paris, 1954.
3. Mikeladze, Sh. E. New Methods of Integrating Differential Equations. Moscow-Leningrad, 1951.
4. Mikeladze, Sh. E. Some Problems of Structural Mechanics. Moscow-Leningrad, 1948

Obtaining High-strength Concrete Using Local Microdispersed Additives

Aleksandre Peikrishvili
Technical University of Georgia, M.Kostava st 77, Tbilisi 0175, Georgia
aleksandre.peikrishvili@gau.edu.ge
DOI: https://doi.org/10.52340/building.2025.72.02.10

Abstract. The article discusses modern approaches to producing high-strength concrete using local microdispersed additives. It examines the principles of modifying the composite structure of concrete and the influence of microsilica, microclay, and metakaolin on the rheological and physical properties of the mixture. The research subject is the effectiveness of silicomanganese dust from the Zestafoni Ferroalloy Plant as a micro-additive on concrete strength. Results of chemical and physical-technical analysis confirm that this residue contains a low amount of active SiO2 and does not provide the required concrete strength. Comparative analysis shows that foreign microsilica with high silicon content significantly increases concrete density, strength, and corrosion resistance. Additionally, the study explores the possibility of using cement kiln dust which, in combination with superplasticizers, contributes to raising the concrete class and alleviating ecological problems.

Keywords: Microsilica; silicomanganese dust; micro-additives; concrete modification; local raw materials.

Introduction.

One of the most decisive and influential factors in the ongoing development of modern concrete technology is the meticulous processing and application of the scientific foundations regarding concrete modification. Currently, one of the most prevalent and effective methods for modifying the internal structure of composite building materials involves the strategic introduction of highly active additives into their basic composition to enhance performance. These mineral additives can be derived from either natural or artificial origins and typically contain various silicate minerals. Depending on their source and processing, these minerals may exist in several physical states, including crystalline, fine-crystalline, colloidal, or amorphous states. Within this category of transformative materials, microsilica, microclay, and metakaolin stand out as the primary and most significant types of additives used to achieve these structural improvements.

The inclusion of these specific mineral additives in a concrete composition significantly helps to maintain the flowability of the mixture for a critical period during the construction process. This retention of flow is exceptionally important in contemporary concrete technology, particularly for the successful implementation of self-compacting concretes that require high mobility. Furthermore, these materials are characterized by distinct rheological properties that ensure the concrete mixture does not undergo segregation, which would otherwise compromise the structural integrity of the material. By using these additives, engineers can ensure that an optimal level of viscosity is maintained for a specific and necessary duration, allowing for proper placement and finishing of the concrete in various architectural and industrial applications.

On a global scale, microsilica has become a staple in the international construction industry, where it is utilized extensively in the production of heavy concretes, foam concretes, and specialized dry construction mixtures. The widespread adoption of this material is explained by its unique and highly desirable physical and chemical properties. Its remarkably high pozzolanic activity is fundamentally determined by its extreme degree of dispersity and the substantial abundance of amorphous silicon dioxide (SiO2) within its structure. Physically, microsilica presents as a super-dispersed powder that possesses an exceptionally large

specific surface area, which allows it to react more efficiently within the cementitious matrix than standard materials.

From a technical perspective, microsilica exhibits a fascinating contrast between its bulk and true density; while its bulk density is relatively low, ranging from 120 to 450 kg/m3, its true density is often ten times higher or more, measured between 2200 and 2300 kg/m3. Chemically, it is characterized by an extremely high content of SiO2 (98%), which exists almost entirely in an active amorphous form. The physical scale of these particles is also extraordinary, with an average size of only 0.1 to 0.2 μm, making them approximately 50 to 100 times finer than standard cement particles. This microscopic size contributes to a massive specific surface area that typically ranges between 13,000 and 35,000 m2/kg, facilitating the dense and high-strength microstructures required for modern infrastructure.

The profound influence of microsilica on the complex process of structure formation within cementitious systems is fundamentally governed by the intricate relationship between two primary mechanisms, which researchers and material scientists categorize as the physical and chemical factors. These factors do not operate in isolation but rather work in a highly synergistic manner to transform the internal architecture of the concrete from the moment water is first introduced until the material reaches its final, fully hardened state. By understanding and manipulating this dual-action modification, engineers can precisely tailor the rheological and mechanical properties of the composite material, ensuring that the resulting building substance meets the increasingly rigorous demands of modern high-performance infrastructure projects.

The physical factor is intrinsically linked to the exceptional ultra-dispersity of microsilica particles, which significantly dictates the behavior of the cement system during its initial coagulation stage. While the mixture is still in its plastic and workable state, these incredibly fine microsilica particles—which are significantly smaller than the cement grains themselves—serve as a strategic micro-filler by occupying the microscopic interstitial spaces and voids that naturally exist between the much coarser grains of cement. This "filler effect" facilitates the creation of a vast and dense network of coagulation contacts between the various solid-phase components, effectively stabilizing the suspension and reducing the likelihood of water bleeding. As the hydration process progresses into the subsequent crystallization stage, this dense packing continues to pay dividends by physically blocking the development of large capillary pores, thereby dramatically increasing the overall density and structural homogeneity of the hardening stone.

Simultaneously, **the chemical factor**, which is deeply rooted in the specific chemical-mineralogical composition of the microsilica, initiates a transformative reaction that fundamentally alters the balance of the cement stone's hydrated phases. The high concentration of active amorphous silicon dioxide within the microsilica reacts chemically with calcium hydroxide—a relatively weak and soluble byproduct of cement hydration—to produce additional volumes of calcium hydrosilicates, commonly known as the C-S-H gel. This chemical metamorphosis is crucial because these secondary hydrosilicates are significantly stronger, more stable, and more adhesive than the initial hydration products. By converting weaker, crystalline components into a robust and dense binder, the chemical presence of microsilica ensures a superior bond between the cement paste and the aggregate, reinforcing the entire matrix at a molecular and microscopic level.

Consequently, the harmonious integration of **high-dispersity microsilica** into a mixture allows for the industrial production of advanced concretes that are characterized by extraordinary compressive strength and remarkably low permeability. Because the internal pore structure is so refined through the filler effect and the chemical bond is made so resilient through

the pozzolanic reaction, the resulting material exhibits a significantly increased resistance to aggressive environmental factors. This effectively prevents the ingress of moisture, salts, and harmful ions that typically lead to the corrosion of reinforcement steel and general material degradation. Ultimately, this comprehensive structural modification translates into a construction material with vastly improved durability and a significantly longer service life, making it an indispensable component for modern engineering challenges.

Tables 1 and 2 present the chemical composition and physical-technical indicators of silicomanganese dust from the Zestafoni Ferroalloy Plant alongside data from similar plants in the former Soviet Union. The data shows that Zestafoni silicomanganese dust is characterized by the lowest content of active SiO2.

Table 1

Chemical composition of some microfillers

Origin of Micro-filler	Name of Micro-reinforcer	Chemical Composition of Micro-fillers							
		SiO2	Fe2O3	Al2O3	CaO	MgO	K2O+Na2O	MnO	SO3
Novoselovskoye	Ferrosilicon	89.7	2	1.7	2.5	1.76	1.89	-	0.3
Chelyabinsk	Ferrosilicon	89.2	2.84	1.68	2.1	1.75	1.43	-	0.5
Ermak	Ferrosilicon	70.1	3.43	2.03	11.4	0.9	0.9	-	0.4
Aktyubinsk	Ferrosilicochromium	66.1	2.2	1.3	0.44	14.65	1.8	-	4.2
Zestafoni	Silicomanganese	25.2	2.64	4.27	18.6	4	2.1	35.8	4.2
Zestafoni	Silicomanganese	35.4	2.3	3.86	4.58	4.2	2.4	39.1	3.4

Table 2

Some physical and technical ndicators of ultrafine waste from ferroalloy production

Manufacturing Plant	Novokuznetsk	Chelyabinsk	Ermak	Aktyubinsk	Zestafoni	Zestafoni
Type of Ultrafine Waste	Ferrosilicon	Ferrosilicon	Ferrosilicon	Ferrosilicochromium	Silicomanganese	Silicomanganese
SiO2 Content, %	89.7	89.2	70.1	66.1	25.2	35.4
Hydraulic Activity	98	94	58	40	14.2	25
Water Demand	40	33	137	43	26	33

Experimental studies utilized silicomanganese dust collected from filters at the Zestafoni plant, which chemical analysis showed contains no more than 20% SiO2, and a Norwegian-produced additive called "Microsilica". According to international standards, the SiO2 content in Microsilica should exceed 85%, a requirement met by the foreign additive. The study considered the high cost of the foreign additive versus the need to utilize Zestafoni silicomanganese dust and the possibility of enriching it with SiO2 by reducing manganese content.

Results in **Tables 3 and 4** show that Zestafoni silicomanganese dust has the lowest active SiO2 content, and experiments demonstrated that its use as a micro-additive in concrete mixtures does not yield adequate results.

Table №3

Composition of Concrete Mixes Modified with Zestafoni Silicomanganese and Norwegian Microsilica

Mix Series No.	Cement (kg/m3)	Khrami River Crushed Stone (5-20 mm) (kg/m3)	Khrami River Sand (0-2.5 mm) (kg/m3)	Khrami River Sand (2.5-5 mm) (kg/m3)	Water (l/m3)	Admixture Type and Dosage (%)	Zestafoni Silicomanganese (kg/m3)	Water/ Cement Ratio
1	400	905	510	275	180	ViscoCrete SF 18 (1.0%)	80	0.45
2	420	855	540	290	170	ViscoCrete SF 18 (1.0%)	84	0.4
Mix Series No.	Cement (kg/m3)	Khrami Crushed Stone (5-10 mm) (kg/m3)	Khrami Crushed Stone (10-20 mm) (kg/m3)	Khrami Sand (0-2.5 mm) (kg/m3)	Quartz Sand (2.5-5 mm) (kg/m3)	Water (l/m3)	Admixture Type and Dosage (%)	Foreign Production Microsilica (kg/m3)
1	400	305	565	490	325	180	ViscoCrete SF 18 (1.0%)	80
2	420	315	585	470	290	170	ViscoCrete SF 18 (1.0%)	84

Table №4

Dependence of concrete compressive strength on the age of the material

Concrete Mix	Admixture	Concrete	Concrete	Concrete	Concrete	Concrete
1	ViscoCrete SF 18 (1.0%)	10.6	21.5	32.3	37.5	45.3
2	ViscoCrete SF 18 (1.0%)	12.8	25.5	34.4	41.8	50.4
Concrete Mix Series No.	Admixture Type and Dosage	Concrete Strength at 1 Day (MPa)	Concrete Strength at 3 Days (MPa)	Concrete Strength at 7 Days (MPa)	Concrete Strength at 14 Days (MPa)	Concrete Strength at 28 Days (MPa)
1	ViscoCrete SF 18 (1%)	18.1	30.8	54.3	73.5	84.6
2	ViscoCrete SF 18 (1%)	21.4	34.5	63.5	80.8	95.7

Testing of Cement Kiln Dust

During the testing of cement kiln dust, Sika Viscocrete SF-18 was used as a plasticizer. One series of samples was prepared without additives or plasticizers, while another series (Series 2) used only Viscocrete SF-18. Samples were tested at 7 and 28 days, with results shown in Table 5.

Table №5

Testing of concrete made with cement Dustmicrofiller

№	Type of Micro-filler	Concrete Composition (kg/m3)						Cone Slump (cm)	Bulk Density (kg/dm3)		Compressive Strength (MPa)	
		Cement	Sand	Crushed Stone	Micro-filler	Plast.	Water		7 Days	28 Days	7 Days	28 Days
1	-	450	800	860	-	-	250	10	2.29	2.33	33.1	52.3
2	-	450	820	880	-	4.5	180	15	2.32	2.34	51.3	73.6
3	Cement Dust	450	785	845	72	4.5	205	15	2.37	2.37	58.4	82

Kiln dust as a potential mineral modifier, a specialized high-performance superplasticizer known as Sika Viscocrete SF-18 was integrated into the mixture to optimize its rheological and mechanical performance. The experimental methodology involved preparing distinct series of samples to ensure a rigorous comparative analysis; specifically, one control series was manufactured without any additives or plasticizers to serve as a baseline, while a second series utilized only the Viscocrete SF-18 plasticizer to evaluate its independent impact on the cementitious system. To evaluate the development of physical-technical properties and the evolution of the material's structure over time, these samples underwent rigorous strength testing at two critical curing intervals: 7 days and 28 days. The precise composition of the modified concrete involved a superplasticizer dosage fixed at 1% relative to the total cement mass, whereas the mineral micro-filler—the cement kiln dust—constituted approximately 16% of the cement mass, ensuring a significant

presence of ultra-dispersed particles within the composite mix.

The subsequent analysis of the experimental results demonstrates that the strategic integration of micro-fillers in tandem with a superplasticizer significantly enhances the compressive strength of the concrete compared to the baseline additive-free versions. This improvement is primarily driven by physical and chemical factors where the ultra-dispersed mineral particles effectively fill the microscopic pores within the hardening stone structure, thereby increasing overall density and the number of coagulation contacts. Furthermore, this process facilitates the modification of the composite structure by potentially altering the balance of hydrated phases, leading to an increased volume of more stable and durable calcium hydrosilicates. Consequently, these findings validate that such modifications effectively enable the elevation of the concrete's functional class, proving that high-performance materials can be successfully achieved using locally sourced additives. Beyond these technical advantages, this research directly addresses the critical industrial challenge of cement kiln dust utilization; by repurposing this residue as a functional component in concrete production, the industry can resolve persistent ecological problems and promote sustainable waste management practices within the construction sector.

References

1. 1. V.V. Malhotra. Innovative Applications of Superplasticizers in Concrete – A Review// CANMET/ACI Symposium on Advantes in Concrete Science Tech. Rome, okt. 7-10, 2007, Proceedings, p.p. 271-314.
2. V. Batrakov, S. Kaprielov. Durabiliti of Concretes Modified bi Silicoorganoc Compounds// CANMET/ACI int. Sump. On Advances in Concr. Technology. LasVegas June, 2005, Supplementari papers, p.p. 609-624.
3. B. Pecur, N. Stirmer. Compatibility of polycarboxylate superplasticizers with cement. of 8th CANMET/ACI International Conference on Superplasticizers and Other Chemical Admixtures in Concrete. Suppl. volume. P. 213-226.
4. m. turZelaZe, g. TaTaraSvili, i. giorgaZe. TviTSemWidroebadi betoni – dRevandeli samSeneblo amocanebis gadawyvetis efeqturi instrumenti. Jurnali „energia", №2 (58), 2011, გვ. 77-79.
5. Д.М. Поляков, С.В. Коваль. Самоуплотняющийся бетон с использованием карбонатного наполнителя. Ж. «Вестник», Киев, 2010 1(81), стр. 107-112.

Planning Experimental Studies of Vehicle Movement Patterns under Various Road Conditions

Konstantine Mchedlishvili, Giorgi Kakhadze
Georgian Technical University, M.Kostava st 77, 0175, Tbilisi, Georgia
kakhadze.g@gtu.ge
DOI: https://doi.org/10.52340/building.2025.72.02.11

Abstract The article is dedicated to the experimental study of the regularities of vehicle movement under various road conditions, the determination of the size of adjustable and controllable variables acting on the Driver–Vehicle–Road–Environment (DVRE) system, the definition of the sequence among variable values to ensure the compactness of the experiment and the effectiveness of the results, and the calculation of the required number of trials and measurement accuracy to obtain reliable and convincing outcomes. The article also discusses conducting the experiment using a so-called "randomized design." For planning the experiments and analyzing the obtained data, the normal distribution law and the so-called "Student's t-test" are applied.

Key words: experiment, number of trials, normal distribution, data analysis

Introduction

Applied science is based on research conducted through theoretical and, predominantly, experimental methods derived from the achievements of fundamental sciences, resulting in solutions to problems that are directly necessary for practical use. Among these is the main goal of our study — a critical analysis of the existing methods, standards, and regulations for studying the regularities of road traffic, improving outdated approaches, and creating new ones. The application of these improved or newly developed methods in practice will ensure the achievement of maximally effective results with minimal time, material, and financial expenditures.

In the early stages of civilization, engineering relied on the results of experimental research, but the analysis and further development of these results belonged more to the realm of art. Instead of the optimal synthesis of mutually conflicting requirements, the main focus was placed on ensuring the style and technologies appropriate to the era, as well as on excessive strength and durability. As an example, we can mention the multilayer pavement structures of ancient Rome's main roads during the classical era, whose strength and durability exceed even the requirements needed for today's automotive loads.

Main Part

Rational planning of an experiment allows us to minimize the duration of the research, avoid major errors, and obtain the maximum amount of useful information with minimal time and labor expenditure. For the effective execution of an experiment, it is necessary to determine in advance the size of the adjustable and controllable variables. To do this, we rely on intuition, experience, and the following two conditions: [1,2,3]

The variation step must be sufficient to reveal a noticeable change in the studied object. For this purpose, we take some baseline value of X, denoted as $X\delta$, and define a step ΔX, which provides the lower and upper bounds of the variation interval — X_{low} and X_{high}.

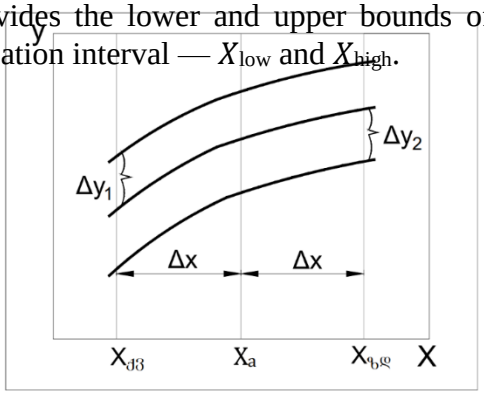

Fig. 1. Scheme for Determining the Variation Step

$X\delta-\Delta X=X_{დბ}$, $X\delta+\Delta X=X_{ზედ}$

The variation step must be such that the increments of the studied object at the lower

and upper bounds cancel each other out:

$$\Delta Y_1 - \Delta Y_2 = 0$$

The variation step must also be small enough to allow the description of the regularities of the studied object's changes within this interval using a linear function. In Fig. 2, it is evident that for linear approximation, the step ΔX is better than ΔX_1.

Such analysis is performed across the entire range of possible values of the variables, and based on this, taking into account the results of preliminary experiments, the required step size is determined.

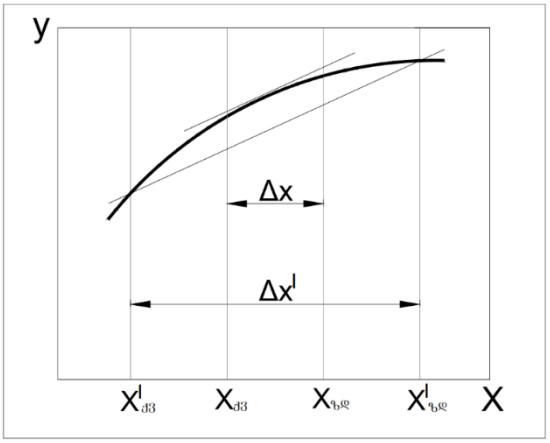

Fig. 2. Selection of the Variation Step Based on the Condition of Linear Approximation

For the experiment to yield effective results and for the experiment itself to remain compact, we must determine in advance the sequence of the variable's values. The theory of experimentation [3] considers two cases here: The first case is when we start from one extreme value of the variable and gradually move toward the other extreme value — for example, from X_{min} to X_{max}.

In the second case, the value of the variable is chosen arbitrarily across its entire range of variation. The first case represents an experiment with a so-called "sequential design," while the second corresponds to an experiment with a "randomized design." Such a design offers several advantages: often, other factors influencing the process under study are not reliably stabilized — this mainly concerns controllable but non-adjustable factors. In our case, these include ambient temperature, rain, and moderate or strong wind, all of which may vary during the course of the experiment. If, during the same period, we continuously vary the studied variable X in a fixed sequence, then the studied output Y may change not only due to variations in factor X, but also under the influence of other, poorly stabilized factors. However, if we vary X randomly, we eliminate the possibility of mixing the effects of meteorological factors and the influence of X on Y. Given the specifics of our experiments, which are conducted outdoors, we always perform the trials in sunny, windless, and dry weather.

Selecting random values for X also eliminates the influence of the operator's changing performance due to fatigue or learning, as well as the limitations of the available time for using the measuring instrument. It is evident that randomization allows us to minimize the "noise" caused by uncontrollable factors. However, in our study, where observations are conducted on pedestrian behavior or the time intervals between vehicles, as well as on the intensity and composition of traffic flow, the experiment is carried out using video recording. If video recording is not used, observers are rotated every 15 minutes when traffic intensity is high, and when traffic is low, one observer can reliably work for 45–60 minutes. Based on the above considerations, and given the characteristics of the studied object, for which obtaining objective information is fully possible through a strict sequential arrangement of variables, we therefore use experiments with a "sequential design."

In our studies, there are often objects that depend on several adjustable and controllable variables. The same object may also be influenced by several uncontrollable factors. In such cases, depending on the number of adjustable and controllable variables, we can conduct two-factor, three-factor, and higher-order experiments. For example, the waiting time of pedestrians at a regulated intersection depends on the duration of the red signal, the width of the roadway, the presence of a median strip, and so on. These are adjustable and controllable variables. In addition, there are uncontrollable factors, such as air temperature, rain intensity, wind strength, and the mentality

of pedestrians and drivers.

In cases of such multi-factorial influences, we can conduct experiments using either a classical or a factorial design. In our studies [5,6], we mainly use multi-factorial experiments with a classical design. For example, consider an object R that is a function of the adjustable and controllable variables X, Y, and Z: $R = f(X,Y,Z)$. In the classical design, all these variables except one are kept constant, i.e., stabilized. The remaining variable is varied across its entire possible range. Then we vary the second variable while keeping the others stabilized at constant levels, and so on. The influence of uncontrollable factors is taken into account through randomization. For instance, consider a two-factor experiment where each factor is varied at five levels. We investigate the maximum speed achievable under stability conditions on a regulated intersection during left turns with a small radius and its dependence on the turning angle α^{o} and the trajectory radius R. The sequence scheme of changes for both factors, each varied at five levels, can be represented as shown in Fig. 3.

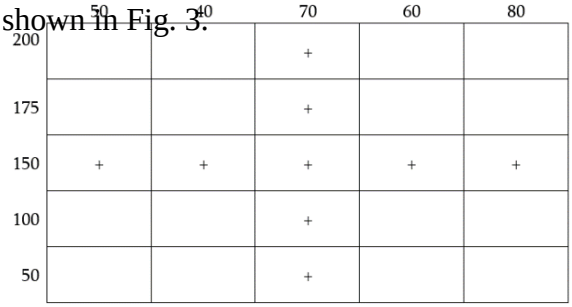

Fig. 3. Randomization matrix of variables at 5 levels

To randomize factors such as vehicle type, driver characteristics, pavement parameters, curve superelevation, etc., it is advisable to conduct the experiment according to the following variable pairings: 200 m – 70°, 75 m – 70°, 150 m – maximum, and so on. Based on our experience, during a classical experiment it is not necessary for the experimental plan to be fully balanced. That is, variables can be varied at different levels. For example, we know that the turning radius is more important than the turning angle of the trajectory. Therefore, we can vary the radius at 8 levels and the turning angle at 5 levels. If a more complex type of mathematical relationship is expected, such as trigonometric, logarithmic, etc., the matrix can be filled more fully, and the experiment can be conducted with a greater nu

mber of combinations of x and y variables. To obtain reliable results from the trials, it is necessary to determine in advance the required number of trials and the accuracy of measurements. Based on our practical experience [5,6], it is advisable to evaluate the reliability of the results using the so-called reliability probability (α). The limits within which the studied quantity is contained with the corresponding reliability probability are called reliable limits, denoted as a_1 and a_2 (Figure 4). The interval between the reliable limits is called the reliable interval $\mu\alpha$. Using preliminary data from observations of vehicle movement modes, we determine the magnitude of the studied parameter's dispersion R.

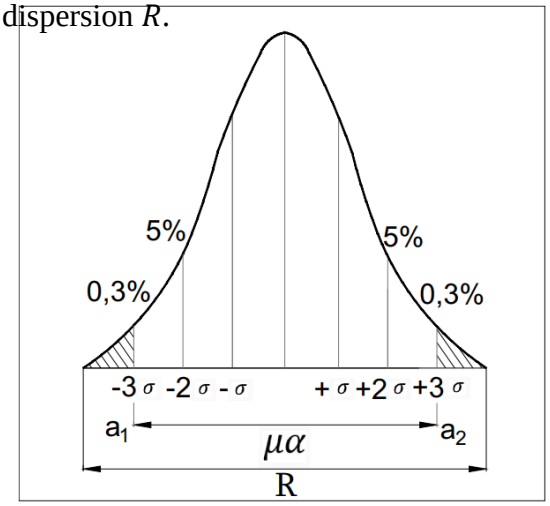

Figure 4. Reliable interval and its limits according to a predetermined reliability probability

The distribution of the studied parameter can follow different regularities. To analyze it, histograms and variation series of the studied quantity are constructed, and then, by fitting the appropriate theoretical distribution curve, statistical investigation is carried out using well-known methods. The reliability of the obtained hypothesis regarding the type of distribution is tested using the Pearson criterion, $P(x)^2$ P=0,05, corresponding to a 95% reliability probability. Analysis of the obtained data and a review of specialized

literature indicate that the distribution of speeds predominantly follows the Gaussian, i.e., the normal distribution law. (Fig. 5)

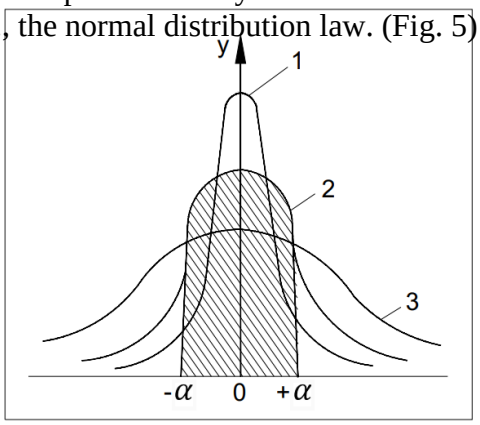

1) σ=0.5; 2) σ=1.0; 3) σ=2.0

Fig. 5. Shape of the normal distribution curve

The distribution of time intervals, on the other hand, more often follows the Poisson or Pearson Type III distribution (Figure 6).

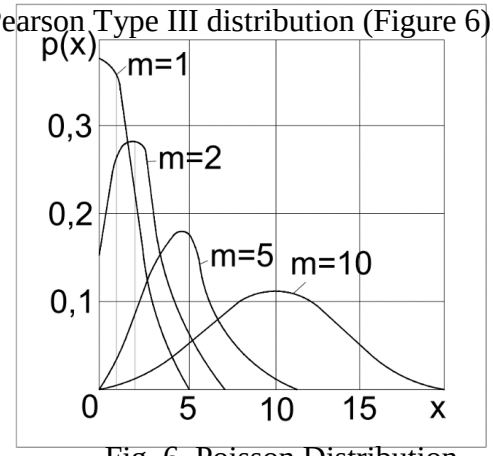

Fig. 6. Poisson Distribution

m-mathematical expectation, i.e., the weighted average value. Under conditions of relatively low intensity, with traffic load levels in the range Z=0.3–0.6, according to our data, the Poisson distribution, in terms of its spread characteristics, approximates the normal distribution. In high-intensity flows, when Z= 0.7–0.85, it corresponds to Pearson's Type III distribution. Since most of our experiments were conducted under traffic loads with Z≤0.6, for the design of experiments and analysis of data, we use the "normal" distribution law. In such cases, to determine reliable limits, we use the number of standard deviations that should be measured to the right and left of the distribution center so that the probability of the distribution within the resulting interval is α [2, 3].

Experience from studies on speed distributions under certain road conditions shows that most values are located within the range X±3σ, which corresponds to a confidence probability of 99.7%. This indicates that we can take the spread magnitude as R=6σ. Accordingly, if the spread magnitude is known from preliminary experiments, the probable value of the standard deviation is σ = R/6.

In road studies, results are traditionally accepted with 85% and 95% confidence, which shows that the existence of the studied quantity within any predetermined interval can be confirmed only with a 15% or 5% allowable error of the total number of cases. To determine a reliable and convincing value of the studied quantity, and subsequently the nature of its distribution, it is necessary to establish the required number of experiments using the following expression:

$$n=\frac{t^2*\sigma^2}{\Delta^2}$$

Where n is the number of trials, Δ is the measurement accuracy, and t is the confidence coefficient, i.e., the function of the reliability probability according to the so-called "Student's criterion" [2, 3]. Its value is chosen according to the required confidence level based on the values presented in the table below.

Table N1

Confidence α%	85	90	95	98	99	99,7
t	1,25	1,7	2,0	2,4	2,6	3,3

Below is the calculation of the minimum number of trials required for analyzing speeds recorded on a specific road section.

Variant I. The speed range on the given road section is V=40–76km/h, i.e., the spread R=36 km/h. Then the standard deviation is $\sigma = \frac{R}{6}$=6km/h σ=6 R=6km/h. We select a confidence level of 85%. From the table, α=85% corresponds to t=1.25. If the measurement accuracy is Δ = 1 km/h, then the minimum number of trials required is:

$$n=\frac{1{,}25^2*5^2}{1^2}$$ =1,56*36=56 trials

For analyzing the distribution of time spent on the section, we perform the following calculation.

Variant I. The time range is t=5–35 min, so the spread is R=30 min. Choosing a confidence level of 85% gives t=1.25, and measurement accuracy Δ=1 min. Then the minimum number of trials required is: $n=\frac{1,25^2*5^2}{1^2}$=1,56*25=39 trials.

If we choose a confidence level of 95%, the required minimum number of trials increases because the Student's criterion becomes t=2. In this case, for speed distribution analysis: $n_v=\frac{2,0^2*6^2}{1^2}$ =144 and for time distribution analysis: $n_t=\frac{2^2*5^2}{1^2}$ =100 trials.

If we reduce the measurement accuracy to Δ=2km/h and Δ=2min, while keeping other parameters the same, the minimum required number of trials decreases accordingly: n_v=36 trials, n_t=25 trials. It should also be noted that for our conducted experiments, the calculation values were taken according to Variant I, i.e., α=85%, t=1.25, Δ=1km/h, and Δ=1 min.

Conclusions

When experimentally studying the patterns of vehicle movement under various road conditions, it is essential to determine the size of the set of controllable and measurable variables acting on the driver–vehicle–road–environment (DVRE) system. The range of variation of the variables should be sufficient to reveal noticeable changes in the studied object. At the same time, the variation should be small enough that the regularities of the changes in the studied object can be described using a linear function. To ensure the compactness of the experiment and the efficiency of the results, the sequence of variable values should be determined in advance. Two approaches are possible here: Sequential Plan Experiment – In this approach, the experiment starts from one extreme value of the variable and proceeds to the other extreme. This method is suitable for objects that depend on several controllable and measurable variables. Depending on the number of such variables, two-factor, three-factor, or higher-order experiments can be conducted, in which one factor is varied while the others are reliably stabilized. Subsequently, the second factor is varied while the remaining factors remain stabilized, and so on. This is the classical sequential plan for multi-factor experiments. Randomized Plan Experiment – When it is impossible to reliably stabilize some of the factors acting on the studied object because they are uncontrollable, it is advisable to select variable values randomly across the entire range. Random variation of the variable protects the experiment from the influence of poorly stabilized factors. For reliable and convincing results, it is necessary to determine in advance the required number of trials and measurement accuracy. Conducting experimental studies on road factors is advisable when the traffic load level does not exceed 0.6, i.e., when a capacity reserve of at least 40% is ensured. Otherwise, high traffic density prevents the influence of road factors on vehicle movement modes from being observed. When the load level is below 0.6, it is possible to use the so-called "normal" distribution law for planning experiments and analyzing the obtained data. The confidence level of the trials is chosen using the Student's criterion. A level of 85% or 95% ensures that errors occur in only 15% or 5% of cases, respectively. Using this criterion, the required number of trials is determined. If necessary, confidence levels of 99% or 99.7% can also be ensured, but this significantly increases the number of trials. Based on our many years of practical experience in conducting experiments, it is advisable in road studies to use confidence levels of 85% and 95%.

References

1. M. Tsikarishvili. Fundamentals of Engineering and Scientific Research. Publishing House "Technical University", Tbilisi, 2021, 152 pp.
2. M. Okroshvili. Fundamentals of Scientific Research. Tbilisi, 2009, 131 pp.
3. V.V. Nalimov. Theory of Experiment. "Nauka" Publishing, Moscow, 1991, 205 pp.
4. V. Sidenko, I. Grushko. Fundamentals of Scientific Research. "Vyshcha Shkola" Publishing, Kharkiv, 1997, 198 pp.
5. K. Mchedlishvili, M. Siradze. Some Features of Engineering Calculations for Road Traffic Regulation. Collection of Works of the Georgian Automobile and Road Institute, No. 3, Tbilisi, 2007, pp. 146–149.
6. K. Mchedlishvili, Z. Bogvelashvili, V. Gabiashvili. Investigation of Traffic Flow Density. Collection of Works of the Georgian Automobile and Road Institute, No. 3, Tbilisi, 2007, pp. 61–65.

Numerical Solution of the Thermally Isolated Crack Problem Using Singular Integral Equations

Gela Matcharashvili
Technical University of Georgia, M.Kostava st 77, Tbilisi 0159, Georgia.
Macharashviligela22@gtu.ge

DOI: https://doi.org/10.52340/building.2025.72.02.12

Abstract The paper discusses the numerical solution of the thermally isolated crack problem using singular integral equations. A circular crack is given in an infinite body, on which the temperature distribution function is known. Determination of the intensity coefficients for stress distribution in a small region near the crack tips is based on a first-kind singular integral equation, which is solved using Markov-type quadrature formulas. The values of stresses in the vicinity of the crack are determined by Cauchy-type integrals; for their computation Professor M. Kublashvili's quadratic formula is used. A specific test problem is discussed. The program "Mathematika" has been compiled in a symbolic language.

Keywords: Thermal Insulation Crack, Singular Integral, Numerical Solution, Harmonic function, Algorithm.

Introduction

The real strength of solid bodies essentially depends on real structural defects. In real materials, there always exist numerous microdefects of various types; under the action of an applied load, their growth in the direction of defect extension gives rise to cracks, which ultimately result in local or complete fracture of the body. As experience shows, this phenomenon is especially characteristic of brittle or quasi-brittle deformable solids.

The study of strength issues for structural elements and cracked structures is of great interest to many well-known researchers.

Many monographs are devoted to the theory of brittle fracture of solids: N. Morozov [1], V. Panasyuk, S. Savruk, A. Datsyshyn [2], V. Panasyuk [3], G. Cherepanov [4], N. Muskhelishvili [5], L. Sedov [6]. A broad review of these works is presented in the monograph [6]. In these works, one of the most important lines of research is accounting for the redistribution of stresses in bodies when cracks and holes arise in them.

Main body

In the present work, numerical solutions of crack problems are studied using a singular integral equation. In particular, the numerical solution of the thermally isolated crack problem is considered.

Let an infinite body contain a thermally isolated crack along a segment. Assume that, in the body without the crack, the temperature distribution is described by a given harmonic function. Then the total temperature can be represented in the following form:

$$T(x,y) = t_0(x,y) + t(x,y), \tag{1}$$

where is the disturbed temperature field caused by the crack. Since the crack is thermally isolated, the following condition holds on its boundary [2]:

$$\frac{\partial T^+}{\partial y} = \frac{\partial T}{\partial y} = 0, \quad |x| < a, y = 0, \tag{2}$$

which, taking (1) into account, can be written as:

$$\frac{\partial t^+}{\partial y} = \frac{\partial t^-}{\partial y} = -\frac{\partial t_0}{\partial y} = \varphi(x), |x| < a, y = 0 \tag{3}$$

From the condition of temperature continuity at the crack tips it follows that:

$$t^+(x,0) = t^-(x,0),$$

when $x = \pm a.$ (4)

Thus, the problem reduces to determining a harmonic function that vanishes at infinity and satisfies conditions (3) and (4).

Represent the disturbed temperature in the following form:

$$t(x, y) = \operatorname{Re} f(z), \quad (5)$$

where $f(z)$ is any piecewise holomorphic function. Then:

$$\frac{\partial t}{\partial x} = \operatorname{Re} F(z); \frac{\partial t}{\partial y} = -\operatorname{Im} F(z), \quad F(z) = f'(z) \quad (6)$$

Let us also introduce the distribution function. Therefore, the stress distribution in a small neighborhood of the crack tip will be known if the stress intensity coefficient is determined. Hence, determining the intensity coefficients $k_1^{\pm}$ and $k_2^{\pm}$ is of essential importance:

$$\psi(x) = \frac{1}{2}\left[t^+(x,0) - t^-(x,0)\right], \quad |x| < a, \quad (7)$$

which describes the temperature jump when crossing the crack line. As is known [2], for $\psi(x)$ one obtains a first-kind singular integral equation:

$$\frac{1}{\pi}\int_{-a}^{+a} \frac{\psi'(t)dt}{t - x} = \varphi(x), \quad |x| < a \quad (8)$$

with the additional condition:

We can obtain a numerical solution of the boundary-value problem (8) and (9) using the algorithm constructed by Zurab Kapanadze:

$$\int_{-1}^{+1} \rho(t) \frac{\phi(t) - \phi(x)}{t - x} dt \approx \sum_{k=1}^{n} A_k \frac{\phi(t_k) - \phi(x)}{t_k - x} (-1 < x < 1) \quad (10)$$

It is implied that $\varphi(t)$ possesses the corresponding smoothness; moreover, as $t_k = x$, in expression (10) the corresponding limit is understood. When $\varphi(t)$ is a $\leq 2n$ polynomial, it is clear that for any $x \in (-1; +1)$ the given quadrature formula is exact; and if the values in (10) are chosen so that the equality holds:

$$\int_{-1}^{+1} \rho(t) \frac{dt}{t - x} - \sum_{k=1}^{n} \frac{A_k}{t_k - x} = 0, \quad (11)$$

then, for the corresponding values of x (by condition (11)), for the following singular integral:

$$\int_{-1}^{+1} \rho(t) \frac{\phi(t)}{t - x} dt (-1 < x < 1)$$

we obtain the quadrature formula:

$$\int_{-1}^{+1} \rho(t) \frac{\varphi(t)}{t - x} dt \approx \sum_{k=1}^{n} A_k \frac{\varphi(t_k)}{t_k - x} (-1 < x < 1), \quad (12)$$

Quadrature formulas of this structure, known in the literature as Gaussian quadrature formulas for singular integrals, are determined completely unambiguously for a given $\rho(t)$ by the values of the $\{x_k\}_{k=1}^{n-1}$ singularity points. From this it follows that the number of values of the singularity parameter x for which the highest algebraic degree of accuracy of formulas of the form (12) is achieved is strictly limited.

In this regard, considering the practical effectiveness of quadrature formulas that have a relatively high degree of accuracy, it is natural to attempt, to some extent, to increase the number of such singularity points x. In relation to formulas of the type (12), this may

be realized at the expense of some reduction in accuracy, but in such a way that the resulting quadrature formulas still have a significantly higher accuracy than the interpolation-accuracy formulas that are used much more often (or formulas close to them). As numerical experiments show, as the value of r is gradually decreased within given bounds, we obtain quadrature formulas with somewhat reduced, yet still near-Gaussian accuracy.

In constructing the most effective high-accuracy formulas for singular integrals of the form (12), computational experiments play a very essential role. In this context, it should once again be noted that the known effectiveness of using increased-accuracy quadrature formulas for singular integrals is confirmed by the numerical solution of problems related to solving integral equations containing Cauchy principal value singular integrals.

In (6), the function $F(z)$ has the following form:

$$F(z)=\frac{F^*(z)}{\sqrt{z^2-a^2}}=\frac{1}{\pi i\sqrt{z^2-a^2}}\int_{-a}^{+a}\frac{\sqrt{a^2-t^2}\varphi(t)dt}{t-z}, \qquad (13)$$

where:

$$F^*(z)=\frac{1}{\pi \mathrm{i}}\int_{-a}^{+a}\frac{\sqrt{a^2-t^2}\varphi(t)dt}{t-z}$$

Knowing what the function $F(z)$ is, from relation (6) we determine the disturbed temperature $t(x,y)$.

For a fixed point z, we can compute the integral by an ordinary quadrature formula, but the order of accuracy decreases substantially as the point approaches the boundary points of $[-a,+a]$ (especially when $z\to\pm a$).

We compute the $F^*(z)$ integral using the quadratic formula constructed by Professor Murman Kublashvili [7]:

$$F^*(z)\approx F_n^*(z)=F^*(1;z)L_v(\varphi;t_0)+p_{v-10}(t_0;z)\frac{\varphi(\tau_{v-1})-\varphi(t_0)}{\tau_{v-1}-t_0}+[p_{v-11}(t_0,z)+p_{v0}(t_0,z)+p_{V1}(t_0,z)+$$

where:

$$+p_{v+10}(t_0,z)]\frac{\varphi(\tau_{v+1})-\varphi(\tau_v)}{\tau_{v+1}-\tau_v}+p_{v+11}(t_0,z)\frac{\varphi(\tau_{v+2})-\varphi(t_0)}{\tau_{v+2}-t_0}+\sum_{\sigma\neq v\pm1}^{n}\sum_{k=0}^{e}p_{\sigma k}(t_0,z)\frac{\varphi(\tau_{v+1})-\varphi(t_0)}{\tau_{v+k}-t_0},$$

$$p_{\sigma k}(t_0,z)=\frac{1}{\pi i}\int_{\tau_\sigma\tau_{\sigma+1}}\frac{\sqrt{(t-a)(b-t)}(t-t_0)}{t-z}l_{\sigma k}(t)dt$$

$(\sigma=1,2,\cdots,n)$.

Table 1 presents an approximate computation table for the integral $F(z)$ using the algorithm given above, for different values of in the neighborhood of the point $z=\pm1$, when $\varphi(t)=\mathrm{Re}(t)+\mathrm{Im}(t)$.

Table 1

n	z	$F(z)$	$F_n(z)$	$R_n(z) = F(z) - F_n(z)$
10	$-1+0.005i$	$3.60173+3.46915i$	$3.8148+3.66829i$	$0.21307+0.19914i$
10	$1+0.005i$	$-3.60173+3.46915i$	$-3.81848+3.66829i$	$-0.21307+0.19914i$
20	$-1+0.005i$	$3.60173+3.46915i$	$-3.69248+3.52953i$	$0.09075+0.06038i$
20	$1+0.005i$	$-3.60173+3.46915i$	$-3.69248+3.52953i$	$-0.09075+0.06038i$
30	$-1+0.005i$	$3.60173+3.46915i$	$3.69248+3.52953i$	$0.04035+0.09338i$
30	$1+0.005i$	$3.60173+3.46915i$	$-3.69248+3.52953i$	$-0.04035+0.09338i$
50	$-1+0.005i$	$3.60173+3.46915i$	$3.63742+3.45305i$	$0.03569-0.01610i$
50	$1+0.005i$	$-3.60173+3.46915i$	$-3.63742+3.45305i$	$-0.03569-0.01610i$

Thus, as can be seen from the table, by means of the above algorithm $z = \pm 1 + 0{,}005i$, at special points (the crack ends) for $n = 50$ an accuracy order of 10^{-2} is achieved.

Conclusion

Thus, the considered thermally insulated crack problem is reduced to a first-kind singular integral equation, in which the singular integral is replased by a numerical calculation scheme developed by us , distinguished by the simplicity of calculations and the relatively high accuracy of the obtained results (Gaussian- type accuracy) as confirmed by the results presented in the table.

References

1. Morozov, N.F. *Mathematical Questions of Crack Theory.* Moscow: "Nauka", 1984, 255 p.
2. Panasyuk, V.V., Savruk, M.P., Datsyshyn, A.P. *Stress Distribution Near Cracks in Plates and Shells.* Kyiv: Naukova Dumka, 1976, 443 p.
3. Panasyuk, V.V. *Limit Equilibrium of Brittle Bodies with Cracks.* Kyiv: "Naukova Dumka", 1968.
4. Cherepanov, G.P. *Mechanics of Brittle Fracture.* Moscow: "Nauka", 1974.
5. Muskhelishvili, N.I. *Some Basic Problems of the Mathematical Theory of Elasticity.* Moscow: Nauka, 1966, 707 p.
6. Sedov, L.I. *Continuum Mechanics,* Vol. 2. Moscow: "Nauka", 1973.
7. M. Kublashvili. *Development of Methods for Studying the Stress–Strain State and Fracture Processes of Bodies with Cracks Using the Method of Singular Integral Equations,* Doctoral Dissertation, Tbilisi, 2004.

A New Structural System of a Transformable Guiding Bridge for Extreme Conditions

Giorgi Sarishvili
Georgian Technical University, M.Kostava st 77, Tbilisi 0159, Georgia.
gsarishvili85@gmail.com

DOI: https://doi.org/10.52340/building.2025.72.02.13

Abstract The article presents a new structural system of a transformable guiding bridge designed for the rapid arrangement of temporary transport crossings under extreme conditions. In modern emergency response, rescue, and military operations, damage to transport infrastructure significantly restricts the mobility of personnel and equipment, which necessitates the use of rapidly deployable and operationally flexible bridge systems.

The paper provides a brief review of existing guiding bridge systems and identifies their main limitations, including restricted span length, installation complexity, and the need for additional supporting elements. Based on this analysis, a transformable guiding bridge concept is proposed, which employs temporary transformable supports during the installation stage and transitions into a single-span working configuration during operation.

The article describes the structural solution of the bridge, its main components, and the installation and deployment technology. The proposed system allows rapid assembly and dismantling using minimal technical resources and personnel. The application of transformable temporary supports reduces the need for auxiliary works within the obstacle zone and enhances operational flexibility in complex terrain and environmental conditions.

The obtained results demonstrate that the proposed transformable guiding bridge system represents an effective and promising engineering solution for the development of temporary transport infrastructure intended for use under extreme conditions.

Keywords: transformable guiding bridge, rapid deployment, temporary bridge structures, installation technology, extreme conditions, emergency and military engineering

Introduction

In extreme conditions such as natural disasters, military operations, or large-scale technological accidents, damage to transport infrastructure significantly restricts the movement of civilian, rescue, and military vehicles [8]. Under such circumstances, one of the most critical engineering tasks is the rapid deployment of temporary crossings that ensure safe and operational mobility with minimal time and resource expenditure [1,5].

Rapidly deployable guiding bridges are widely used to address such challenges; however, most existing structural systems exhibit several limitations, including strict constraints on span length, the need for additional supports during installation, significant self-weight, and complex assembly procedures [3,6]. These factors reduce the effectiveness of such bridges in complex terrain and unstable environmental conditions.

This paper presents a new structural system of a transformable guiding bridge that utilizes temporary transformable supports during the assembly stage and transitions to a single-span operational scheme during service. This approach allows for increased span length without the construction of additional permanent piers and significantly reduces installation time and technical resource requirements [4,9].

1. Review of Existing Guiding Bridges and Problem Formulation

Rapidly deployable guiding bridges are essential elements of temporary transport infrastructure used in civilian, rescue, and military operations [2,5]. Their primary purpose is to overcome short- to medium-span obstacles within a limited time using prefabricated structural components.

Most existing guiding bridge systems are based on the sequential installation of steel sections using cranes or specialized transport equipment. Temporary intermediate supports are often required during installation, which increases assembly complexity and dependency on the geometric and geotechnical conditions of the obstacle [3,5].

Some systems incorporate transformable or extendable supports; however, such solutions are typically limited by allowable support height and length, making their application in deep or complex obstacles problematic [6]. Analysis of existing systems indicates the need for a structural solution that reduces installation complexity and enhances adaptability under extreme conditions [9].

2. Structural Design of the Transformable Guiding Bridge

The proposed transformable guiding bridge structural system is based on a modular approach and is designed for rapid installation and multiple reuse [1,6]. The bridge consists of initial, intermediate, and final sections that are prefabricated and adapted to transportation constraints.

A distinctive feature of the system is the integration of transformable temporary supports within the intermediate sections. These supports carry the primary loads during installation and ensure temporary stability of the span structure [4,9]. The adjustable length of the supports enables adaptation to terrain and soil conditions without the need for additional permanent piers (Figure 1).

After completion of assembly, the transformable supports are folded, and the bridge transitions into a single-span operational configuration, reducing redundant structural elements and improving service performance [7].

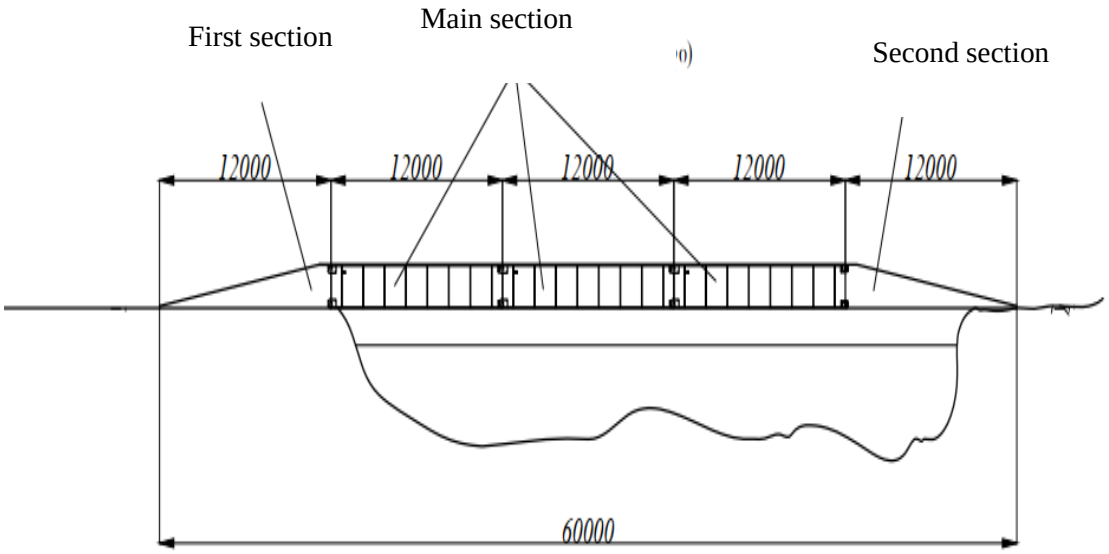

Figure 1 — Structural scheme of the transformable guiding bridge

3. Bridge Assembly and Deployment Technology

The assembly and deployment technology of the bridge is developed based on principles of rapid deployment and operational safety [5,8]. Installation begins with transporting the bridge sections to the obstacle site and placing the initial seion in its working position. Figure 2 — Stages of assembly and deployment of the transformable guiding bridge

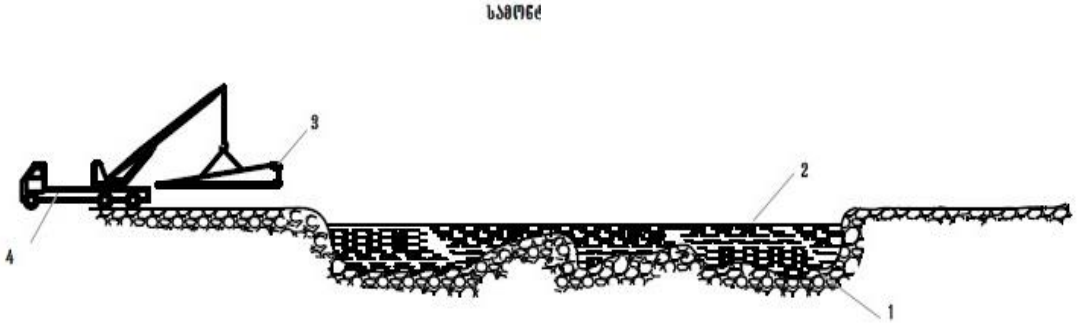

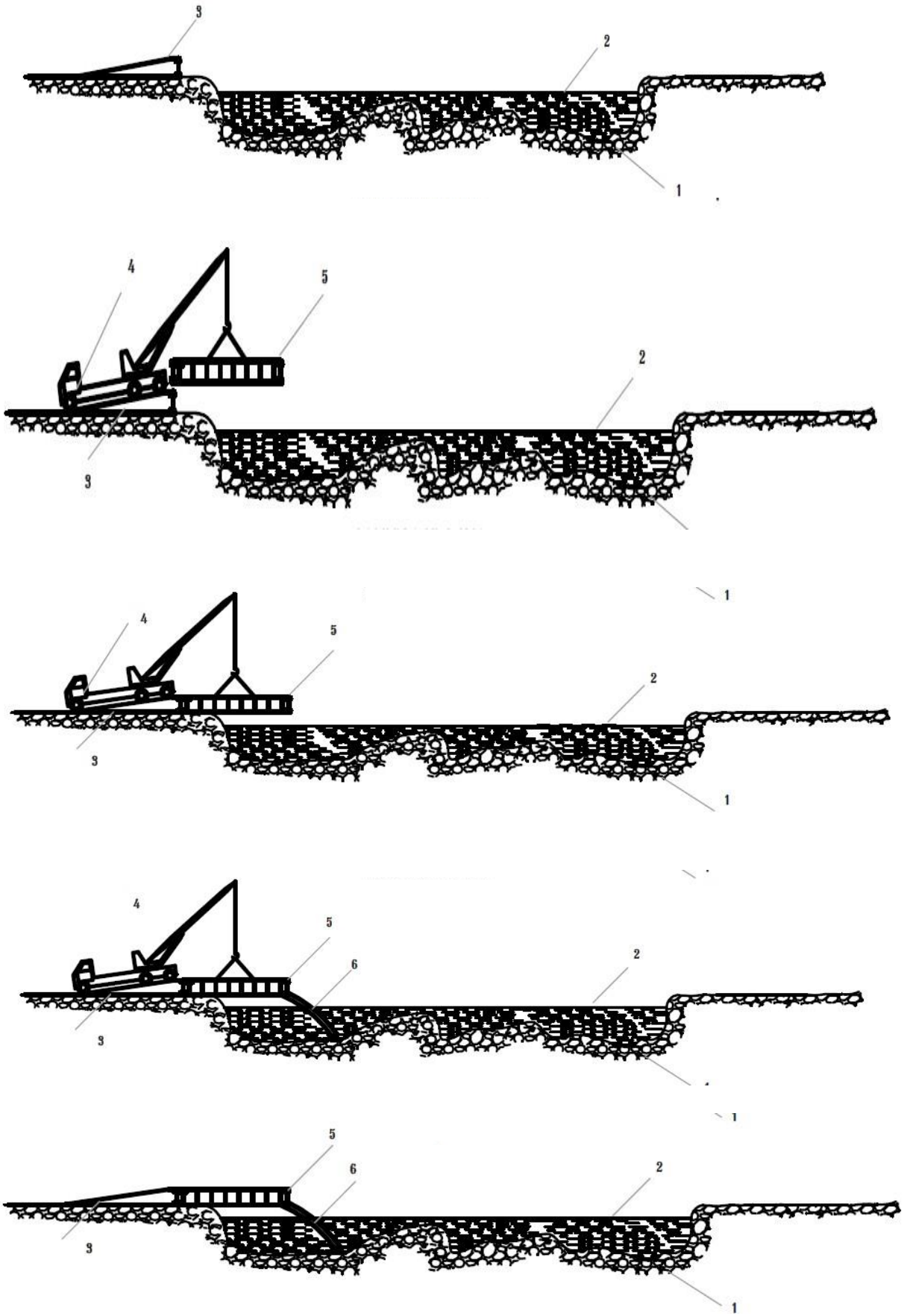
3
2
1
4
5
2
3
1
4
5
2
3
1
4
5
6
2
3
1
5
6
2
3
1

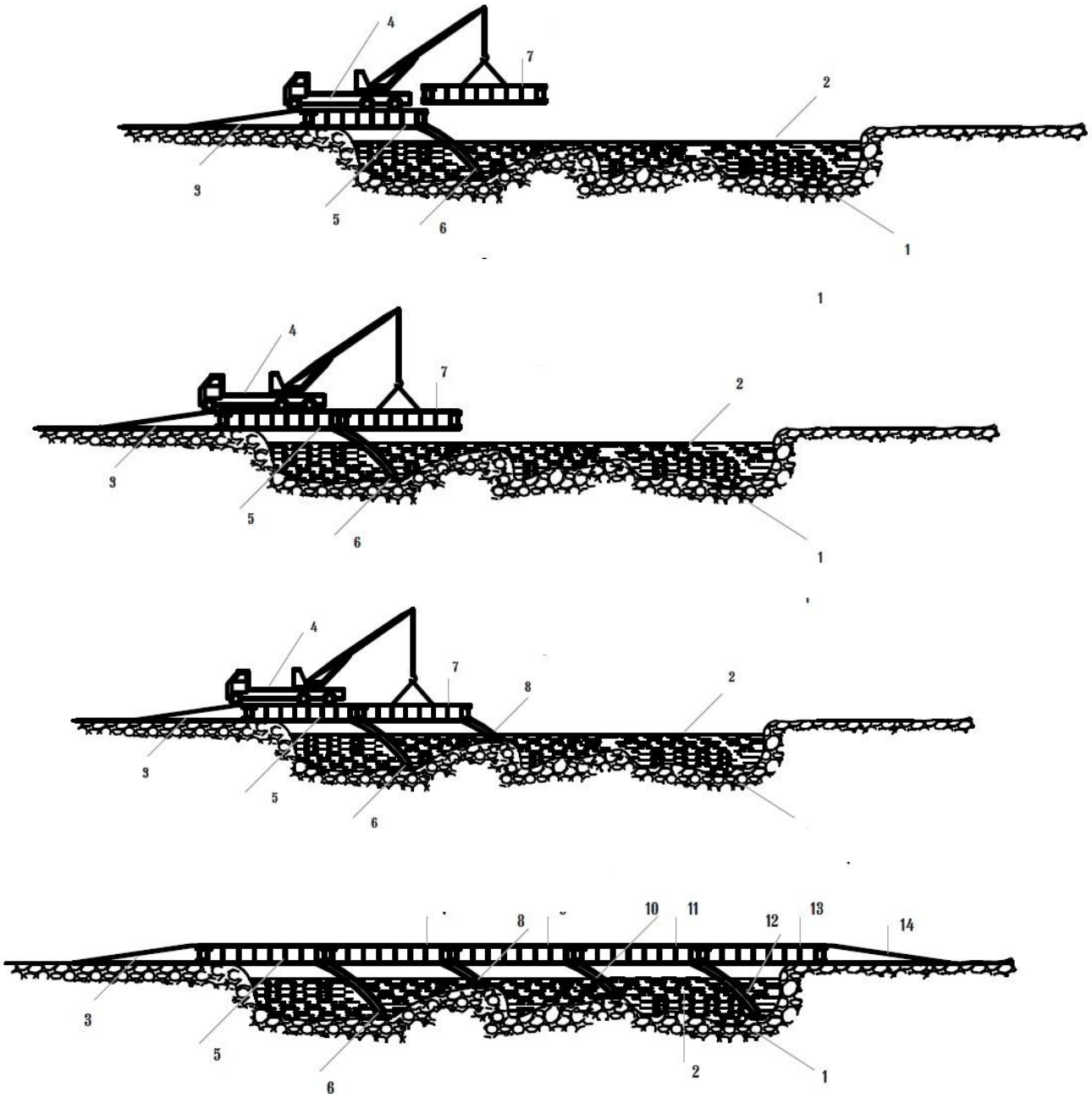

Figure 2 — Stages of assembly and deployment of the transformable guiding bridge
1 Riverbedm , 2 River, 3 Initial section, 4 Crane, 5 Intermediate section No. 1, 6 Deployable transformable support leg No. 1, 7 Intermediate section No. 2, 8 Deployable transformable support leg No. 2, 9 Intermediate section No. 3, 10 Deployable transformable support leg No. 3, 11 ntermediate section No. 4, 12 Deployable transformable support leg No. 4, 13 Intermediate section No

During installation of the intermediate sections, the transformable temporary supports are activated, providing temporary structural stability and reducing dependency on environmental conditions [6,9]. Upon completion of assembly, folding of the supports allows the bridge to transition into a single-span working state.

The proposed technology enables bridge assembly and dismantling within 2–3 hours using a minimal number of personnel [1,5].

4. Advantages and Application Potential of the Proposed System

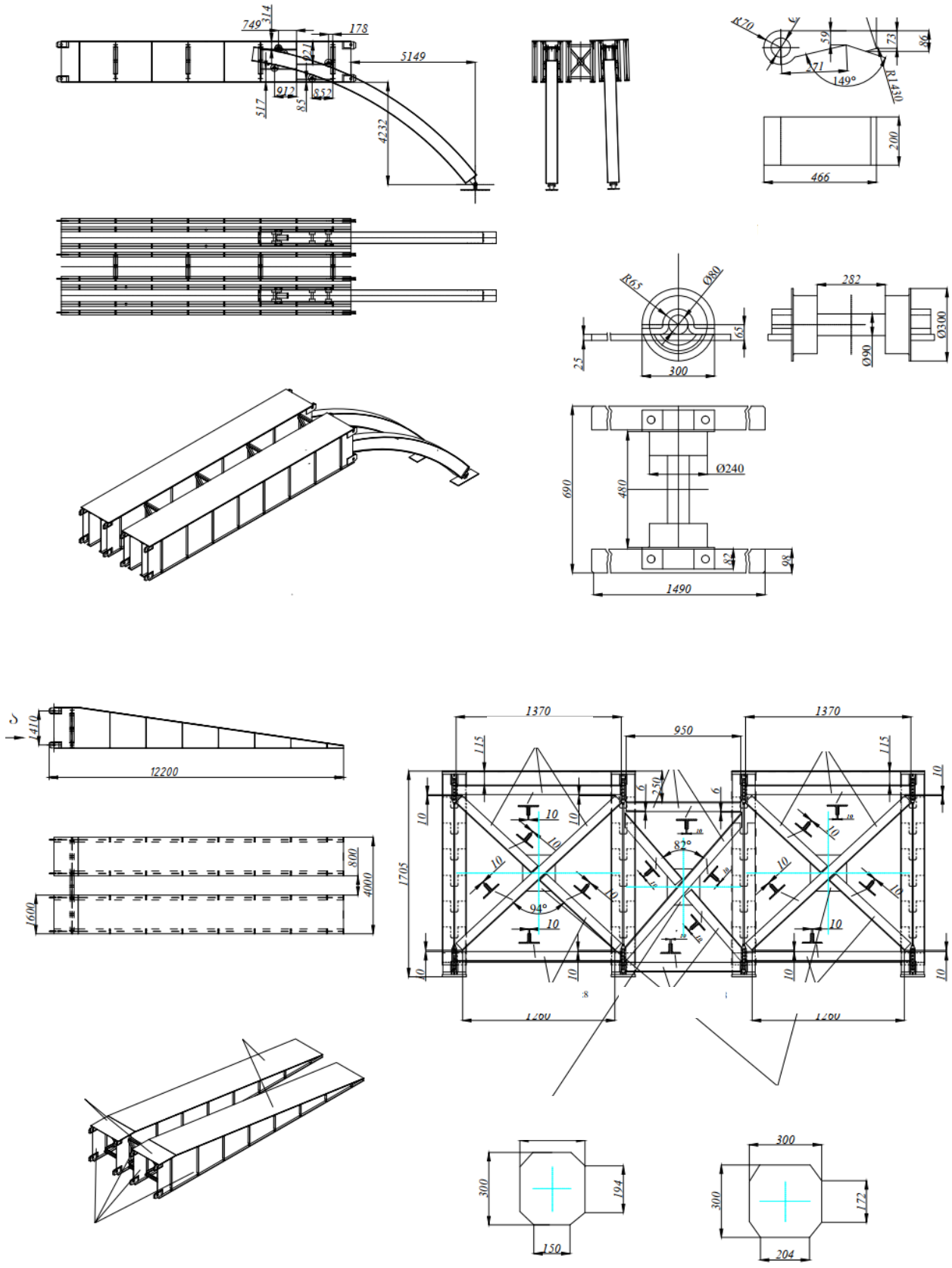

Figure 3 — Operational state of the bridge and performance of transformable supports

The proposed transformable guiding bridge system is characterized by reduced installation time, structural flexibility, and high adaptability to varying terrain conditions [4,9]. The use of temporary transformable supports minimizes the need for additional works within the obstacle zone and enhances system reliability in unstable environments (Figure 3).

The modular nature of the structure and optimized transport dimensions allow for multiple reuse of the bridge in civilian, rescue, and military operations [2,8].

Conclusions

This paper presents a new structural system of a transformable guiding bridge that effectively addresses key challenges in the field of rapidly deployable bridge systems [3,6]. The proposed solution ensures rapid installation, structural flexibility, and reduced operational resource requirements under extreme conditions.

The modular structure and use of transformable temporary supports provide stability during installation without the need for additional permanent piers. Transition to a single-span operational scheme after assembly reduces redundant elements and improves service performance, particularly in scenarios where access to the opposite side of the obstacle is limited or unsafe.

The presented assembly and deployment technology allows for bridge installation and dismantling within a short time using minimal technical resources and personnel. The adaptability of the transformable supports to terrain and soil conditions significantly expands the operational applicability of the system in complex and extreme environments.

The obtained results confirm that the proposed system represents a promising solution for the development of temporary transport infrastructure and creates a foundation for its practical implementation in various operational scenarios [4,9].

References

1. Austroads. *Guide to Bridge Technology: Rapid Bridge Construction*. Sydney, 2018.
2. NATO. *Military Load Classification of Bridges*. STANAG 2021, Brussels, 2016.
3. Chen, W., Duan, L. *Bridge Engineering Handbook*. CRC Press, 2014.
4. Smith, J., Brown, T. Rapid deployment bridge systems for emergency response. *Engineering Structures*, 2019, Vol. 198, pp. 109–120.
5. U.S. Army Corps of Engineers. *Design of Temporary Bridges*. EM 1110-2-2104, 2017.
6. Li, H., Zhao, Y. Modular steel bridge systems for extreme conditions. *Journal of Bridge Engineering*, 2020, Vol. 25(6).
7. EN 1993-2. *Eurocode 3: Design of steel bridges*. CEN, Brussels, 2006.
8. FEMA. *Temporary Infrastructure Solutions in Disaster Zones*. Washington, 2018.
9. Wang, P. Transformable support systems in temporary bridges. *Structural Engineering International*, 2021.

Development of Lightweight Energy-Efficient Construction Blocks Incorporating Recycled Plastic and Alternative Materials

Merab Baratashvili, Tornike Baratashvili.
Akaki Tsereteli State University, Kutaisi, Georgia
merabib@gmail.com

DOI: https://doi.org/10.52340/building.2025.72.02.14

Abstract: This study investigates the formulation, characterization, and performance of energy-efficient construction blocks utilizing recycled plastics combined with alternative raw materials. The objective is to reduce cement consumption, thereby lowering CO_2 emissions, while maintaining structural strength and thermal insulation in compliance with European standards. River sand, crushed brick, basalt aggregate, volcanic ash, and shredded secondary plastics were used. Thermal conductivity, compressive strength, and density tests confirm that the blocks achieve a density of 500–650 kg/m³, compressive strength of 2.2–3 MPa, and thermal conductivity below 0.4 W/m·K.

Keywords: Energy-efficient blocks, recycled plastic, thermal insulation, cement reduction, lightweight construction, sustainable materials

1. Introduction

Concrete and cement-based construction materials are major contributors to global CO_2 emissions. Traditional cement production consumes large amounts of energy and releases significant CO_2 per ton. Reducing cement usage without compromising structural integrity is a key challenge in sustainable construction.

Recycled plastics offer potential for lightweight construction, improving thermal insulation and reducing environmental impact. Combining plastics with secondary aggregates, such as crushed brick, volcanic ash, and basalt, enables blocks with lower density while retaining sufficient compressive strength.

This study focuses on the systematic development of such blocks and provides experimental evaluation of their thermal and mechanical performance.

2. Materials and Methods

2.1 Raw Materials

- **Cement:** Ordinary Portland Cement, reduced proportion (10–15%)
- **Aggregates:** River sand, crushed brick, basalt
- **Volcanic Ash:** Pozzolanic additive to improve microstructure
- **Recycled Plastics:** Shredded secondary plastics, density 150–250 kg/m³, non-toxic, non-reactive

2.2 Block Composition

The proportion of each component was optimized to achieve:

- **Density:** 500–650 kg/m³
- **Thermal Conductivity:** <0.4 W/m·K
- **Compressive Strength:** 2.2–3 MPa

2.3 Experimental Methods

- Blocks were cast in standardized molds and cured for 28 days.
- **Density (ρ):** Measured according to EN 772-13
- **Compressive Strength (σ):** Tested according to EN 1015-11
- **Thermal Conductivity (λ):** Measured with a heat flow meter method

3. Results and Discussion

3.1 Material Performance

- Recycled plastics reduced the overall weight, allowing block density as low as 500 kg/m³.
- Cement reduction by 40–50% did not compromise compressive strength.

- Thermal insulation improved due to microvoids created by plastics, achieving $\lambda < 0.4$ W/m·K.

3.2 Optimization

- The ratio of volcanic ash to cement was critical for maintaining structural integrity.
- Crushed brick and basalt acted as fillers, increasing strength while reducing cement demand.

3.3 Environmental Impact

- Cement reduction leads to lower energy consumption and CO_2 emissions.
- Utilizing recycled plastics diverts waste from landfills, promoting circular economy principles.

Composition and Properties of Blocks **Table 1**

component	Proportion %
Crushed Brick	20–25
Cement	10–15
Crushed Brick	20–25
Basalt	10–15
Volcanic Ash	10–15
Recycled Plastic	15–20
Density (kg/m³)	500–650
Compressive Strength (MPa)	2.2–3
Thermal Conductivity (W/m·K)	<0.4

mparative Performance **Table 2**

~Type of Block	Density (kg/m³)	σ (MPa)	λ (W/m·K	Cement Reduvti
Conventional	1800	12-15	1.2	0
Proposed	500-650	2.2-3	<0.4	40-50

figure 1. Experimental setup with embedded temperature sensors (place photo here)

Figure 2. Block structure

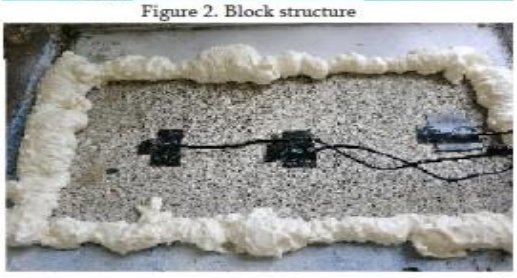

Figure 3. Block hermetically attached to the stand

4. Mathematical logarithm of block mix fraction optimization

The starting parameter in the research was the heat transfer coefficient, the maximum energy-efficient norm of which is determined by the Government Resolution No. 354. In the manufacture of secondary plastic blocks, in order to ensure the strength of lightweight blocks, we used a large 40% dose of cement. To reduce the specified dose, we added various inert materials to the mixture during the manufacture of the block, which increased the volumetric weight of the block mixture, and this addition, in turn, allowed us to reduce the proportion of cement. River sand, quarry basalt-containing gravel were used as additional admixtures. Residual slag from the factory's blast furnaces, porous light admixture accompanying coal, volcanic ash, crushed brick mass, and residual secondary raw materials accumulated over decades at the lithophone factory. The raw materials of the Gumbri mines, which were sent to Azerbaijan for oil refining, were tested on a stand at high temperatures, the raw materials from the mine were decomposed under the influence of a temperature of 53 for 15 minutes. When compiling the material proportions, we took into account two crucial parameters: the heat transfer coefficient and the strength of lightweight concrete. After completing the studies, it was determined that when preparing the mixture using the presented materials, the block made of the finished mixture fully met the specified indicators. In order to correctly describe the specified proportion, the logarithm of the mathematical description of the process was used. The logarithmic relationship between density and thermal conductivity has the form:

$\lambda \to aL_n(\rho) - b$

where; a, b are coefficients whose values are determined empirically:

$a = 0.02, b = -0{,}05$

Accordingly:

$\lambda \to 0.02L_n(\rho)$ -0.05

Mathcad It allows the ability to present the characteristics of materials in a tabular form using the above logarithm.

Table 3. Relationship between density and heat transfer

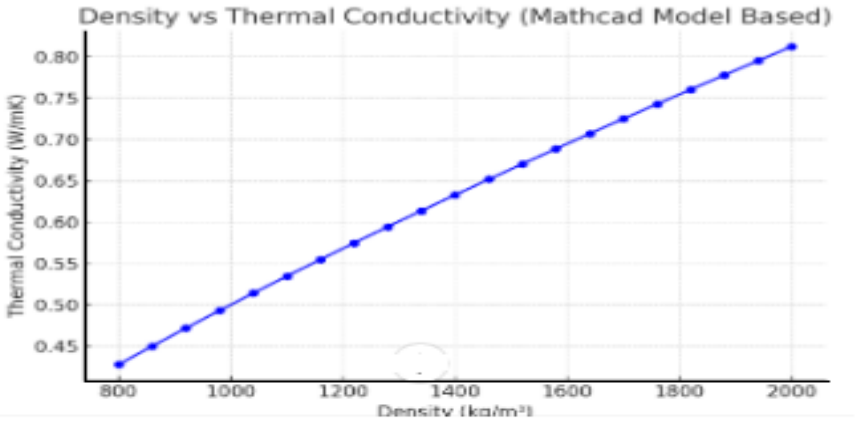

Diagram 1. Relationship between density and thermal conductivity

Density of the mixture $(kg \cdot m^3)$	Thermal conductivity $\lambda(W/m \cdot k)$
800	0.19
1000	0.22
1500	0.30
2000	0.36

Diagram 1 presents a graphical representation of the relationship between thermal conductivity and densityDependence. Through a mathematical optimization model, it is possible to determine the required parameters in order to provide the desired, specified characteristics according to the resolution. C $, P, F$ The corresponding indicators for the optimal proportion of plastic, cement and filler material. $U \leq$ Targeted heat transfer and $\rho \geq$ Minimum allowable strength of lightweight blocks.

$\log(U) \rightarrow a \cdot \log(C) + b \cdot \log(p) + c \cdot \log(F)$

Where:

a, b, c

The coefficients determining the physical and mechanical properties of a material are,

U - The heat transfer coefficient is.

C, P, F -It is an indicator of the percentage of cement plastic and filler material.

$\rho = k \cdot C + m \cdot P + n \cdot F$

Where: k, m, n Relevant materials

$k = 5.0, m = 2.0, n = 8.0$

The results obtained for a specific case are presented in Table 5.

Sample	C(%)	P(%)	F(%)	Density $\rho, kg \cdot m^3$
Volcanic ash	30	10	60	840
Quarry gravel with basalt	25	15	60	820
River sand	35	10	55	860

5.Conclusion

The study demonstrates that integrating recycled plastics and secondary aggregates in construction blocks:

- Achieves lightweight, energy-efficient materials
- Reduces cement usage and associated CO_2 emissions
- Maintains compressive strength and complies with European thermal standards
- Supports sustainable building practices and circular economy principles

References

1.Smith, J., et al., "Recycled Plastics in Construction Materials," *Construction and Building Materials*, 2023.

2.European Committee for Standardization, "EN 998-1:2016 Specification for Mortar and Masonry Units," 2016.

3.Brown, A., "Lightweight Concrete with Waste Materials," *Journal of Sustainable Construction*, 2022.

4.Zhao, X., "Thermal and Mechanical Properties of Polymer-Modified Blocks," *Materials Today*, 2021.

Prefabricated Reinforced Concrete Structures – Innovation in Modern Construction

Giorgi Gogoladze
Technical University of Georgia, M.Kostava st 77, Tbilisi 0159, Georgia.
Gogoladze.giorgi24@gtu.ge

DOI: https://doi.org/10.52340/building.2025.72.02.15

Abstract Prefabricated reinforced concrete structures represent a significant innovation in modern construction, responding to the growing demand for speed, quality, sustainability, and economic efficiency. This paper examines the development, principles, and advantages of prefabricated reinforced concrete systems, emphasizing their role in contemporary civil engineering. The study outlines the historical evolution of prefabrication, describes its technological and geometric characteristics, and compares prefabricated systems with traditional monolithic construction. Special attention is given to construction speed, quality control, structural performance, and environmental sustainability. The integration of advanced design tools such as CAD and BIM, along with modern jointing and hybrid construction techniques, is discussed as a key factor in improving structural reliability and precision. Global case studies and practical applications demonstrate the successful use of prefabricated reinforced concrete in residential, industrial, and high-rise buildings. The paper also highlights the growing relevance of prefabricated systems in Georgia, where industrial construction is gaining momentum. Overall, prefabricated reinforced concrete structures are presented as a forward-looking solution that supports efficient, durable, and environmentally responsible construction in the 21st century.

Keywords: Prefabricated reinforced concrete; Precast construction; Modular building systems; Sustainable construction; BIM and CAD technologies; Industrialized construction; Structural efficiency; High-

Introduction

The rapid pace of modern construction demands new, flexible, and efficient technologies. Fast construction, energy efficiency, and sustainable architecture have become standard today. Prefabricated reinforced concrete structures attract special attention as an innovative approach, combining industrial precision with the dynamism of the construction process.

Prefabricated reinforced concrete structures are considered one of the most significant achievements in modern civil engineering. The principle involves the pre-production of individual concrete elements in controlled environments and their subsequent assembly on-site. This approach reduces construction time, cost, and ensures standardized high-quality outcomes.

History of Prefabricated Reinforced Concrete

In the early 20th century, architects such as Le Corbusier, Walter Gropius, and Soviet engineers experimented with modular and prefabricated systems.

The development of prefabricated reinforced concrete structures began in the mid-20th century when it became clear that standard buildings required fast, safe, and high-quality solutions. The initial system included simple

blocks, which gradually evolved into modern high-strength panels.

What are Prefabricated Reinforced Concrete Structures?

Prefabricated reinforced concrete structures are factory-made blocks, slabs, columns, or

wall elements that are later assembled on site. This approach reduces construction time, ensures high quality control, and minimizes human error.

Innovative Advantages

Prefabricated reinforced concrete structures differ significantly from traditional monolithic systems in terms of construction speed, cost efficiency, and quality control. While monolithic construction involves on-site formwork, reinforcement, and pouring of concrete, prefabrication allows most of these processes to be completed in a controlled factory environment. This ensures higher precision, minimizes weather-related delays, and provides better surface quality. From a structural standpoint, prefabricated elements can achieve equal or greater strength when designed correctly, as they are produced under optimal curing conditions. However, monolithic systems still have advantages in complex geometry and seismic continuity. In economic terms, prefabrication reduces labor costs and accelerates project delivery, but requires higher initial investment in production facilities and transportation logistics. Therefore, the optimal choice often depends on the project scale, location, and labor conditions.

In terms of performance, monolithic concrete offers continuous structural integrity with fewer joints, which can be advantageous in high-seismic areas. Prefabricated systems, on the other hand, use advanced jointing techniques and flexible connectors that maintain structural safety while enabling rapid assembly. Modern hybrid construction frequently combines both approaches—prefabricated columns and slabs with in-situ connections—to achieve the benefits of speed and structural monolithicity.

- Time efficiency — elements are produced simultaneously with site preparation work.
- High quality and accuracy — factory production ensures uniform standards.
- Eco-friendliness — waste can be recycled during production.
- Economic efficiency — labor costs are reduced, and project completion time is shorter.

Sustainability and Environmental Aspects

Sustainability has become a key consideration in modern construction. Prefabricated reinforced concrete structures play a vital role in reducing the environmental footprint of the building industry. Because elements are produced in factories, material waste can be reduced by up to 30%, and excess concrete or steel can be recycled efficiently. Controlled production also allows precise batching of materials, minimizing overuse and emissions associated with on-site mixing.

Energy efficiency is another strong advantage. Prefabricated panels can be integrated with thermal insulation layers and energy-saving finishes, reducing heating and cooling demands over the building's lifetime. Moreover, the reduced construction time lowers on-site energy consumption and transportation emissions. Some advanced factories now use renewable energy sources and eco-friendly admixtures to further decrease the carbon footprint of production.

From a life-cycle perspective, prefabricated buildings are easier to dismantle, and their components can be reused or recycled at the end of service life. This circular approach aligns with global sustainability goals and contributes to the development of greener cities. The combination of industrial efficiency and environmental awareness positions prefabricated reinforced concrete as a key element of sustainable construction in the 21st century.

Application Areas

Prefabricated reinforced concrete structures are widely used in residential, industrial, and infrastructure projects. Their flexibility and quality allow builders to quickly construct multi-story buildings, industrial facilities, bridges, and sports facilities.

Innovative Technologies

The technological process of producing prefabricated reinforced concrete elements begins with precise design and planning. Computer-aided design (CAD) and Building Information Modeling (BIM) systems are used to generate accurate molds and reinforcement layouts. The process starts with the preparation of steel reinforcement, which is cut, bent, and welded according to design specifications. High-quality formwork is then prepared, ensuring accurate dimensions and surface smoothness.

Design and Geometric Characteristics

Prefabricated reinforced concrete structures are designed based on modular coordination principles. Standard dimensions allow for interchangeability and efficient assembly. Common prefabricated elements include slabs, columns, beams, wall panels, and staircases. These components are typically designed to fit together through specialized joints and connectors that ensure structural stability and alignment.

Designing prefabricated systems requires careful consideration of geometry, load paths, and transportability. Elements must be strong enough to withstand lifting and transport stresses while maintaining precise tolerances for on-site assembly. Joint types vary from dry mechanical connections with steel plates and bolts to wet joints that use high-strength grout or concrete for continuity. Modern 3D modeling tools facilitate detailed coordination between structural, mechanical, and architectural components, ensuring precision during fabrication and erection.

Global Experience

In Europe, Asia, and the USA, prefabricated reinforced concrete structures are widely adopted, including high-rise residential and commercial projects. Hybrid systems combining steel and concrete create practically durable constructions.

Images

Fig. 1 – Factory-made concrete panels

Fig. 2 – Prefabricated elements assembly on site

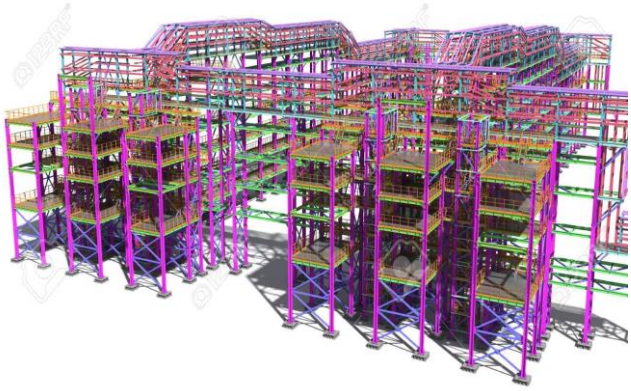

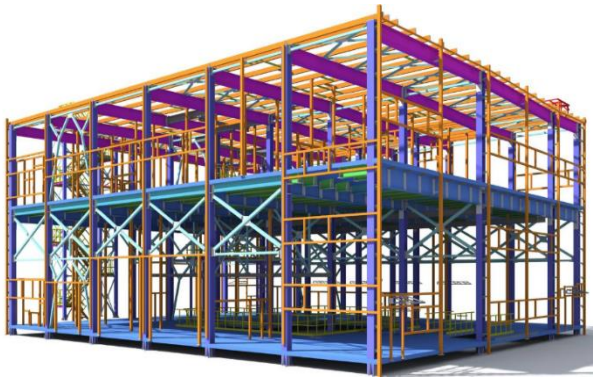

ig. 3 – BIM modeling example

g. 4 – Industrial building with prefabricated elements

Fig. 5 – High-rise building structure

Prefabricated reinforced concrete structures - in residential buildings

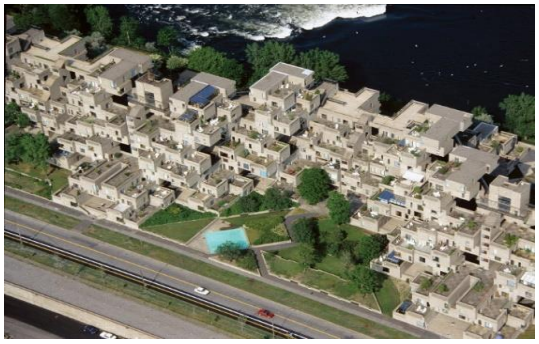

Habitat 67 – Montreal, Canada (Modernized Units in the 21st Century)

Originally built in 1967, however, since the 2000s, some of the modular construction has been renovated and new residential units have been added, using prefabricated reinforced concrete.
Type: Residential complex, modular concrete units.
Significance: Shows that modular concrete is still used in residential complexes in the 21st century.

De Zalmhaven (Rotterdam, Netherlands)
This building was planned to be approximately 215m high and 61 floors high.
The construction process used 100% precast elements – walls, floors, facades, etc.
Construction method: The elements were manufactured in a factory, then lifted by crane, and assembled according to the floors – this significantly reduced on-site work time and emergency installation work.
Key message: This is a modern line that is being used in high-rise buildings with "precast technology" and shows that such a system is already at the forefront.

Mischek Tower (Vienna, Austria)
Located in the 22nd district of Vienna, at Leonard Bernsteinstrasse 8.
Height: approximately 108 m, floors: 36 (+4 basements).
The building is constructed of precast concrete elements, making it one of the first of its kind in the world.
Interesting technical detail: It was built in 1998–1999 and was one of the tallest residential buildings in Austria at the time.
Why it's worth watching: It's a good example of how this type of construction can be used in a high-rise residential project in a European context, and also shows us the combination of sophisticated design and industrial production.

Prefabricated Systems in Georgia

Interest in industrial construction is growing in Georgia. In recent years, local factories have emerged producing pre-stressed concrete elements, panels, and blocks. This trend is especially relevant in industrial and residential buildings where time and resource optimization is crucial.

Conclusion

Prefabricated reinforced concrete structures are not only a technological innovation but also a pathway to the future, where the construction process becomes faster, safer, and more environmentally balanced. Such approaches create innovative architecture that meets the demands of the modern world.

Reference

1. International Federation for Structural Concrete (fib). Prefabricated Concrete Structures. Lausanne: fib, 2022.
2. Neville, A.M. Properties of Concrete. 6th Edition. Pearson, 2012.
3. Smith, R.E. Prefab & Modular Construction. New York: McGraw-Hill, 2019.
4. Bakhtadze, G. Innovative Construction Systems in Georgia. Tbilisi: Technical University, 2021.

Steel Structure Inspection Using a Laser Scanner Device with Finite Element Method

Revaz Sakhvadze, Levan Sturua
Georgian Technical University, M.Kostava st 77, Tbilisi 0159, Georgia.
Sakhvadze.r@gtu.ge
DOI: https://doi.org/10.52340/building.2025.72.02.16

Abstract The following research covers optimal solutions for design of connection joints in metal structures based on digital modeling and 3d scanning devices. The paper discusses the properties of metal as a building material, welds and bolted joints, where to use the FEM finite element method in practical application, as well as the stages of CAD computer modeling. Computer aided design covers the development of geometric shapes in a digital format. The structural model is designed using a portable laser scanning device. One of the joints is selected and a unit of force as a load is applied. The finite element method is the most common tool for solving engineering problems. Problems may concern structural loads, temperature transfer, fluid flow or electromagnetic potential. To solve given issues, finite element analysis involves transforming a large complex system into smaller elements. While it is easier to solve a small element using given variables, it can be solved for a large system.

Key words: CAD, 3D, SCANNER, MESH, CNC, CAM, FEM.

Introduction

Generally, steel structures in construction projects have advantages mostly for its physical and mechanical properties and therefore the ability to solve specific tasks. Steel structures are mostly required for their specific characteristics as a building material over the reinforced concrete. Steel structures and steel as a material could be considered in construction projects because of its weight, rigidity - to maintain strength both in compression and in tension, mobility - to move as a component. Therefore, steel structures in the construction projects were used to reduce the time required to complete the process. Timelines in the construction process, large scale projects, high quality and reliability, budget, aesthetics, these are the reasons to create or select new technologies for manufacturing structural components, ensure transportation of products, and a high level of process organization and automation. In the design of steel structures, it is important to choose proper connection nodes, calculate loads, manufacturing technologies and the use of different configurations. In general, for any form of design it is crucial to define elements and their mutual fastening connections. In reality, a clear boundary between a separate element and separately formed connections is often erased, since functionally they are combined with each other. The process of shaping a structure begins with the selection of elements and connections. The form of a structure is a specific set of many different elements, in a connection with each other, that constitute a certain system. The search for and study of new forms of construction design, today involves a wide range of researchers and specialists. It should be noted that it is the main challenge of the art and science of design. The challenge of designers is to determine not only the optimal form of the structure, but also the best and most acceptable ways of its implementation, of achieving its own form. It is this aspect, the identification of actually possible and accessible ways of shape, that largely serves as the main characters for assessing the quality of the technical solution and the solution of the problem of designing a structure. CAD technologies plays a leading role in construction practice, which facilitates the processes of implementing large-scale projects and additionally creates new opportunities. On the other hand, in modern engineering and technology, it is widespread to use three-dimensional scanning equipment in practice, which allows the conversion of complex and intricate geometric shapes into

digital vector format. The solution of the construction of buildings is a complex process, especially with the adaptation to digital manufacturing technologies, computer modeling and computing systems. Obtaining a geometric form through digital devices and computer modeling reduces the amount of time spent on project implementation. It also facilitates the manufacture of accurate prototypes and makes it possible to achieve different, difficult-to-obtain geometric forms. The capabilities of the hardware devices are always limited, requiring specific knowledge and qualifications depending on application and purpose. Given factors must be taken into account at each stage of project implementation and design.

Main Part

Digital manufacturing is versatile and is commonly used to complete engineering tasks, as well as in medical, biological, chemical and other technical or natural science directions. In construction practice, the use of given method requires certain limitations and restrictions, which can be classified in the following sequence during the design process: 1. Determination and analysis of the capabilities of the material used in the construction process; 2. Determination of the potential of digital production equipment, preparation, modification, equipment, according to the selected material and work specifications; 3. Design of a computer model based on the capabilities of the equipment; 4. Design of a computational structural model, setting specific functional and architectural requirements, checking reliability; 5. Use of a computer aided model CAD for programming digital equipment, writing a path and code for CNC device and digital manufacturing process CAM. Therefore, digital production is preceded by the generation of a computer model. This stage can be completed using various computer programs, directly drawing the geometry of the model in vector format. It is worth noting the existence of digital archives of drawn models and stores where ready-made forms are located. In addition, for our research, we will be able to obtain a model by measuring a physically existing object with a three-dimensional scanning device, during which the ctual forms are automatically converted into vector format. After computer modeling, it is possible to use it not only for the purpose of digital production, but also for the calculation of the structure, by converting it into a digital structural model. The practice of computer calculation of a structural model dates back to the 1960s. Computer modeling, on the basis of which the above-mentioned process and digital production are carried out, has been widely established in engineering since the second half of the 1980s. Scanning devices are based on two methods of obtaining data: 1. Laser Based – which involves sending a set of rays from the device's sensor in the direction of the object and determining the coordinates of the segments that make up the surface on the x, y, z axes through the feedback of the rays from the object; 2. Photogrammetric – this method involves perceiving the contours of the object's surface from different viewing angles using a photoactive sensor and a lens with the help of the focus effect; 3. Combined – when, in addition to determining the geometric shapes of the surface, determining the texture and colors of the surface is also actual. Data can be obtained in different sizes, which refers to the resolution of scanning geometric shapes. Objects scanned with high resolution often complicate software processing processes, so it is common to divide the object into sections and perform work in parts, depending on the capabilities of the computer. The study uses the Sense 3D scanner (Figure 1), which is based on the photogrammetric method of data acquisition.

Fig. 1. Sense 3D Scanner

The object choosed for scanning and research is a steel joint connection with traverses (Figure 2).

Fig. 2. Object for 3D Scanning

To create a high-precision model, it is recommended to scan the object several times, and then integrate each of them into the appropriate computer program (Figure 3). A shape decoding algorithm can be used in the integration process. The aforementioned algorithm decodes such primary figures as an ideal surface cone, cylinder, cube, etc. The system consisting of combinations of the aforementioned figures can be compared with the actual scanned model, which allows us to determine deviations from ideal shapes.

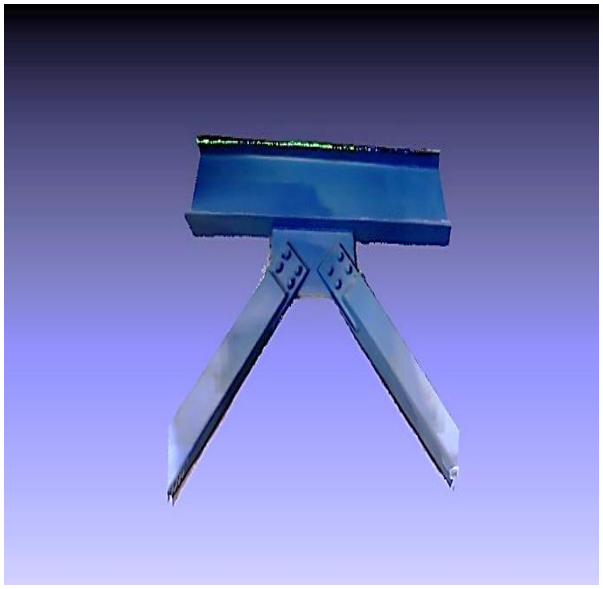

Fig. 3. Scanned Object

To build a digital computational model, used the computer aided software - Solidworks, where it is possible to both model and assign appropriate physical and mechanical characteristics to the components of the model. First, the model is built using an actual data from obtained by 3D Scanner device (Figure 4).

Fig. 4. Computer Aided Model

It is important to assign physical and mechanical characteristics directly to the scanned object (Figure 5). For this process, it is necessary to a complete and high-resolution object by scanning, which is achieved by capable computer equipment and a powerful scanning device.

Property	Value	Units
Elastic Modulus	2039420	kgf/cm^2
Poisson's Ratio	0.29	N/A
Shear Modulus	815768	kgf/cm^2
Mass Density	0.00787	kg/cm^3
Tensile Strength	3314.0575	kgf/cm^2
Compressive Strength		kgf/cm^2
Yield Strength	1835.478	kgf/cm^2
Thermal Expansion Coefficient	1.22e-05	/°C
Thermal Conductivity	0.124044	cal/(cm·sec·°C)
Specific Heat	107.075	cal/(kg·°C)
Material Damping Ratio		N/A

Fig. 5. Phisical and Mechanical Properties of Material

After creating geometric shapes, they are transformed into a digital structural model,

each of whose constituent segments is a finite element. The larger the amount for this element (Figure 5), the more difficult the calculation process becomes for a software.

Fig. 6. Body Mesh Prepared for FEA

The geometric shape model is converted into a mesh. Generating the mesh allows for FEA calculations. Each component of the mesh represents a finite element. Finite elements are connected to each other according to physical and mechanical properties of material. Determining physical and mechanical characteristics is necessary to obtain stress-strain values in structural elements (Figure 7), and its connections (Figure 8).

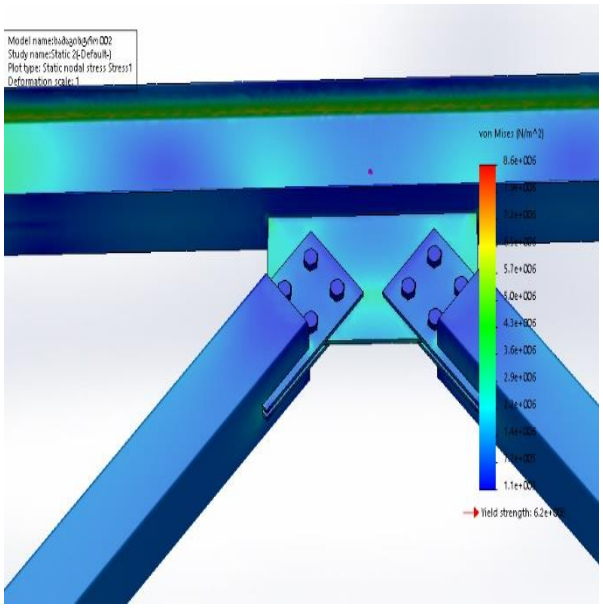

Fig. 7. Stress Distribution with CAD Model

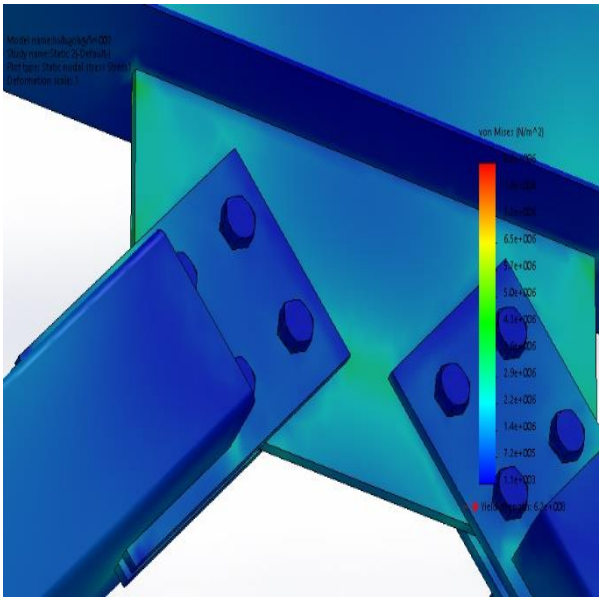

Fig. 8. Bolt Connections

Based on CAD modeling, in addition to defining stress and strain, FEA gives the ability to determine the actual displacement (Figure 9).

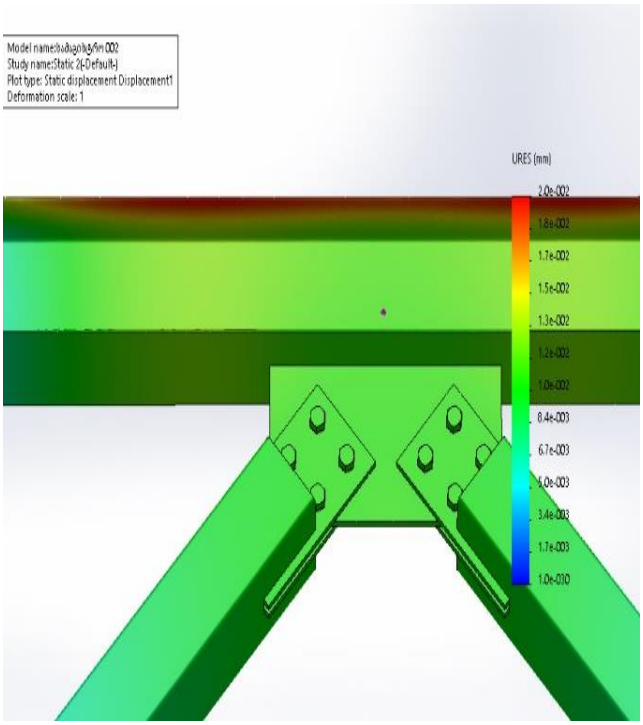

Fig. 9. Actual Displacement

Conclusions

The given method makes it possible to improve the structural model and connection

nodes, in particular, to cut out sections where the stress is insignificant and to reduce the weight of the frame. In the case of solving problems using this method, the created digital models can be used at the level of computer aided manufacturing CAM, which significantly simplifies and speeds up construction processes. Involving digital manufacturing technologies into construction processes significantly reduces not only time spent on completing the tusk but also significantly lowers the costs and expenses on building materials.

Reference

1. Practical Stress Analysis with Finite Elements (3rd Edition) 3rd ed, Bryan J Mac Donald, Glasnevin Publishing, June 22, 2020.
2. PRACTICAL FATIGUE & DURABILITY ANALYSIS, Nitin S. Gokhale, Finite To Infinite, November 9, 2021.
3. Structural Steel Design 6th Edition, Jack McCormac, Stephen Csernak, Pearson, August 3, 2017.
4. Structural Steel Design 1st Edition, Abieyuwa Aghayere, Mercury Learning and Information, May 19, 2025.
5. Schaum's Outline of Structural Steel Design 1st Edition, Abraham J. Rokach, McGraw Hill, January 22, 1991.
6. Structural Steel Design: A Practice-Oriented Approach (2nd Edition), Abi O. Aghayere, Jason Vigil, Pearson, July 23, 2014.
7. Design of Steel Structures 3rd Edition, Jr. Gaylord, Edwin H, McGraw-Hill Publication, September 1, 1991.

The Influence of Pile Length on the Settlement and Internal Forces of a Piled Raft Foundation

Giorgi Bichiashvili
Georgian Technical University, M.Kostava st 77, Tbilisi 0159, Georgia.
bichiarchery@gmail.com

DOI: https://doi.org/10.52340/building.2025.72.02.17

Abstract This study primarily investigates the effect of pile length on the settlement and internal forces of a piled raft foundation, as well as the influence of raft-to-soil contact. The analysis was performed under both static and dynamic loading conditions. The modeling parameters included a fixed pile diameter (D = 0.5 m) and a constant pile spacing (S_p = 4.5D). The pile length was varied (Lp = 28D, 32D, 36D, and 40D). The raft dimensions were 10x10 m with a thickness of 1.00 m. The subsurface conditions were modeled based on a soil profile consisting of six layers: silty sand with traces of clay, silty sand, medium stiff clay, and dense sand. The soil mass was simulated using a semi-infinite element. The analysis was conducted using the finite element software package PLAXIS 3D version 2013, a code for soil and rock analysis. The software was used to determine the bending moment, shear force in the raft, and the settlement magnitude.

Key Findings:

1. **Effect of Pile Length for a Piled Raft Foundation (raft in contact with soil):**
   - **Under static load**, increasing the pile length resulted in a **29% reduction** in raft bending moment, a reduction to **0.5%** in raft shear force, and a **40% decrease** in settlement.
   - **Under dynamic load**, a similar reduction in parameters was observed: bending moment decreased by **29%**, shear force reduced to **0.5%**, and settlement decreased by **40%**.
2. **Comparison of Two Design Models:**
   - The **bending moment** in the raft for the model where the raft is rigidly connected to the piles (no soil contact) is **7% greater** than for the piled raft foundation model (with contact).
   - The **shear force** in the raft for the rigidly connected model is also **2% larger** than for the model with the raft bearing on the soil.
   - The **settlement** for the model with the raft rigidly connected to the piles is **10% higher** than

1. INTRODUCTION

The straining action and the settlement in piled raft foundation are affected by many different factors such as pile length, pile diameter raft thickness, and type of soil but to a varying degree.

2. Analytical Analysis by Finite Element Analysis:

The used computer program was for the proposal of a three-dimensional finite element package of a PLAXIS 3D version 2013 model to simulate the theoretical effect of pile length in pile raft foundation

2.1 Proposed model:

In the present study, a theoretical analysis has been done for a selected site (in a governmental project in Semesta city, Beni-suef, Governorate, Egypt).Fig. (1) illustrates a borehole for the previous site that was chosen to be used in the analysis. The soil consists of four layers and is simulated by a semi-finite element isotropic homogenous elastic material. The analysis program consists of a piled-raft

foundation consisting of 25 piles their diameters are fixed (D = 0.5m) and the spacing between piles is fixed (Sp = 4.5D) and they have various pile lengths (Lp= 28D,32D,36D, and 40D). Analysis carried out on two categories as follows

- rested piled raft
- raft act as a slab connected the

piles The details and variations of these selected parameters are listed in tables from (1) to (3). and figures (2) and (3)

3. Analytical Analysis by Finite Element Analysis:

The used computer program was for the proposal of a three-dimensional finite element package of a PLAXIS 3D version 2013 model to simulate the theoretical effect of pile length in pile raft foundation

3.1 Proposed model:

In the present study, a theoretical analysis has been done for a selected site (in a governmental project in Poti, Georgia). Fig. (1) illustrates a borehole for the previous site that was chosen to be used in the analysis. The soil consists of four layers and is simulated by a semi-finite element

. isotropic homogenous elastic material. The analysis program consists of a piled-raft foundation consisting of 25 piles their diameters are fixed (D = 0.5m) and the spacing between piles is fixed (Sp = 4.5D) and they have various pile lengths (Lp= 28D,32D,36D, and 40D). Analysis carried out on two categories as follows

- rested piled raft
- raft act as a slab connected the

piles The details and variations of these selected

-

parameters are listed in tables from (1) to (3). and figures (2) and (3)

Depth (m)	legend of borehole ■	end of layer	S.P.t or%Rec	un confined QUKN/m²	Description
1					
2		2			Silty sand and trace of clay
3					
4		4			Silty sand
5					
6					
8					
10		12	12	100	medium stiff clay
11					
12					
13					
14					
15					
16					
17					
18					
19					
20					
21					
22		30	33		dense sand
23					
24					
25					
26					
27					
28					
29					
30					

Fig. (1): Borehole Log

N0.	Number of piles	pile diameter (m)	The contact of the raft with the soil	Length Of the piles	Pile spacing	Raft Thickness (m)
1				28D		
2				32D		
3	25	0.5	Rested on the soil	36D	4.5D	1
4				40D		
5						
6			The raft			
7			act as a	28D		
8			slab	32D		
	25	0.5	connected	36D	4.5D	1
			the piles	40D		

Table (2): Properties For Soil Layers

Parameters	Name	Silty sand and traces of clay	Silty sand	Medium to stiff clay	dense sand	unit
Material model	-	**Moher column**	**Moher column**	**Moher column**	**Moher column**	-
Thickness	T	2	2	8	18	m
Young's modulus	Es	7500	8000	3000	15000	kN/m^2
Unit weight	ɣ	17	16.6	17	18	kN/m^3
Poisson ratio	υ	0.3	0.4	0.3	0.25	-
Cohesion	c	25	12.5	30	0	kN/m^2
Friction angle	Ø	25	35	0	37	°

Table (3): pile and raft properties

Parameters	Pile	Raft
Material model	Elastic	Elastic
Types of material	Concrete	Concrete
Diameter (m)	0.5	-
Raft thickness (m)	-	1
Unit weight (kN/m3)	25	25
young's modulus Es (kN/m2)	24*10^6	24*10^6
Poisson ratio (υ)	0.2	0.2

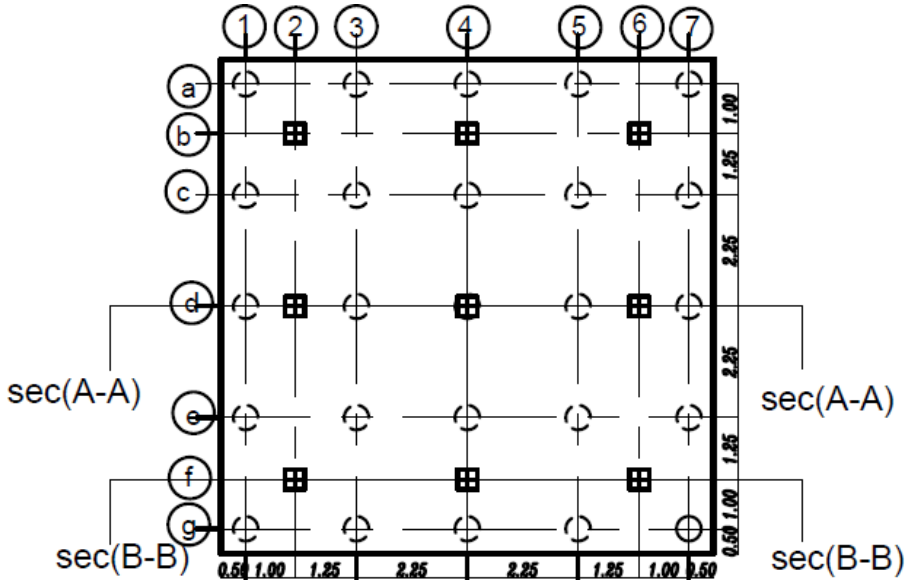

Fig (2) plane of piled raft foundation

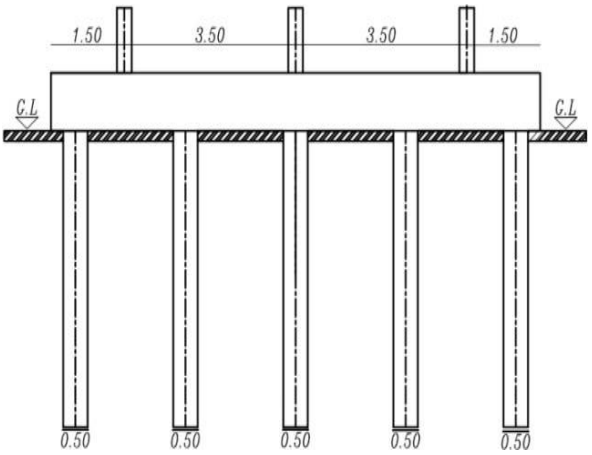

Fig (3) Cross section of piled raft foundation rested on the soil

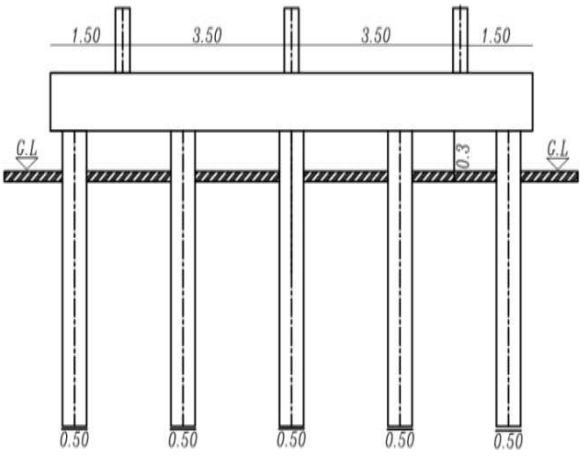

Fig (4) Cross section of piled raft foundation as raft act as slab connected the piles

Finite element model:

Figures (3) and (4) show the cross sections of the piled raft in the two cases rested on the soil and the raft act as a slab connected the piles (Lp=32D, D =0.5 m Sp =4.5D)

3 -Parametric study

The effect of pile length on the following:

i. The settlement of piled raft
ii. The bending moment on the raft
iii. The shear force on the raft

4. 1. Finite Element Results:

The obtained results of selected examples for different cases are shown in figures (6 to 17) as follows:

Figure (6) and (7) shows the bending moment on the raft in the two cases rested on the soil and the raft act as a slab connected to the piles from the soil (Lp = 32D, D = 0.5 m, and Sp =4.5D).

Figures (8) and (9) show the vertical displacement of the soil under the raft in the (x-y) plane (as shading) for the two cases (Lp = 32D, D = 0.5 m, and Sp =4.5D).

Figures (10) and (11) show the vertical displacement of soil under the raft in(x-z) plane (as shading) for the two cases (Lp = 32D, D = 0.5 m, and Sp =4.5D).

Figures (21) and (23) show the shear force on the raft for the two cases (Lp = 32D, D = 0.5 m, and Sp =4.5D

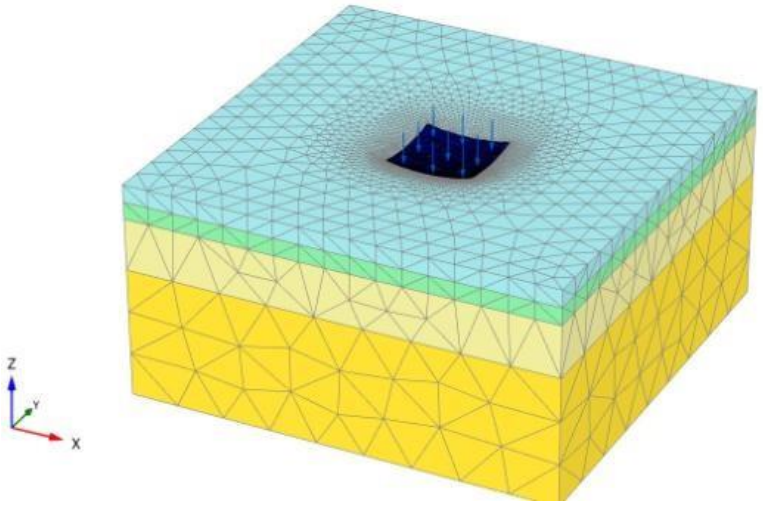

Fig (5) Deformation pattern of the finite element mesh representing the piled raft system with Lp = 16 m.

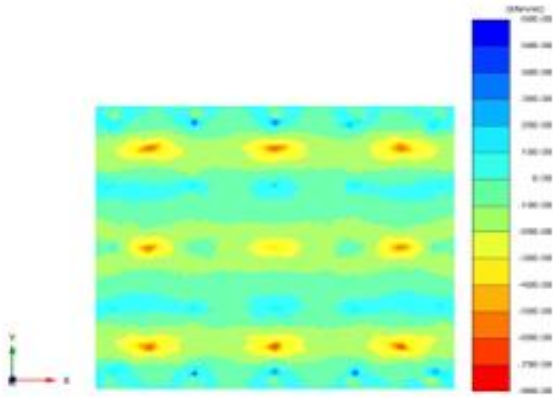

Fig(8) Bending moment in the soil-contacting piled raft (L_D = 32D)

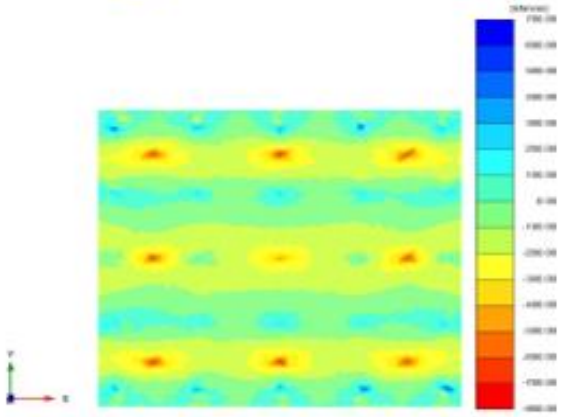

Fig(7) Bending moment in the pile-connected slab (L_D = 32D)

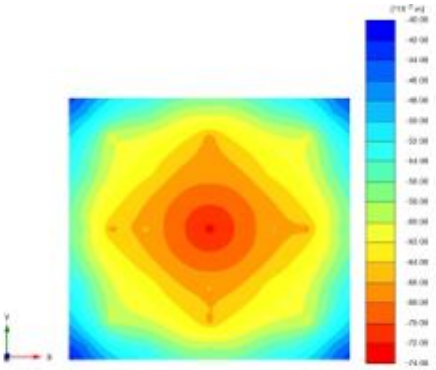

Fig (8) Vertical soil displacement beneath the raft in a soil-contacting piled raft foundation (L_D = 32D)

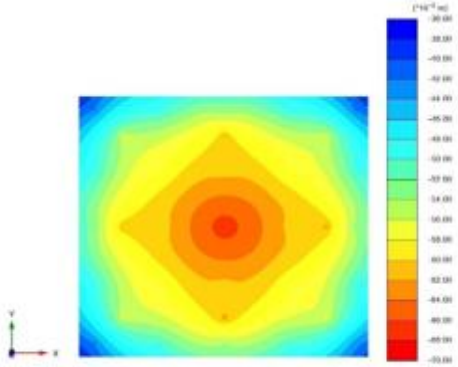

Fig(9) Vertical soil displacement beneath the raft in a pile-connected slab foundation (L_D = 32D)

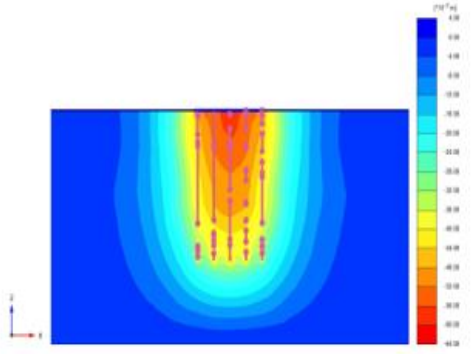

Fig (10) Vertical settlement contours (XZ plane) in the soil for a soil-contacting piled raft foundation (L_D = 32D)

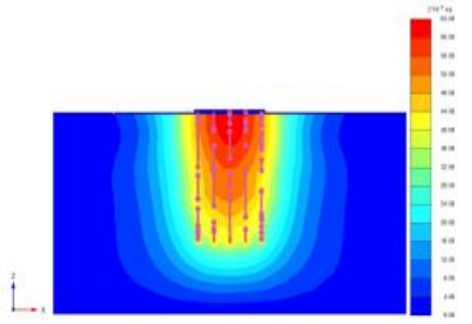

Fig (11) Vertical settlement contours (XZ plane) in the soil for a pile-connected slab foundation (L_D = 32D)

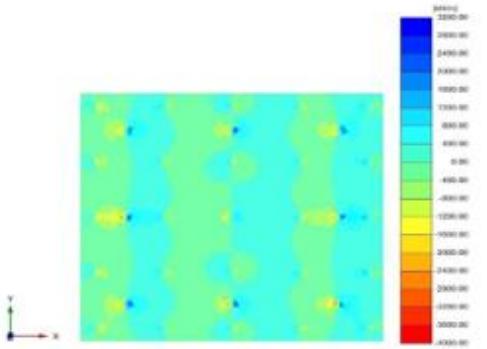

Fig (12) Shear force in the raft for a soil-contacting piled raft foundation (L_D = 32D)

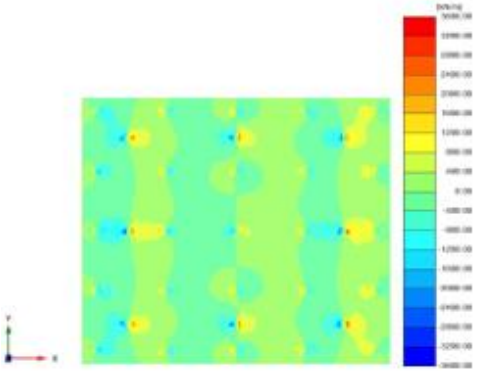

Fig (13) Shear force in the raft for a pile-connected slab foundation (L_D = 32D)

5 m), with raft thickness 1m in sec A from these figures, it can be shown with increasing pile length from 28D to 40 D the shear force on the raft decreased from 1%to0.5% in the case of piled raft rested on the soil and the shear force on the raft decreases from1%to0.5%. in the case of piled raft with raft act as slab connected the pile.

Figures (24), (25) shows the relation between the shear force on the raft in the two cases with various pile lengthwhere Lp = (28D, 32D, 36D, and 40D) for (D = 0.5 m), with raft thickness 1m in sec B .it can be observed that with increasing pile length from 28D to 40D the shear force on the raft decreases from 1%to0.5%. in the case of piled raft rested on the soil and the shear force on the raft decreases from 1%to0.5%. in the case of piled raft with raft act as a slab connected the pile.

Figures (26), (27) and fig (38) show comparison in the settlement, bending moment and shear force between piled raft foundation rested on the soil and piled raft foundation with raft act as slab connected the piles where lp=28D and raft thickness(1m). it can be concluded that the settlement in the piled raft in the case of raft act as slab connected to the piles is greater than the case of rested piled raft by 10%, the bending moment in the raft in the case of a raft act as a slab connected to the piles is greater than the case of a rested piled raft by 7% and the shear force in a raft in the case of a raft act as a slab connected the piles is greater than in the case of a rested piled raft by 2%.

Figures (29), (30) shows the relation between settlement on the raft in the two cases with various pile length = where Lp = (28D, 32D, 36D, and 40D) for (D = 0.5 m), with the effect of dynamic load and static load, with raft thickness 1m in sec A. It can be observed that with increasing pile length from 28D to 40D the settlement decreases 40% in the case of piled raft rested on the soil and settlement decreased 35% in the case of piled raft with raft act as slab connected the pile.

Figures (31) and (32) shows the relation between the bending moment of the raft with the effect of dynamic load and static load, in the two cases with various pile length where Lp = (28D, 32D, 36D, and 40D) for (D = 0.5 m), with raft thickness = 1m in sec A. It can be observed that with increasing pile length from 28D to 40D the bending moment in the raft decrease 29% in the case of piled raft rested on the soil and the bending moment in the raft decreases from 20% in the case of piled raft with raft act as slab connected the pile. Figures (33), (34) shows the relation between the shear force on the raft in the two cases with various pile length where Lp = (28D, 32D, 36D, and 40D) for (D = 0.5 m), with the effect of dynamic load and static load with raft thickness 1m in sec A from these figures, it can be shown with increasing pile length from 28D to 40 D the shear force on the raft decreased 0.5% in the case of piled raft rested on the soil and the shear force on the raft decreases 0.5%. in the case of piled raft with raft act as slab connected the pile.

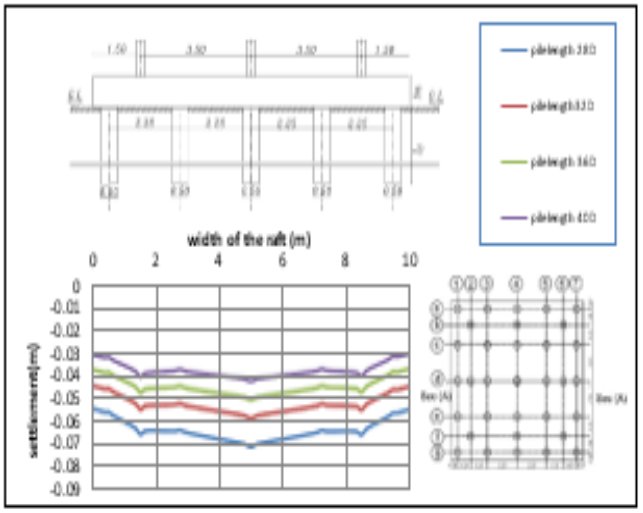

Fig (14) Relationship between pile length and settlement at Section A for a soil-contacting piled raft foundation

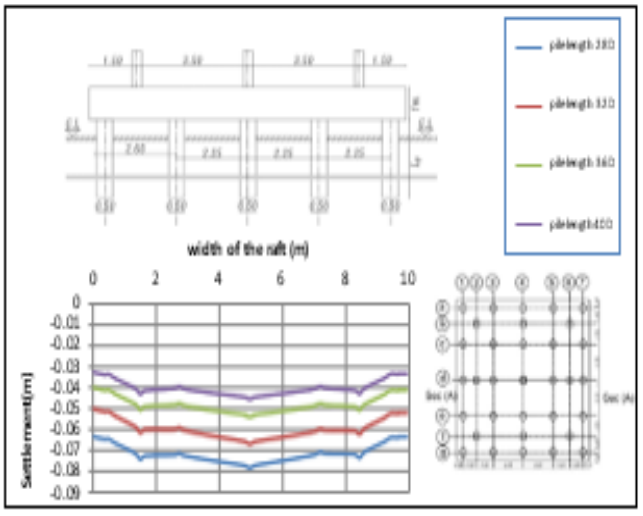

Fig (15) Relationship between pile length and settlement at Section A for a pile-connected slab foundation.

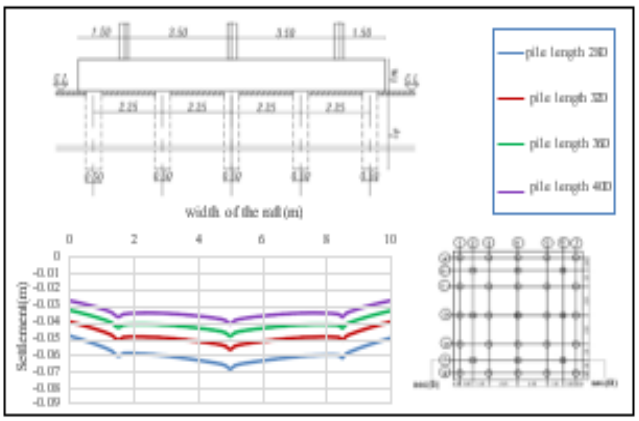

Fig (16) Relationship between pile length and settlement at Section B for a soil-contacting plied raft founda

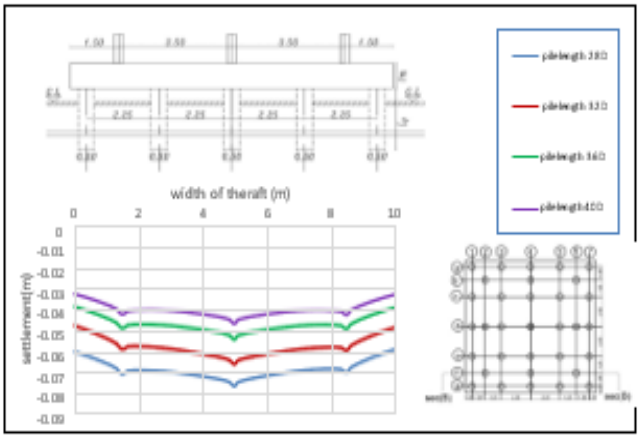

Fig (17) Relationship between pile length and settlement at Section B for a pile-connected slab foundation.

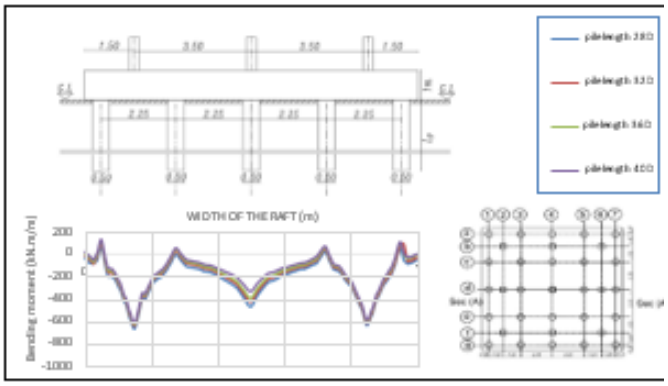

Fig (18) Relationship between pile length and raft bending moment at Section A for a soil-contacting pile foundation.

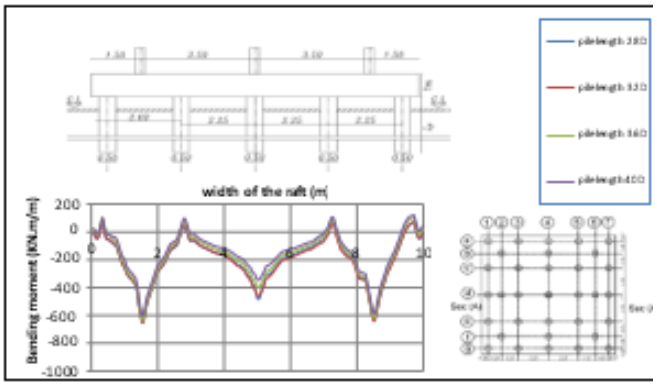

Fig (19) Relationship between pile length and raft bending moment at Section A for a pile-connected slab foundation.

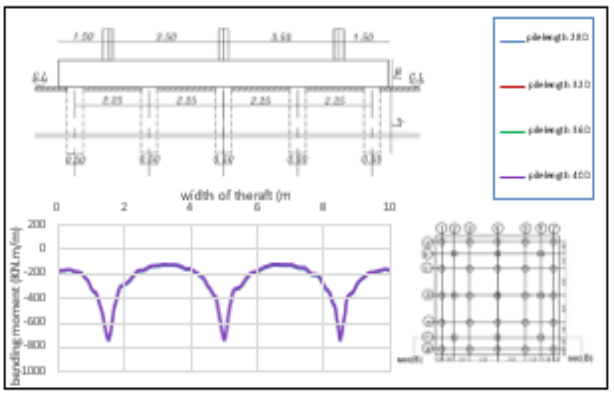

Fig (20) Relationship between pile length and raft bending moment at Section B for a soil-contacting piled raft foundation

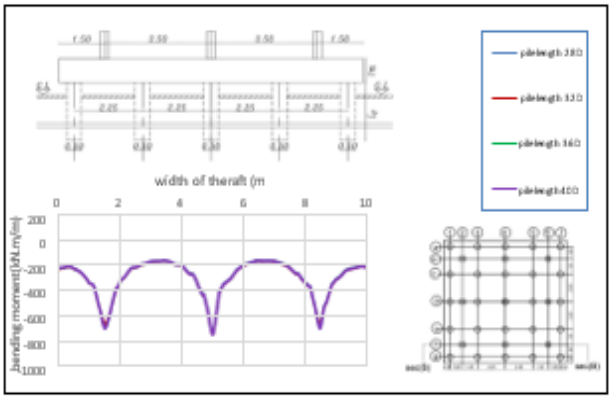

Fig (21) Relationship between pile length and raft bending moment at Section B for a pile-connected slab foundation.

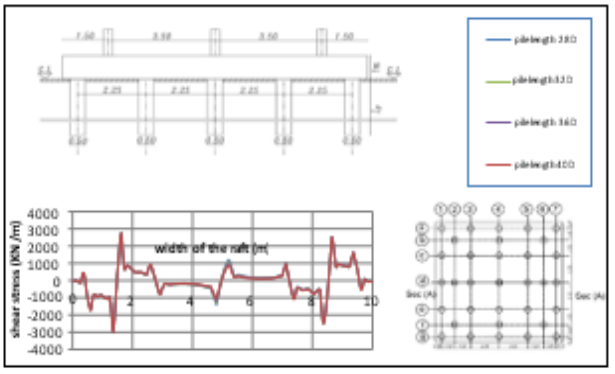

Fig (22) Relationship between pile length and raft shear force at Section A for a soil-contacting piled raft foundation

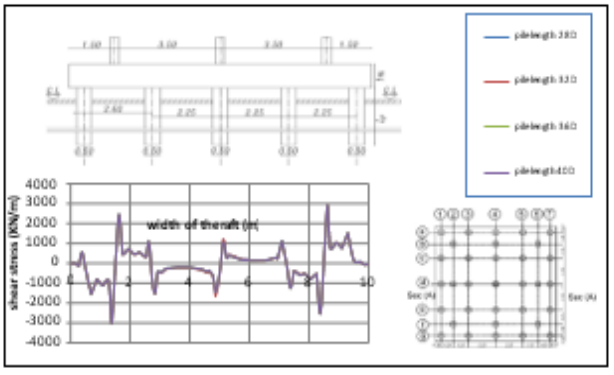

Fig (23) Relationship between pile length and raft shear force at Section A for a pile-connected slab foundation.

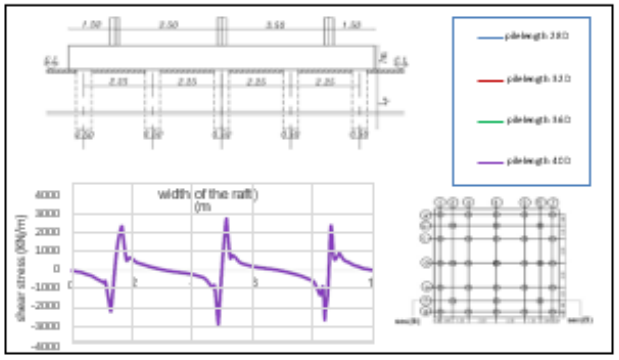

Fig (24) Relationship between pile length and raft shear force at Section B for a soil-contacting piled raft foundation

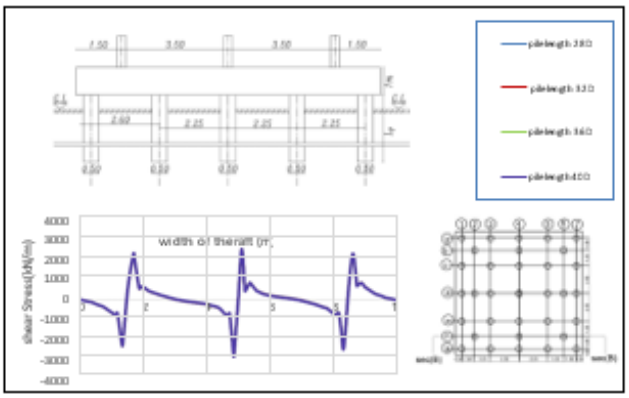

Fig (26) Relationship between pile length and raft shear force at Section B for a pile-connected slab foundation.

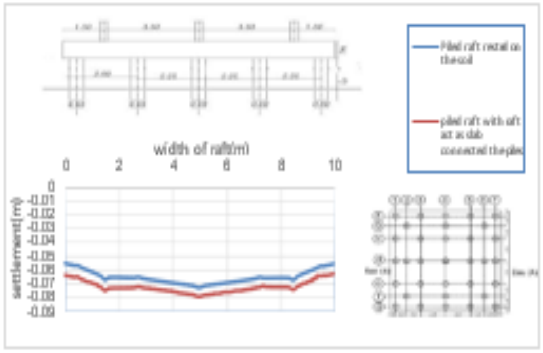

Fig (28) Settlement comparison: soil-contacting piled raft foundation vs. pile-connected slab foundation.

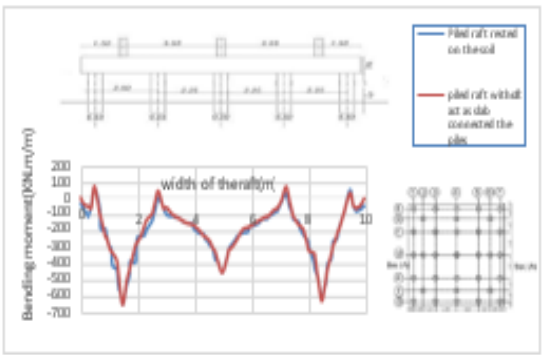

Fig (27) Bending moment comparison in the raft: soil-contacting piled raft foundation vs. pile-connected slab foundation.

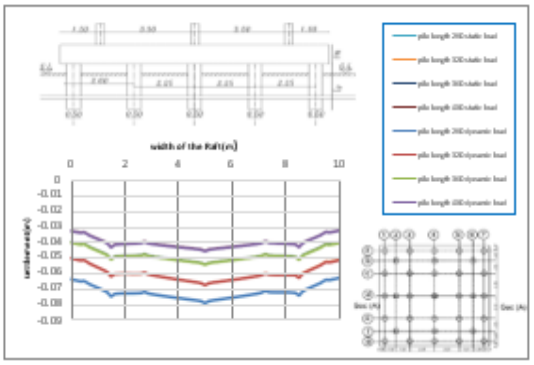

Fig (30) Relationship between pile length and settlement at Section A for a pile-connected slab foundation under static and dynamic load

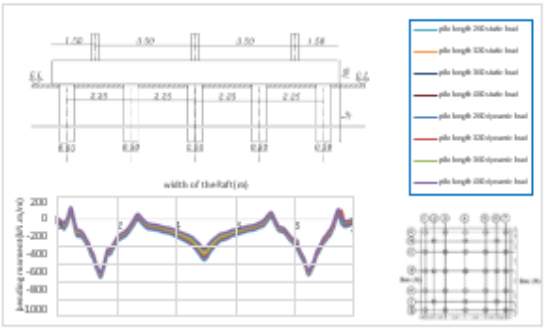

Fig (31) Relationship between pile length and raft bending moment at Section A for a soil-contacting piled raft foundation under static and dynamic load

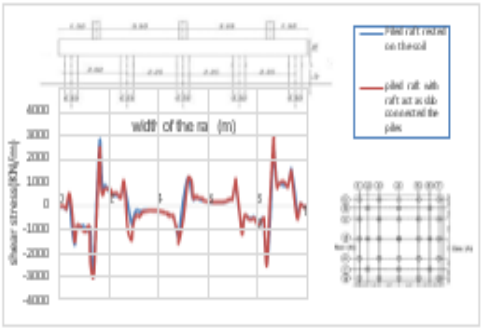

Fig (28) Shear force comparison in the raft: soil-contacting piled raft foundation vs. pile-connected slab foundation.

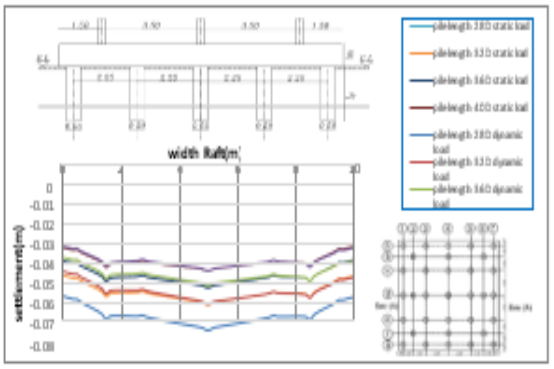

Fig (29) Relationship between pile length and settlement at Section A for a soil-contacting piled raft foundation under dynamic load

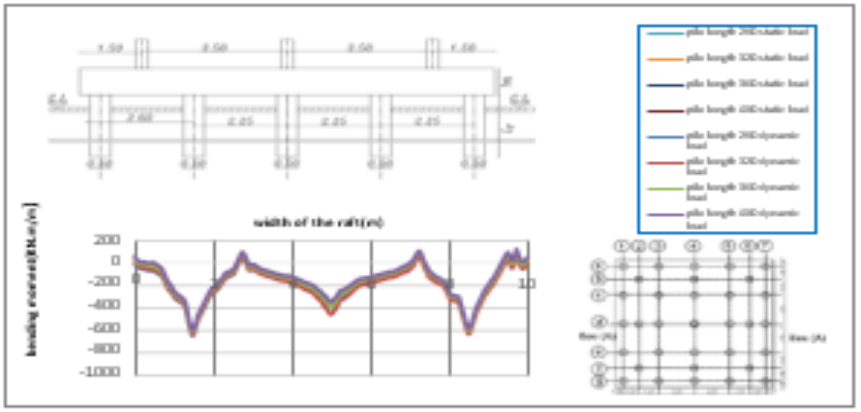

Fig (32) Relationship between pile length and raft bending moment at Section A for a pile-connected slab foundation under static and dynamic load

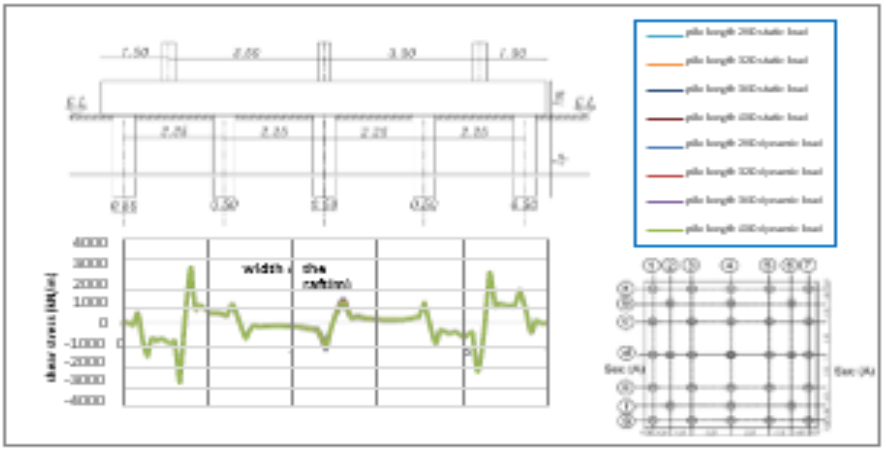

Fig (33) Relationship between pile length and raft shear force at Section A for a soil-contacting piled raft foundation under static and dynamic load

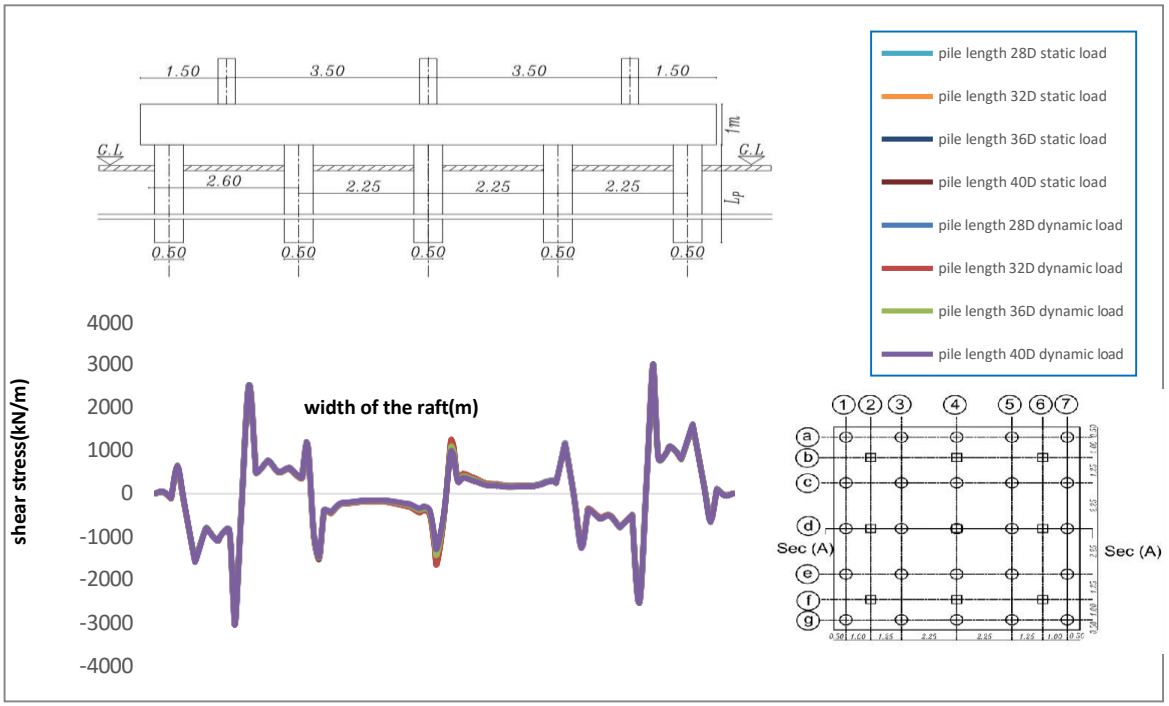

Fig (34) Relationship between pile length and raft shear force at Section A for a pile-connected slab foundation under static and dynamic load

Conclusions:

From the present study, the followings are concluded:

1. In the case of rested piled raft increasing pile length leads to

- The bending moment in the raft decreases 29%
- The settlement decreases 40 % of piled raft foundation
- the shear force in the raft decreases from to 0.5%

2. In the case of a raft act as a slab connected the piles increasing pile length leads to

- The bending moment in the raft decreases 20%
- The settlement decreases 35 % of piled raft foundation
- the shear force in the raft decreases 0.5%

3. The comparison between the two cases piled raft rested on the soil and piled raft act as a slab connected the piles

The bending moment in the raft in the case of a raft act as a slab connected to the piles is greater than the case of a rested piled raft

- by 10 %
- the settlement in the piled raft in the case of raft act as slab connected to the piles is greater than the case of rested piled raft by 7%
- The shear force in a raft in the case of a raft act as a slab connected the piles is greater than in the case of a rested piled raft by 2%

4. The effect of pile length with dynamic force

In the case of rested piled raft increasing pile length leads to

- The bending moment in the raft decreases 29%
- The settlement decreases 40 % of piled raft foundation

5.the shear force in the raft decreases from 0.5% In the case of a raft act as a slab connected the piles increasing pile length leads to

- The bending moment in the raft decreases 20%
- The settlement 35 % of piled raft foundation
- The shear force in the raft decreases 0.5%.

From Restoration to Interpretation: Historical Memory in the Architecture of Renato Rizzi

Nino Imnadze, Mariam Botchorishvili,
Georgian Technical University, M.Kostava st 77, Tbilisi 0159, Georgia.
n.imnadze@gtu.ge

DOI: https://doi.org/10.52340/building.2025.72.02.18

Abstract: This article analyzes one of the key debates in 21st-century architecture—the integration of contemporary architecture within historical urban fabric and the relationship between cultural heritage and modernity—through two projects by the Italian architect Renato Rizzi: "*Casa Museo Depero"* (1992–2008, Rovereto, Italy) and the "*Gdańsk Shakespeare Theatre"* (2004–2014, Poland). Although functionally different, both projects are united by Rizzi's conceptual approach, which is based on a critical dialogue with the material and immaterial layers of the past. In the first case, the research examines the restoration and adaptation of interior space within an existing medieval structure, while in the second case it explores the abstract reconstruction of cultural memory on the site of a former Elizabethan theatre. The study demonstrates that for Rizzi, historical architecture is not a static heritage object or a museum artifact, but a living process that generates new architectural forms and meanings through interpretation. The comparative analysis reveals that in both projects historical metaphors are synthesized with contemporary technologies and architecture. As a result, Rizzi's architecture is simultaneously contextual and contrasting, transforming historical reference into a contemporary spatial narrative. The "Gdańsk Shakespeare Theatre" integrates three fundamentally different systems: the architectural interpretation of historical memory, technologically driven architectural form, and open urban space designed for social and cultural interaction. The research concludes that Rizzi rejects superficial historicism and formal imitation, proposing instead an interpretative architectural strategy in which history is understood as a living text. Through rereading and translating this text into contemporary architectural language, his projects establish architecture as a mediator between past and present, memory and innovation, tradition and modernity.

Key words: Historical urban fabric; Cultural heritage; Reconstruction; Poetics of space; Architectural concept

Introduction

One of the most important topics in 21st-century architectural debates is contemporary architecture within historic urban fabric and the integration of cultural heritage buildings with modernity. The synthesis of architecturally and temporally distant spaces through a contemporary language is a challenge both for the city and for professionals, as it requires from the creator a deep knowledge of innovative technologies and philosophical vision. Therefore, the topic is highly relevant, since the spatial and artistic image of any city is formed through temporal intervals, which determines its diversity, growth, and continuous development. The aim of this article is to explore the relationship between the new and the old in connection with the physical world and cultural memory through the discussion of specific objects. During the research process, another no less important issue emerged, related to understanding the visible and invisible instruments that shape architectural form. The direction defined by our research is concentrated on the work of the Italian architect and theorist, Professor at the University of Venice (IUAV), Renato Rizzi. Our interest in his work is driven by two factors. First is the architect's attitude toward contemporary architecture, about which he states: *"Contemporary architecture is losing its voice; it speaks the language of the market, not of memory"* (R. Rizzi). In other words, Renato Rizzi's architecture is not commercial.

Second is the form of dialogue he initiates with space, place, and history, which is connected to phenomenology and the poetics of space, and is therefore highly individual. In interviews regarding the restoration of cultural heritage monuments, Rizzi notes: *"Reconstructing history does not mean reproducing an old form unchanged; rather, it requires rereading and interpreting it. Only in this way can we integrate it with contemporary life"* (Rizzi, 2015, public lecture, GTS archive).

Research Methodology. The present study is based on qualitative, comparative–conceptual analysis. The research methods include spatial-formal analysis of architectural objects; interpretation of historical-cultural context; analysis of visual materials (photos, plans, and sections); examination of primary and secondary sources: interviews with the architect, lectures, essays, and academic literature. The study relies on a phenomenological approach where architecture is considered as spatial experience and a material form of cultural memory. Comparative analysis allows the identification of Renato Rizzi's conceptual strategies in the context of contemporary architecture integration into historical environments.

Theoretical framework: the architectural interpretation of place, space, and form as a dialogue with the built environment and history. Within this context, two works by Renato Rizzi are examined the reconstruction of the "Casa d'Arte Futurista Depero" and the Shakespeare Theatre.

Main Part

"Casa d'Arte Futurista Depero" (Figures 1,2) opened in 1959 in a former bank and exchange building located in the historical center of Rovereto, Italy, at the initiative of Italian Futurist artist and designer Fortunato Depero, based on the multidisciplinary concept of the "house-studio" he developed in 1919–1920. Since 2009, after reconstruction, Depero's house reopened as a Futurism museum. The reconstruction was carried out according to the project of architect Renato Rizzi. His concept was based on conveying the idea of constant movement of Futurism while preserving the building's authentic appearance and updating the museum interior functionally and technologically.

Fig. 1

Fig.2

For Rizzi, the Depero Museum is not only an exhibition space but also an "energy machine," which transforms the relationship between time and space into an architectural form. The architect preserved the historical façade and continued Depero's aesthetics in the interior: decorative system, theatricality of space, and color philosophy (sharp, contrasting, resonant, and dynamic). Rizzi used geometric forms and color ratios in the interior, predominantly authentic white as a counterpoint, red-black, and blue. This solution continues Depero's idea of creating an illusion of "acoustic dynamics" with color tonalities. Moreover, through functional transformation of the interior, the two-story building was turned into an eight-room museum without violating the scale and exterior appearance. At the same time, the reconstruction created an "illusion of

movement" inside, evoking a Futurist experience for the visitor. To develop Depero's idea of "moving art," the interior was divided into modules, allowing dynamic rotation of exhibitions. Thus, the museum became not a historical memorial, but a living Futurist experiment combining two eras. This shows that for Rizzi, restoration is not only a technical or functional act but a philosophical one: not "returning to the past" but "continuously moving toward the future." Rizzi's approach treats history not as "restorable material" but as an initial idea that must be recreated in any era.

Discussion. Thus, Rizzi seeks a critical interpretation of Depero's Futurist movement through newly created spatial layers (two additional levels), which establish a tense dialogue with the old spaces. The new spaces (halls) create transitional spaces in time. Rizzi's intervention approaches theatrical and stenographic thinking and conveys Depero's Futurist atmosphere. In doing so, it emphasizes that new architecture must engage in active dialogue with the old—through rethinking history rather than through stylization. Nevertheless, Rizzi's attitude toward old, historical architecture is contextual. From this perspective, he approaches the vision of Carlo Scarpa, though in a completely different manner. A comparative analysis between interventions carried out in different epochs—within Italian heritage spaces of the 20th and 21st centuries—may seem paradoxical on our part. However, the analysis reveals that Carlo Scarpa interprets the historical context not as a direct response in form or material, but as an integration with history at the level of detail, time, and spatial articulation. His reconstruction of the "Castelvecchio Museum" (Verona, 1959–1973) offers a solution in which new forms interact with historical "layers" with masterful precision. The focus is on the poetry of detail. Scarpa preserves the old and artistically, carefully, and poetically connects it with the new. In contrast, Rizzi creates a new geometric dynamism through spatial modeling. For both architects, the dramaturgy of space, the movement of visitors, and the historical-cultural context are of fundamental importance. Renato Rizzi, through the restoration of the Casa d'Arte Futurista Depero, created a new type of museum in which history and contemporaneity do not simply complement one another, but are transformed into a new architectural form. Comparative analysis shows that, despite certain shared tendencies with Carlo Scarpa's approach to restoration, Rizzi's reconstruction differs in its philosophy and brings it closer to expressive, Futurist thinking. He succeeded in preserving the energy of Futurism and created a space that functionally, technologically, and aesthetically responds to the museum requirements of the 21st century. Rizzi not only physically restored a historic building but also created an architecture of time and movement—a transitional space between art and time.

The **Shakespeare Theatre** in the city of Gdańsk (Poland) is one of Renato Rizzi's (co-author: Jerzy Limon) most interesting, realized projects, in which the author's cultural and philosophical vision is clearly revealed (Fig. 3).

Fig. 3. Shakespeare Theatre in Gdańsk. Architect: Renato Rizzi

Historical Context. In the 17th century, Gdańsk possessed a rich theatrical tradition. It was an important port and cultural center throughout the Baltic region. An open-type English so-called "Elizabethan" public theatre was located here (Gdański Teatr Szekspirowski, 2016, official statement). It

was one of the first spaces in Eastern Europe where Shakespeare's plays were performed. Ideologically and typologically, it corresponded to London's Globe Theatre.

Theatre Concept. The Shakespeare Theatre opened in 2014. It is located on the site where, in the 17th century, an open wooden stage—the so-called Elizabethan stage—once stood. From an urban planning perspective, the new theatre is positioned between the medieval city and the contemporary urban fabric (Fig. 4).

Fig. 4. Shakespeare Theatre on the boundary between historic and contemporary development

The foundation of Rizzi's architectural approach is the idea that "the reconstruction of history should not occur through the transfer of old forms, but through rereading and interpretation, which will be synthesized with contemporaneity and speak the language of contemporary architecture" (2013–2015), as he himself notes in interviews, lectures, and architectural essays. The theatre explicitly employs the principle of the urban artifact as a materialized embodiment of the city's history and collective memory. Consequently, it represents a part of the contemporary city's urban structure space for socio-cultural dialogue and historical reconstruction. The massive, geometric, horizontal, smooth black volume metaphorically evokes a "fortress." This is not merely an aesthetic choice, but a semiotic architectural sign. In terms of scale, the theatre does not disrupt the city's urban silhouette and respects the historical context. Its spatial and volumetric composition, as well as architectural forms and details, are inspired by the brick Gothic style of 14th–15th century Gdańsk. It responds to the city's historical symbol and dominant landmark, the Basilica of the Crown (Fig. 5).

Fig. 5. Shakespeare Theatre against the background of the historic city. Closed and open roof

Within the "walls" of the theatre, the inner surface of the building contains perimeter "paths" or "streets" that create spaces allowing anyone to move through them without entering the theatre's interior. Through this solution, a new type of public space was created, serving as a continuation of the historic city's urban fabric. Visitors find themselves between historical memory (the medieval space) and contemporary theatrical spaces. From these paths, extraordinary views of the city unfold. (Figs. 6, 7).

Fig. 6. Panoramic views of the historic and contemporary city from the paths

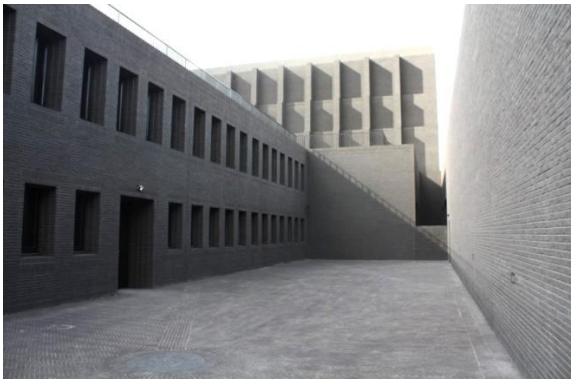

Fig. 7. Inner paths recreating a medieval atmosphere

Fig. 8. Transformable roof

The black color of the façade contrasts radically with the theatre interior. The interior is much warmer, more social, and dynamic. It directly reflects the spatial archetype of the Elizabethan theatre. The multi-level wooden galleries, together with staircases, create spaces resembling "streets" and "squares," evoking the image of a small town. The most important innovation is the movable roof, which can open and close within a few minutes, allowing the theatre to function under the open sky (Fig. 8). In this way, the tradition of XVII century open-air performances restored. Also noteworthy is the modular and transformable stage system, which directly relates to the Elizabethan stage typology and becomes multifunctional. The stage adapts to Gdańsk's cultural events (Fig. 9). Performances are held in three formats: under an open roof (Elizabethan style), in a traditional format, (audience seated facing the stage), and in an arena format (audience seated around the stage).

Fig. 9. Multifunctional, transformable stage space

The Gdańsk Theatre is a flexible theatrical laboratory that transcends the limitations of classical theatre. It combines historical metaphor with contemporary technologies and the building's geometry. Accordingly, the project stands out both through formal contrast and its engagement with historical context, making it an independent architectural phenomenon.

Discussion. The theatre's architecture transcends any classical theatre type, as the building itself becomes a place of interaction between space, city, and people. However, the space surrounding the theatre building—enclosed by walls—is isolated from the outside world. It is self-contained and assigns semantic meaning to the structure of the historic city. Its location, form, and scale create a detached yet integrated artifact that mediates between the layers of the old city and contemporary requirements. It is not a nostalgic replica, but an interpretation. The building responds to key principles of urbanism: flexibility as an essential quality of cultural infrastructure; openness as a form of accessible public space; integration as a mechanism for deepening the city's social fabric; reinterpretation as a continuation of historical texture. The theatre can be understood as a symbolic bridge between the city's historical past and its contemporary cultural future. It successfully unites architectural interpretations of memory, technological innovations, and urban synthesis. Rizzi's approach can be associated with the theories of Aldo Rossi. Like Rossi, Rizzi embraces the rigor of form and transforms it into a structure that transcends time. Rossi viewed the city as a carrier of collective memory and architecture as the material embodiment of memory. His buildings connect to the city's historical layers. Rizzi's Shakespeare Theatre is constructed on the same principle: it symbolically connects to the history of the "place" and responds through a massive volume, the "emptiness" of interior spaces, minimalist details, and contemporary technologies (the movable roof) that react to the world. The theatre is not merely a "typology," but a "process." Thus, Renato Rizzi's Shakespeare Theatre is based not on

replication of history, but on interpretation: the theatre is not a reconstruction of a 17th-century theatre, but an architectural response to the city's historical memory. With this work, Rizzi opposes the dominant formal experiments in contemporary architecture and openly declares: *"Architecture can be a theatre for the soul—a stage where a person remains alone with oneself."* For him, architecture is a space of thought that speaks to us. A building does not merely occupy territory and space but creates an urban narrative that gives the city a new cultural identity. The new building, constructed at the beginning of the 21st century, is considered a physical, cultural, and semiotic dialogue with the historical artifact that existed in 17th-century Gdańsk and with the contemporary demands developing today in the field of theatrical architecture.

Conclusions

Thus, in the present article, we analyzed two buildings designed by the Italian architect Renato Rizzi the "Casa Museo Depero" (1992–2008, Rovereto, Italy) and the "Gdańsk Shakespeare Theatre" (2004–2014, Poland) within the context of historical memory. The first involves restoration within an existing medieval architectural framework, with the adaptation of interior spaces; the second represents an abstract reconstruction of cultural memory on the site of an Elizabethan theatre. Both projects are united by Rizzi's conceptual approach: creating spaces through dialogue with the material and immaterial layers of the past, which simultaneously reflect history and contemporaneity. The comparative analysis includes historical approaches, spatial and material strategies, urban roles, and conceptual narratives. The research demonstrates that for Rizzi, historical architecture is not a static heritage, but a participant in a living dialogue that generates new forms and meanings. His architectural language rejects superficial historicist imitation, while at the same time remaining rooted in local identity. For Rizzi, "history is not a static museum remnant, but a living text whose "reading" and "translation" create a new layer of interpretation". (Rizzi, 2015)

Reference

1. Rossi, A. (1982). *The Architecture of the City*. Cambridge, MA: MIT Press.
2. Scarpa, C. (2007). *Carlo Scarpa: Architecture and Design*. New York: Rizzoli.
3. Rizzi, R. (2015). *Lectures on Architecture, Memory and Interpretation*. Venice: IUAV Archives.
4. Gdański Teatr Szekspirowski. (2016). *Official Publications and Architectural Description*. Gdańsk.
5. Frampton, K. (1995). *Studies in Tectonic Culture*. Cambridge, MA: MIT Press.
6. Norberg-Schulz, C. (1980). *Genius Loci: Towards a Phenomenology of Architecture*. New York: Rizzoli.
7. https://iqd.it/en/architects/renato-rizzi/
8. https://www.archdaily.com/595895/gdansk-shakespearean-theatre-renato-rozzi
9. https://ec.europa.eu/regional_policy/en/projects/poland/gdansk-shakespeare-theatre-building-an-impressive-venue-for-art-and-education
10. https://www.theatre-architecture.eu/db.html?theatreId=235
11. https://en.teatr.com.pl/portfolio-item/gdansk-shakespeare-theatre/
12. https://journals.openedition.org/shakespeare/1624?lang=en
13. Claudia Tinazzi "Renato Rizzi "To be an Architect you must be in the Grip of an Obsession". Spaces of Memory Commentaries on 21ts Centure Buildings. Edited by Luigi Spinelli 2020
14. https://www.tonellihotels.com/en/futurist-house-of-art-fortunato-depero
15. https://www.trentino.com/en/highlights/museums-and-exhibitions/casa-d-arte-futurista-depero/

Peculiarities of the construction of rotating buildings

Irakli Kvaraia, Lasha Bochorishvili
Georgian Technical University, M.Kostava st 77, Tbilisi 0159, Georgia.
i.kvaraia@gtu.ge, lashabochorishvili12@gmai.com
DOI: https://doi.org/10.52340/building.2025.72.02.19

Abstract The main goal of architects when designing, depending on the purpose of the buildings, is to create the most perfect and convenient working or living conditions for people. One of the important factors in this regard is to ensure the orientation of the building's facade in such a way that daylight and sunlight penetrate as much as possible. Based on the above, to meet this requirement, buildings are often equipped with wide windows, glazed balconies, or their facade parts are completely covered with stained glass. Many buildings include a large number of terraces and open balconies. Many architects have gone further and have already implemented many projects where the building itself or its floors rotate and it is possible to orient it in the desired direction. The idea of building rotating buildings arose at the beginning of the last century and gradually developed to such an extent that for several years now very interesting projects of rotating skyscrapers have been developed. Due to its engineering solution, the construction of such buildings is associated with significant costs, and their implementation is only related to finding financing.

Keywords: building, rotation, construction, frame, mechanism, steel.

1.Introduction

The first rotating building project was presented in 1920 by the architect Vladimir Tatlin. He also built a wooden model for the building of the Third International. The new headquarters of this international communist organization, at that time the tallest building in the world, was to be built in St. Petersburg. In fact, the project was a visual embodiment of a communist utopia. The building was to become a monument that stood out from all others. If it had been built, it would certainly have become one of the wonders of the world, but an overly ambitious design prevented its implementation. The 400-meter-high building consisted of two interconnected metal spiral structures. Four different geometric figures
were suspended from it, each rotating at a different speed around its own axis. The lowest, cube-shaped building was dedicated to the legislative body and made only one rotation during the year. It was planned to hold large gatherings, congresses and conferences there. The pyramid-shaped building above was intended for the executive bodies. It made one rotation per month. The third, cylindrical building in height was to house the information center, publishing house, printing house and other services with an agitation-propaganda function. The cylinder would make one rotation per day. The highest, hemispherical figure made one rotation in one hour and was presumably dedicated to artists and art workers (Fig. 1).

According to the author's idea, the tower was to become a symbol of the reunification of humanity, which was divided during the construction of the Tower of Babel, and in its design, constructivist, it would be built entirely from locally produced materials. In capitalist countries, such high-rise buildings were faced with marble, ivory and other expensive materials. Tatlin wanted to create the tower with the main elements of Soviet

industry (iron, steel, glass, etc.). It was of great importance to the working class, because at that time everywhere, including in the field of art, they wanted to establish a new and clearly socialist identity. Tatlin's tower was unique because the construction concerned the entire socio-economic class of people. Although it was not implemented, it still made such a strong impression that it is still a source of inspiration for architects.

Fig. 1. Model of Tatlin's Tower

2. Main part

The world's first residential house that rotates around its own axis was built in 1935 in the village of Marcelli, near Verona, Italy. Tatlin's idea was implemented almost 15 years later by the Genoese engineer and investor Angelo Invernizzi, who built a rotating private house with the help of famous engineers and architects. It was built in the style of modernism and during a period of great interest in the use of solar energy. The building is also known as the "Sunflower Villa" because its fruits are always directed towards the sun (Fig. 2). From an engineering point of view, the building is a masterpiece of rationalism and futurism. The building consists of two parts. The first part is a three-story reinforced concrete support platform with a diameter of 44 meters. Inside it is a rotating axis, and on the surface there is a green courtyard, where three circles of railway tracks are made. The second part is movable. It is a two-story building. Its two rectangular parts are connected to each other at an angle of 900, with a 40-meter-high tower in the middle. The supporting part of the tower is built of a metal frame, and here, as in the building, bricks and reinforced concrete are also used. From above, the object resembles a large and slowly moving sundial. Its weight is more than 1,500 tons and movement on the tracks is carried out in both directions by 15 locomotive wheels and a 3-horsepower electric motor. The moving part takes 9 hours and 20 minutes to rotate 3600 degrees, or its speed is 4 mm/s. Currently, this building houses a museum.

Fig. 2. The first rotating house

After this object, many more rotating houses were built around the world at different times, and there are even more ideas and projects for their embodiment. Among such buildings, several deserve special attention for their original engineering solutions. One of these is the three-story house of architect Ralph Disch in Freiburg (Germany), which was built in 1994. The house that follows the sun was named after the decorative plant "heliotrope". The flowers of this plant change

their position during the day in the direction of the sun's movement, that is, they always look at the sun. This building was built taking into account this principle. In addition, it is interesting that the house rotates using solar energy. Which is generated by 6.6 kW of solar panels located on its roof. It is worth noting that the panels, whose total area is 56 m2, generate 5-6 times more electricity than is needed to fully power the house. Therefore, it is also considered an ecological building. The panels also move freely along with the movement of the sun, which allows for maximum accumulation of electricity, and the movement of the house itself creates a certain atmosphere for the residents. It should also be noted that the windows of the house are double-glazed, which has high thermal insulation properties and has the ability to control the climate (Fig. 3).

Fig. 3. "Heliotrope" in Freiburg

The idea of creating absolutely ecological buildings is relevant not only for residential, but also for public buildings. In particular, the solution of the "Heliotrope" - a rotating house was used by the same architect when developing the "Heliotrope" hotel project, which was supposed to show a wider scope of the use of kinetic construction. And possibilities. Unfortunately, due to lack of funds, it could not be implemented.

A two-story house with 4 duplex-type residences built on Prince Edward Island in Canada is very interesting due to its simple solution. It makes one full turn around its central axis throughout the day. Its rotation almost completely repeats the principle of movement of a children's carousel. For this, first, a circular pool-like underground structure was built from monolithic reinforced concrete, and then a rotating frame from steel profiles was arranged in its internal space. This frame is actually the foundation of the building, on which two floors were built using light metal structures (Fig. 4).

Fig. 4. Rotating foundation

Fig.5. Around the Sea"

According to the authors of the project, this is the only apartment building that rotates with an elevator, and all rooms in the building necessarily face the ocean. In addition, this structure required not only precise calculations, but also furniture and accessories are arranged

with pre-calculated fastenings. In order not to restrict the movement of the house, communications were laid in its central part. In order to ensure the best possible view around, the windows and doors of the building have wide frames, and the second floor is equipped with a circular balcony. Therefore, the building fully corresponds to its name. "Around the Sea" means "around the sea" (Fig. 5).

In 2004, a rotating private house was built on a mountainside in San Diego (USA), with unusually good views. It was designed by the Johnstons, a couple who live there, who did not have a special architectural education. The base of the kinetic structure of the house is a cylindrical base, made of a metal frame with movable and stationary platforms. The movement is carried out by an electric motor. Since it is hot in California, the facade is made of black tinted glass. The movable platform is the floor of the living area of the house, and 8 bearings are enough to move it. Using a conventional remote control, it is possible to adjust the speed of rotation of the building, one full revolution is carried out, the fastest movement is carried out in 33 minutes. The building has a circular balcony and all communications, elevator and entrance door are located inside its cylindrical axis. A two-car garage is located on the first, immovable floor of the building (Fig. 6).

Fig. 6. Rotating house in San Diego

Many more examples of low-rise rotating houses can be cited, which are found in different countries of the world. Modern architects, creating a new project, always try to make specific changes to make it different from standard types of buildings. One of such features is high-rise rotating buildings, which, along with the architectural solution, are interesting for their rotational motion. The most difficult thing at this time, based on the laws of physics, is to ensure the stability of the floors moving asynchronously around the axis of the building (Fig. 7).

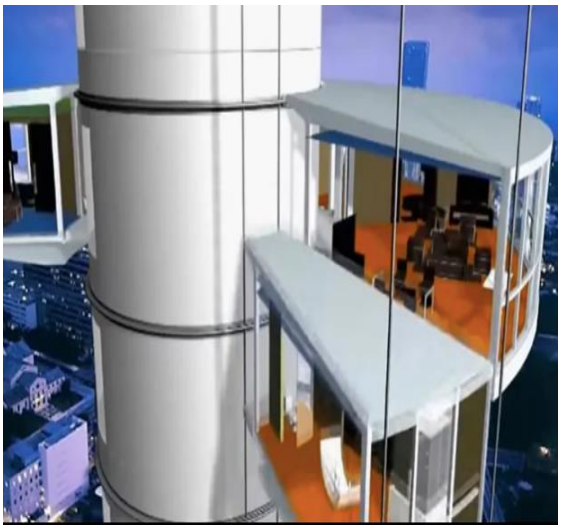

Fig. 7. Floor connection

Most of the low-rise buildings built earlier were completely rotary. In the case of separately movable floors, the architectural and constructional solution is also supplemented by ensuring their functionality. This requires an individual engineering approach in each particular case. Therefore, along with the names of the authors of such objects, i.e. architects, the creators of the rotating mechanism are also indicated. One of the first such high-rise buildings was built in 1991 in Curitiba, Brazil, whose architect is Burno de Franco, and the design of the rotating device was created by engineer Alan Holtzman. This building is considered the first complex in the world where the floors can rotate independently of each other. The building is

15-story. The first four floors are stationary, while the remaining eleven can completely independently make one rotation around the central core, where all communications and nodes are concentrated, in 60 minutes (Fig. 8).

Fig. 8. Rotating house in Brazil

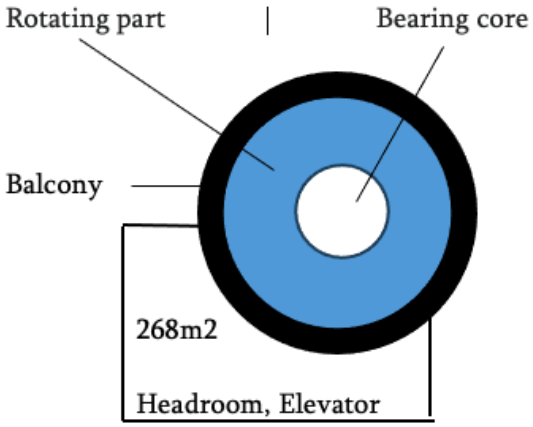

Fig. 9. Rotating Part

The complex is located in the city center, in an elite area. The cost of the apartments is much higher than the cost of ordinary apartments, since their owners receive not only apartments, but also the ability to change the view from the windows at their own discretion. There is only one elite apartment on each floor, where prominent citizens of Brazil live. Such a decision was made with the view that in the case of several apartments, there could be major misunderstandings regarding the rotation of the floor. Therefore, the total area of the floor is 268 m2. All conditions for comfortable living are created in the apartments. In addition, more than 30 m2 is occupied by a large terrace with a panoramic view. Communications pass through the central core here too and there are sewers. And the fixed part houses the entrance, stairwell, elevators and a number of other auxiliary storage rooms (Fig. 9).

The most important object among the rotating buildings is the "Rotating Tower" (rotating tower) 80-story skyscraper (height 420 m) under construction in Dubai. All floors rotate independently in both directions and complete one revolution in 90 minutes. The building is constructed around a central, monolithic reinforced concrete cylindrical core, with individual sectors of the floors suspended (Fig. 10).

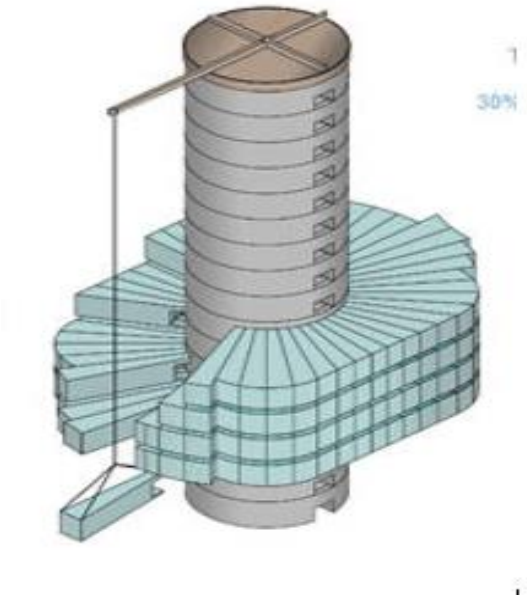

Fig.10. Connecting the sectors

The lower 20 floors of the building will house offices of well-known firms and companies. The next 15 floors will be

devoted to a six-story hotel. The remaining 45 floors are apartments with pools and greenery, the price of which is incredibly high. The staircase, elevators, entrance, and communications are in the central core. There are wind turbines between the floors, which will generate much more electricity than is needed for consumption. In addition, the configuration of the floors is such that as a result of their free rotation, the facade of the building will always be different, making it truly incomparable. Figure 12 shows several such facades of the building obtained as a result of the rotation of the floors.

Conclusion

1. The idea of rotating buildings has been around for more than a century. The first such building was built in 1935 in Italy, where a museum is now located. Since then, mainly low-rise buildings have been built, which rotated around their axis, in most cases, using a carousel-like structural solution;
2. The most difficult is the structural solution of a rotating building, when it is necessary to ensure the movement of floors in both directions, completely independently. All such cases individually require the creation of special rotating systems, which is always interesting. The first such rotating high-rise building was built in Brazil in 2001, where 11 rotating floors were suspended around a central metal axis;
3. Currently, the construction of a 420-meter-high, 80-story rotating house in Dubai is nearing completion. Its floors are suspended and installed on a central core using prefabricated sectors. The floors are configured in such a way that their movement constantly changes the facade of the entire building, which makes this building unique.

Literature:

1. T. Khmelidze. Composite Constructions. Publishing House "Universal", Tbilisi. 2024. 449 p.;
2. I. Kvaraia, S. Gelahvili. The Use of Concrete in The Construction of Skyscrapers. BUILDING. Sientific-Technical Journal N1(69), 2024. P.108-114;
3. I.Kvaraia. Seismic protection systems in construction and their arrangement. Technical University. Tbilisi. 2023. 124 p.
4. I.Kvaraia. Innovative technologies in construction. Technical University. Tbilisi 2020. 194 p.;5.
5. Chad Randl. Revolving Architecture: A History of Buildings that Rotate, Swivel and Pivot. 2008. 208 pp.

Investigation of Structural Behavior and Computational Modeling of a Transformable Guiding Bridge

Giorgi Sarishvili
Georgian Technical University, M.Kostava st 77, Tbilisi 0159, Georgia.
E-mail:gsarishvili85@gmail.com
DOI: https://doi.org/10.52340/building.2025.72.02.20

Abstract This paper investigates the structural behavior and computational modeling of a transformable guiding bridge system intended for rapid deployment in extreme operational conditions. The performance of temporary guiding bridges is governed not only by their structural configuration but also by the accurate evaluation of internal forces and deformations arising during both installation and service stages, which is particularly critical for emergency, rescue, and military engineering applications.

The distinguishing feature of the proposed bridge system lies in its transformable structural behavior. During the installation phase, the bridge functions as a temporary multi-span structure supported by deployable auxiliary supports, whereas during service it is converted into a single-span system. This transformation leads to a significant redistribution of internal forces and necessitates a computational approach capable of capturing both structural states.

A realistic calculation model was developed to represent the actual behavior of the bridge, incorporating modular geometry, temporary transformable supports, and appropriate boundary conditions. Structural analysis was carried out using MIDAS Civil 2024 software, based on the displacement-based finite element method. The model considers permanent, live, and temporary installation-related loads corresponding to unfavorable working conditions.

The results demonstrate that maximum bending moments, shear forces, and deflections occur during the installation stage but remain within allowable normative limits. The study confirms that the application of transformable temporary supports significantly improves structural safety and constructability. The proposed guiding bridge system provides a reliable and efficient solution for rapidly deployable transport infrastructure in extreme environments.

Keywords: transformable guiding bridge, structural performance, finite element analysis, temporary bridge, extreme conditions

1. Introduction

The reliable operation of rapidly deployable guiding bridges under extreme conditions requires a comprehensive understanding of their structural behavior throughout all stages of deployment and use. In temporary transport infrastructure, particular attention must be paid to load-bearing capacity, stiffness, and serviceability during both installation and operational phases [5].

Transformable guiding bridges exhibit a dual structural behavior. During installation, they operate as temporary multi-span systems supported by auxiliary deployable supports, while in service they are transformed into single-span structures. This transition induces a redistribution of internal forces and represents a critical aspect of their structural assessment [1].

Most existing research on rapidly deployable bridges addresses permanent or semi-permanent systems [1], whereas the combined analysis of transformable structures considering both installation and service stages remains limited in open literature [4]. This gap highlights the

relevance of the present study.

The objective of this paper is to analyze the structural performance and computational model of a transformable guiding bridge system and to assess its suitability for application in extreme operational conditions [2,5].

2. Computational Scheme and Structural Model

To evaluate the structural response of the transformable guiding bridge, a computational model was developed representing both the installation and operational stages. The model accounts for modular geometry, temporary transformable supports, and realistic boundary conditions reflecting actual deployment scenarios [1,5].

The bridge is modeled as a modular steel girder system. During installation, deployable temporary supports create a multi-span structural scheme. Upon completion of assembly, these supports are folded, and the bridge operates as a single-span system. This modeling strategy allows identification of the most unfavorable structural conditions [4].

Temporary supports are represented as adjustable vertical elements providing intermediate reactions during installation. Primary structural members are modeled using beam-type finite elements, enabling calculation of bending moments, shear forces, and deflections. Support conditions are defined in accordance with common temporary bridge design practice and applicable standards [2,3].

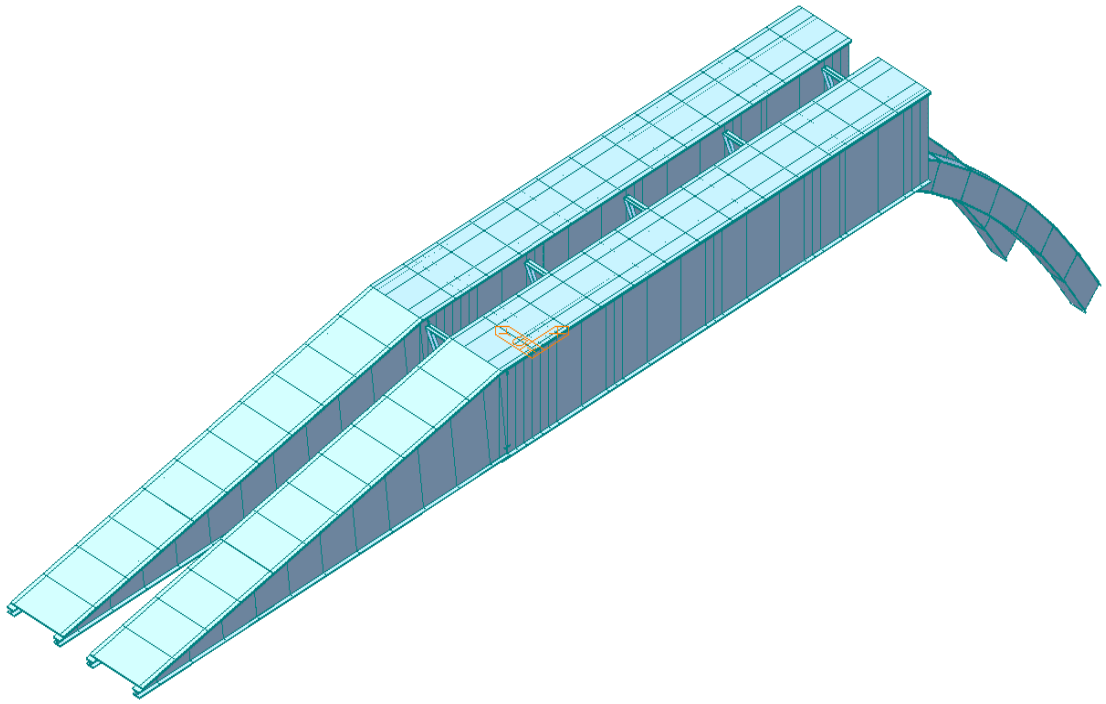

Figure 1 — Structural computational scheme of the transformable guiding bridge

Structural analysis was performed using MIDAS Civil 2024 software, employing the displacement-based finite element method, which is widely used for bridge analysis due to its reliability in evaluating internal forces and deformations.

3. Loads and Computational Parameters

The computational analysis considers load combinations relevant to rapidly deployable bridges operating under emergency and extreme conditions. Permanent loads include the self-weight of the structural elements, calculated based on geometric properties and material

densities and applied as distributed loads along the span [1].

Live loads are represented by the NG-60 vehicular load model, which corresponds to unfavorable loading scenarios typically adopted for temporary military and emergency bridges [5]. The load model is applied to generate critical internal force effects in accordance with engineering practice [1,5].

Temporary loads associated with staged installation are also included, accounting for the sequential placement of bridge sections and activation of temporary supports. Where appropriate, dynamic amplification effects are considered to reflect moving-load influence on the structural response [1,2].

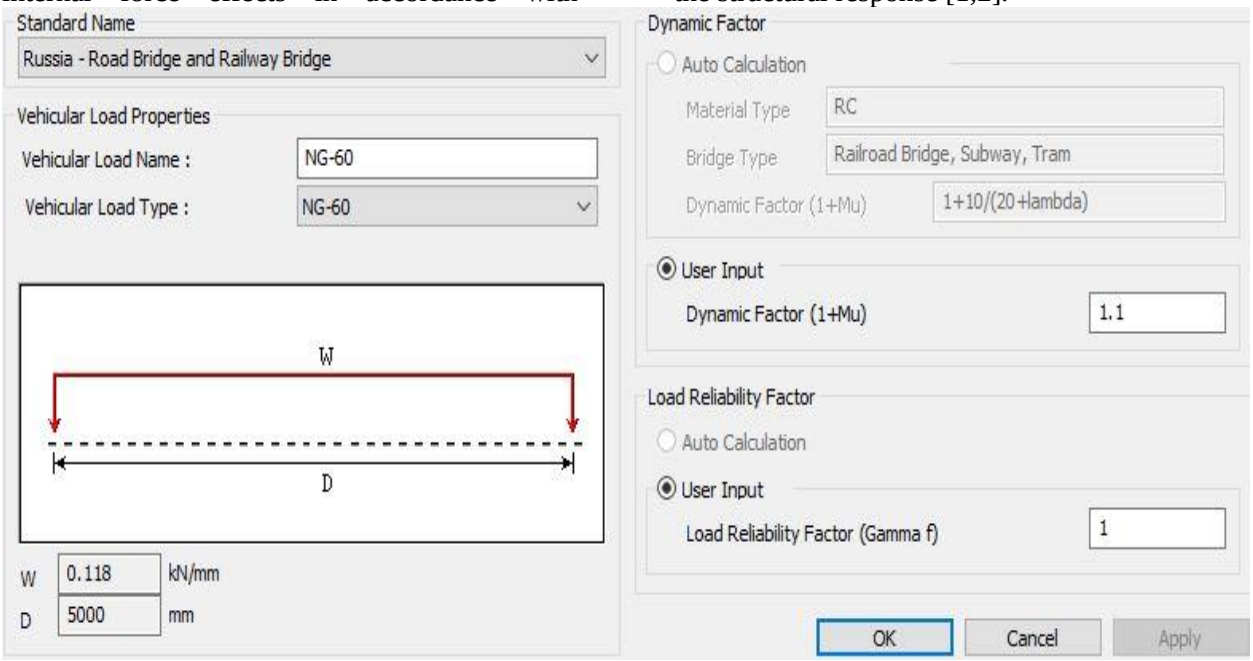

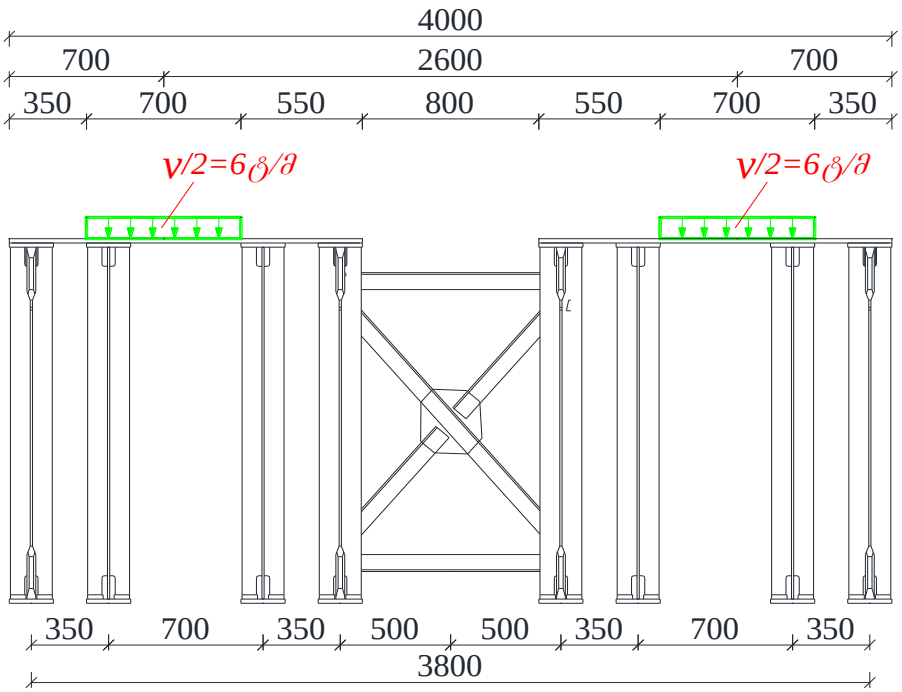

Figure 2 — Application of the NG-60 live load model on the bridge span

4. Results and Discussion

The presented results correspond to the most unfavorable computational stage, which occurs during installation when temporary supports are engaged. Analysis of bending moments indicates that the maximum bending moment (My) develops near the mid-span region. The obtained values remain within allowable limits, confirming adequate structural strength under critical conditions [2,3].

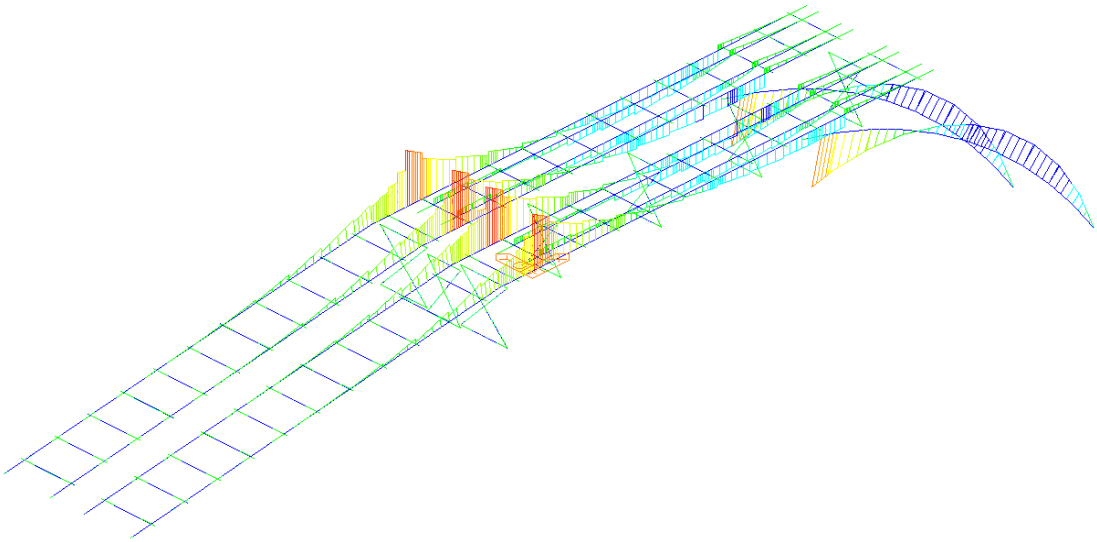

Figure 3 — Bending moment (My) distribution for the critical installation stage

Shear force analysis shows peak values in regions adjacent to support locations, which is consistent with the expected behavior of girder-type bridge systems. The calculated shear forces do not exceed the design capacity of the structural members under the adopted load combinations [1,2].

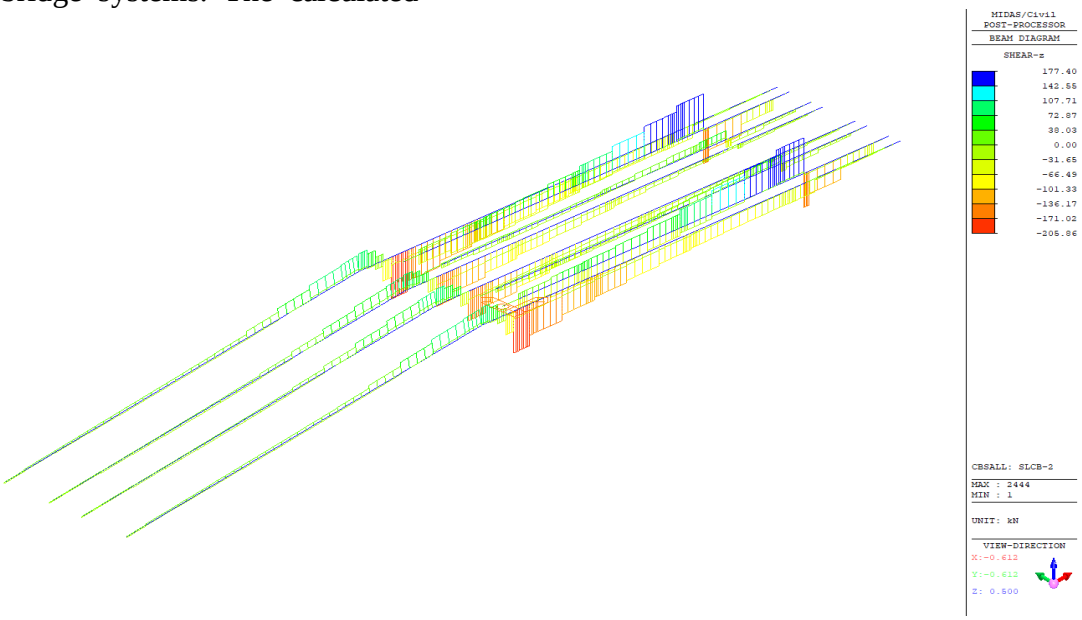

Figure 4 — Shear force (Qz) distribution for the critical installation stage

Deflection analysis demonstrates that maximum vertical displacement (Dz) occurs at mid-span and remains below the serviceability limits specified by relevant design standards for steel bridge structures [2,3].

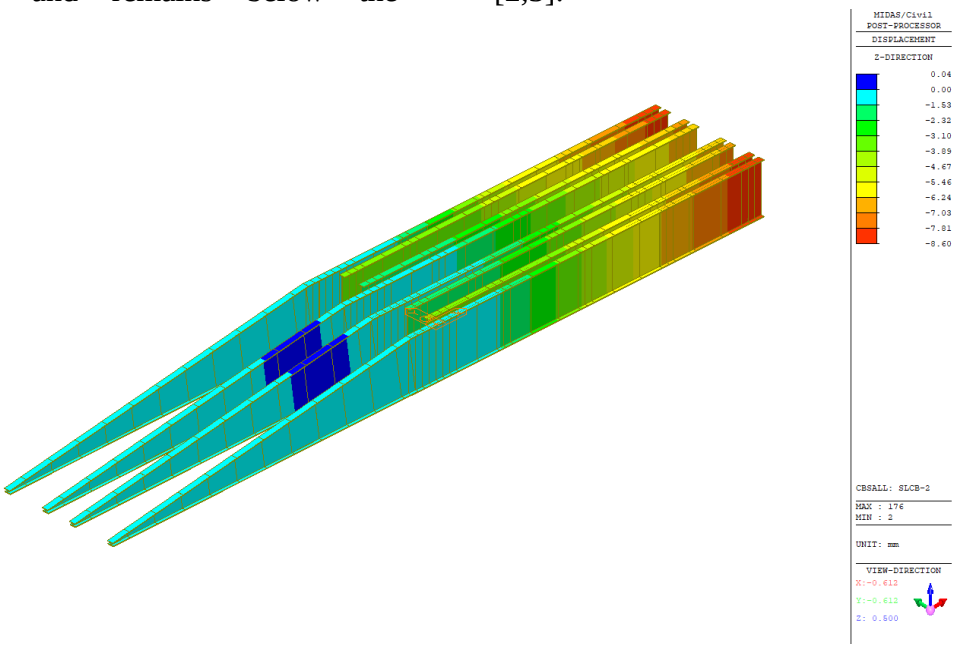

Figure 5 — Vertical deflection (Dz) diagram for the critical installation stage

Overall, the results confirm that the use of transformable temporary supports significantly reduces peak internal forces during installation, enhancing structural safety and constructability. The transition to a single-span operational configuration does not introduce unfavorable structural effects [4,5].

5. Conclusions

This study presented a structural performance analysis and computational model of a transformable guiding bridge system designed for rapid deployment under extreme conditions. The proposed modeling approach effectively captures the bridge behavior during both installation and operational stages, reflecting its transformable nature [4].

The results indicate that the most critical structural conditions occur during installation, while bending moments, shear forces, and deflections remain within allowable limits prescribed by relevant standards and established temporary bridge practice [2,5]. The application of transformable temporary supports improves stability during assembly and supports safe and efficient deployment.

The proposed guiding bridge system represents a practical and adaptable engineering solution for temporary transport infrastructure, offering reduced installation time and enhanced operational reliability. The adopted computational methodology provides a foundation for further optimization and future development of transformable bridge systems [1,4].

References

[1] Chen, W., Duan, L. *Bridge Engineering Handbook*. CRC Press, Boca Raton, 2014.
[2] EN 1993-2:2006. *Eurocode 3: Design of steel structures – Part 2: Steel bridges*. CEN, Brussels, 2006.
[3] Austroads. *Guide to Bridge Technology: Rapid Bridge Construction*. Austroads Ltd., Sydney, 2018.
[4] Wang, P. Transformable support systems in temporary bridge structures. *Structural Engineering International*, 2021, Vol. 31(2), pp. 215–223.
[5] U.S. Army Corps of Engineers. *Design of Temporary Bridges*. Engineer Manual EM 1110-2-2104, Washington, 2017.

.Research on Cracks Caused by Nonlinear Deformation of a Reinforced Concrete Slab

Irine Katchiuri

Georgian Technical University, M.Kostava st 77, Tbilisi 0159, Georgia.

i.katchiuri@gtu.ge

DOI: https://doi.org/10.52340/building.2025.72.02.21

Abstract The article develops a software package based on a calculation method for cracks caused by nonlinear deformations in reinforced concrete slabs with discontinuous parameters. The system's functionality is based on a mathematical apparatus for modeling cracks in reinforced concrete slabs. The subsystem is presented as a package of problem-oriented procedures for determining the Stress-Strain State (SSS), along with a subsystem of mathematical and software algorithms for SSS determination, which is housed in a library of load modules. The subsystem software consists of a package of applied software modules that perform specific mathematical and logical functions. A new method for calculating the deformation and stability of plates with discontinuous-parameter cracks has been developed. Based on this method, calculation results for specific problems have been obtained. The effectiveness of the method lies in the use of a standard set of approximating functions at each loading stage; these functions represent solutions to linear problems and can be constructed using any known calculation methods.

Keywords: Plate, Crack, Model, Software, Deformability.

Introduction

In the modern construction industry, significant importance should be assigned to works aimed at researching the physical nature of the strength and deformation capacity of concrete and reinforced concrete. Such research reveals the resistance mechanisms of these materials to the deforming and destructive impacts of structural and other factors. Specifically, from the perspective of modern solid-state fracture mechanics, the study of the patterns of formation and development of various types of structural cracks in concrete and reinforced concrete is of great interest. The strength and deformation capacity of concrete and reinforced concrete—specifically the intensity of deformation development under constant loads, long-term strength in aggressive environments, the endurance limit, and similar issues—depend on the structural cracks formed and accumulated within the concrete.

Based on the analysis of the research results, a study of cracks caused by the nonlinear deformations of reinforced concrete slabs has been developed. We have studied the methodology, the deformed state of concrete and reinforced concrete, and the process of crack formation. [1]

The patterns of crack formation and development, as well as the quantitative assessment of their magnitudes based on the degree of reinforcement and the type of aggregate, are presented in works [1; 2; 3].

Experimental studies and their comparisons, conducted on the basis of theoretically obtained results, are presented in work [4].

One of the primary issues determining the deformation and crack resistance of reinforced concrete (RC) slab structures is the consideration of the specific properties of reinforced concrete. As a two-component structural material, reinforced concrete differs from other materials due to several characteristic properties. For instance, properties such as heterogeneity, anisotropy, and crack initiation create certain difficulties in the calculation and design of building structures.

Various deformation models are currently used to describe the deformation and failure of RC slab structures. They can be conventionally divided into the following groups:

The First Group: Models in which the stress-strain state of a two-component composite

material is considered at a point separately for concrete and separately for reinforcement. In this case, the physical equation for a section or a characteristic element is formulated based on the combined deformation of the composite, which includes concrete and steel. Furthermore, the elastic or elasto-plastic deformations of the reinforced concrete are accounted for in the relationships obtained according to the calculated state diagrams. The merit of these models lies in their generality and universality.

The Second Group: This group includes so-called microstructural deformation models. The idea behind these models, initially considered for the construction of models for frame elements, involves examining a characteristic area of the RC element between two adjacent cracks, where the averaged deformations of the reinforcement and concrete are determined using a special procedure.

For the development of a general theory for calculating RC structures, it was of great importance to reduce the problem of the stress-strain state of an RC element to the calculation of a bar with variable stiffness and to apply conventional methods of structural mechanics. The integral deformation model is determined by the loading level, regime, and duration, as well as by the strength and deformation characteristics and the cross-section.

The Third Group: This group of physical models includes so-called block models of RC deformation. The concept behind these models represents the structure as being composed of distinct blocks.

Although block models allow for a more detailed description of deformation processes in cracked sections, the solution to the contact problem of reinforcement-to-concrete bonding still relies on empirical relationships for determining bond forces and the shear modulus. Based on the above, this work is undoubtedly of high relevance.

Main Part "The production of fundamentally new and improved structural and other progressive materials accelerates the development of electronics, mechanical engineering, construction, the national economy, and other fields." Regarding construction, this primarily concerns structural materials—concrete and reinforced concrete—the use of which increases annually. This highlights the importance of the economic consumption of these materials, upon which the overall improvement of construction efficiency depends.

However, it is not only the pursuit of increased economic efficiency in the use of concrete and RC that dictates the necessity of perfecting their properties. Their scope of application is constantly expanding; accordingly, the requirements that concrete and RC must meet are increasing. This has led to intensive efforts, both domestically and abroad, to improve the economic indicators of using concrete and RC in various types of structures and operational conditions, as well as to find ways to endow them with properties that respond to new operational demands. These efforts are conducted in various directions, among which a significant role is played by the refinement of calculation methods for building structures. This allows for the identification of hidden reserves and the evaluation of reliability with a high degree of certainty, as well as the creation of traditional concrete types with improved indicators of durability, strength, and deformation.

Equally important are the works concerning the refinement of characteristics that determine the feasibility of using concrete and RC as structural materials, as well as more reliable methods for the quantitative determination of these characteristics.

Furthermore, significant importance should be assigned to studies whose task is to research the physical nature of the strength and deformation capacity of concrete and RC to reveal the mechanisms of resistance of these materials to the deforming and destructive impacts of structural and other factors. Specifically, from the standpoint of modern fracture mechanics of solids, there is great interest in studying the patterns of the formation and development of various types of structural cracks in concrete and RC. The strength and deformation capacity of

concrete and RC—specifically the intensity of deformation development under constant loads, long-term strength in aggressive environments, the endurance limit, and similar issues—depend on the structural cracks formed and accumulated within the concrete.

Reinforced concrete is one of the most common and versatile materials in modern structural engineering. It is characterized by high strength, long service life, and a variety of forms. RC slab-type elements are widely used in both roofing and foundation structures. The formation of cracks in an RC slab is usually a manifestation of nonlinear mechanical processes. This process can be caused by a complex set of factors, such as excessively high applied loads, plastic deformation of the material, concrete shrinkage, creep and relaxation, thermal expansion and contraction, uneven impact on supports, or a non-homogeneous structure.

One of the most crucial issues determining the deformation and crack resistance of RC structures is the nature of reinforced concrete itself. As a two-component structural material, it differs from other materials by a range of characteristic properties. For example, properties such as heterogeneity, anisotropy, and crack initiation create certain difficulties in the calculation and design of building structures.

Regarding the novelty of the research, a study of cracks caused by the nonlinear deformations of RC slabs will be developed based on the analysis of research results. We will study the methodology, the deformed state of concrete and RC, and the process of crack formation, focusing on the patterns of crack initiation and development, as well as the quantitative assessment of their magnitudes based on the reinforcement ratio and the type of aggregate.

Thus far, during the construction of calculation equations, we have only formally touched upon the physical side of the problem. However, for fabricated slabs such as those made of reinforced concrete, substantiating the physical essence of the basic relationships is important not only for algorithmization and the construction of calculation models but also for understanding the phenomena occurring in RC structures under structural and deformational impacts. This ensures the exclusion of gross errors during the analysis of the nonlinear behavior of structures.

Normal cracks in longitudinal and transverse ribs, depending on the nature of the stress state, are reinforced either with distributed reinforcement or with reinforcing bars. The appearance of these cracks is associated with the action of No. 1 tensile forces.

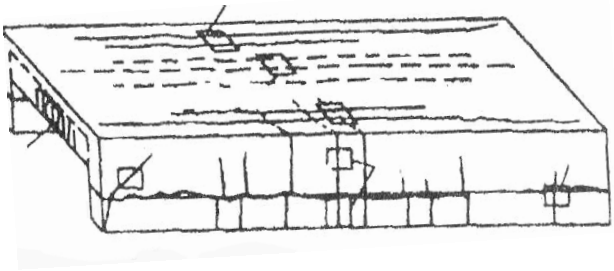

Fig. 1. Schematic diagram of crack formation

Inclined cracks near the supports of longitudinal ribs and in the corner zones of the shell are caused by principal tensile stresses on inclined planes. Depending on the nature of the stress state, the cracks in these zones are oriented orthogonally.

Two types of cracks may appear on the surface of the plates:

Longitudinal cracks at the junctions of the flange and the ribs.

Longitudinal cracks in the middle part of the flange span.

Longitudinal cracks along the connecting elements: their formation is associated with the action of shear forces *S* between the elements of the composite structure near the supports. The initiation and subsequent

opening of these cracks are resisted by the bonds in the shear joint. Such bonds may include transverse reinforcement, dowel-type, or adhesive joints. The presence of transverse rod-connections in the contact zone of the element layers creates additional shear stiffness in the joint.

Composite reinforced concrete shells and corrugated panels are characterized by longitudinal curvature. The types of cracks are as follows:

Longitudinal cracks on the upper and lower surfaces of the flange, associated with the action of transverse bending moments.

Cracks in the end ribs, associated with the action of longitudinal tensile forces in the corresponding zones of the ribs.

Cracks in the upper chords of longitudinal diaphragms, caused by longitudinal tensile forces. The locations of these cracks are determined by the sign of the bending moment in the upper chord of the diaphragm.

Inclined and diagonal cracks in the support and corner zones. In different types of slabs, this type of crack can have varying effects on their load-bearing capacity.

When analyzing the nature of crack formation in composite slab panels, the following can be noted: most of the cracks arising in these structures belong to the type that is orthogonal to the working reinforcement. Consequently, when studying the deformation of this class of structures, orthotropic physical models of reinforced concrete can be utilized. An exception is made for inclined and diagonal cracks, which must be considered based on an anisotropic model. However, as is well known, during the calculation process when resolving static indeterminacy, even quasi-orthotropic or even quasi-isotropic models may be used for these types of cracks.

As a result of investigating the nature of crack formation for the structures under consideration, the model presented in the work (for the first-level calculation scheme) is adopted as the physical model, with certain refinements regarding the evaluation of crack opening. Generally, for elements e1 and e2 operating under plane stress conditions, the relationship between deformations and stresses can be represented as follows:

$$\begin{Bmatrix} \varepsilon_x \\ \varepsilon_y \\ \gamma_{xy} \end{Bmatrix} = \begin{vmatrix} C_{11} & C_{12} & C_{13} \\ C_{12} & C_{22} & C_{23} \\ C_{13} & C_{23} & C_{33} \end{vmatrix} \times \begin{vmatrix} N_x \\ N_y \\ N_{xy} \end{vmatrix} \quad (1)$$

Or

$$[\bar{\varepsilon}] = [C_{ji}] \cdot \{\bar{P}\} \quad (2)$$

For elements e3 and e4, which operate under mixed stress conditions, according to the adopted hypotheses, we can write

$$\begin{Bmatrix} \varepsilon_x \\ \varepsilon_y \\ \gamma_{xy} \\ k_y \end{Bmatrix} = \begin{vmatrix} C_{11} & C_{12} & C_{13} & C^*_{12} \\ C_{12} & C_{22} & C_{23} & C^*_{22} \\ C_{13} & C_{23} & C_{33} & C^*_{23} \\ B^*_{12} & B^*_{22} & B^*_{23} & B_{22} \end{vmatrix} \times \begin{vmatrix} N_x \\ N_y \\ N_{xy} \\ M_y \end{vmatrix} \quad (3)$$

In expressions (1) and (2), C_{ji} is the stiffness matrix, the determination of which depends on the type of cracks and the reinforcement of the elements.

It is easy to see that the values of the stiffness coefficients in the constructed governing equations are directly related to the types of cracks. For instance, the first group of coefficients, C_{ji} determines the cross-sectional stiffness of the shell panel elements under tension (compression) and shear. Accordingly, this group of coefficients is associated with the first and second types of cracks. The coefficients in this group are calculated by multiplying the corresponding diagrams (stress/strain profiles) of the unit functions. For the first-level calculation scheme, the relationships of the deformational model of a quasi-continuous body are used, according to which the contribution of the tensioned concrete between the cracks is accounted for by introducing the coefficient ψ_{bt}

Let us examine the sequence of operations for calculating the first group of stiffness coefficients using shell panels as an example.

After the initiation of the first type of normal cracks, the zones of crack propagation on the structure's surface are determined in accordance with the given calculation scheme of the cross-section and the distribution diagrams of longitudinal forces in this section obtained during the current iteration of the calculation. To achieve this, the shell panel is divided along its length into \$m\$ sections (m = 1, 2, ..., k), and within each section, the relative deformations of the tensioned concrete across the height of the cross-section are calculated using the following formula:

$$\varepsilon_{bt}(x,s)=\left[\sum_{c}\bar{U}_{c}'(x)\bar{\xi}(x)-\sum_{i}V_{i}''(x)\xi_{i}(s)\right] \quad (4)$$

For each calculation element, based on the obtained values of $\varepsilon_{bt}(x,s)$ (i=1, 2, ..., n), a distribution diagram $\varepsilon_{bt}(x)$ is constructed along the height of the structure's cross-section. The maximum deformation value, εbt,max, is then determined for the current iteration of the calculation. The condition for checking the initiation of a crack within the calculation element is written as follows:

$$\varepsilon_{bt,\max}\le\varepsilon_{btu} \quad (5)$$

Where ε_{btu} is the ultimate tensile strain value of the concrete. The numerical values of these strains can be determined as follows:

$$\varepsilon_{btu}=\frac{0,75R_{bt,ser}\gamma_{b4}}{E_b\nu_{btu}} \quad (6)$$

Where

$$\nu_{btu}=\nu_{btR}\left[1-1,05\nu_{btR}\sqrt{0m46-0,35\nu_{btR}}\right]$$

$$\nu_{btR}=0,6+0,15\frac{\gamma_{b4}R_{bt,ser}}{2,5} \quad (7)$$

For the elements in which cracks have appeared, the values of the $\psi_{bt,t}(s)$ coefficients are determined by the formula:

$$\psi_{bt,t}(s)=\frac{N_1(s)}{N_{crc}}(1-\psi_s) \quad (8)$$

where N_{crc} is the generalized crack formation force in the cross-section of the element in the direction of the principal tensile forces. The force N_{crc} can be

determined by the general formula (9), if for the rib under consideration we take $\alpha = 85°$ and $m_{sy} = 0$

$$N_{crc} = \frac{\gamma_{b4} R_{bt,ser}}{\nu_{btu}} \left[t + 2\left(\alpha_{sx} m_{sx} \sin^2 \alpha + \alpha_{sy} m_{sy} \cos^2 \alpha \right) \right] \quad (9)$$

t is the thickness of the corresponding element. m_{xx}, m_{xy} – are the reinforcement parameters along the x and y axes. a_{sx}, a_{sy} – are the ratios of the elastic moduli of reinforcement and concrete along the x and y axes. α is the inclination angle of the principal plane, which is generally determined by the formulas for an anisotropic element. m_{sx}, m_{sy}, α_{sx}, α_{xy} are determined by the following expression:

$$m_{sx} = \frac{A_{sx}}{S_x} \; m_{sy} = \frac{A_{sy}}{S_y} \; \alpha_{sx} = \frac{E_{sx}}{E_0} \; \alpha_{sy} = \frac{E_{sy}}{E_0} \quad (10)$$

where S_x and S_y are the distances between the reinforcement bars relative to the x and y axes.

The value of the edge thickness (taking cracks into account) at the i -th height of the section (i = 1,2,..., n) is determined from the expression:

$$t_i(s) = t_r \psi_{bt,i}(s) \quad (11)$$

The values of the stiffness coefficients $\bar{I}_{dc}(x,c)$ for (d, c = 0,1) for elements with cracks are calculated by the formulas:

$$\begin{aligned}
\bar{I}_{00}(x,c) &= 2\left[E_{b,1} t_r (h_1/2)(\psi_{bt,1} + \psi_{bt,2}) + E_s A_s \right] \\
\bar{I}_{01}(x,c) &= 2\left[E_{b,1} t_r (h_1/2)(\psi_{bt,1} + \psi_{bt,2}) + E_s A_s \right] \\
\bar{I}_{11}(x,c) &= 2\left[E_{b,1} t_r (h_1/2)(\psi_{bt,1} + \psi_{bt,2}) + E_{b,2} t_r \left((z-h_1)/2\right) \times \right. \\
&\times \left. \left(\psi_{bt,3} + \psi_{bt,4}\right) + E_{b,2} t_r b_{b,1} \left(\bar{h} - z - t_p\right) + E_{b,2} t_{p,2} (t_b/2 + b) + E_s A_s \right]
\end{aligned} \quad (12)$$

Calculation of the second group coefficients of the main diagonal $I_{ji}(x,s)$ $(j,i = 1)$ after the appearance of normal cracks in the edges of the structure; and the appearance of the crack is taken into account in the calculation by introducing the reduced thickness of the edges.

$$\begin{aligned}
I_{11}(x,s) = 2\{ & E_{b,1} t_r \psi_{bt,1} (h_1/2)(z^2 - z h_1/2 + h_1^2/12) + + E_{b,1} t_r \psi_{bt,2} (h_1/2)(z^2 - 3z h_1/2 + 7h_1^2/12) + \\
& + E_{b,2} (7t_r/3) \psi_{bt,3} \left((z-h_1)/2\right)^3 + E_{b,2} (t_r/3) \psi_{bt,4} \left((z-h_1)/2\right)^3 + \\
& + E_{b,2} (t_r/3) \nu_{b,1} \left((\bar{h} - z - t_p)/2\right)^3 + E_{b,2} (t_p^2/2) \nu_{b,2} \times \times \left[\left(\bar{h} - z\right)^2 + \left(t_p/2\right)\left(\left(z - \bar{h} + t_p\right)/2\right) \right] + \\
& + E_{b,2} t_b \nu_{b,2} (\bar{h} - z)^2 + E_s A_s (z-a)^2 \}
\end{aligned} \quad (13)$$

The determination of the equivalent reduced thickness of the edges (t_i) is performed using expression (11). The group of $I^*_{\mu}(x,s)$ coefficients is calculated by introducing the $\psi_{bti}(s)$ coefficient.

$$I_p^*(x,s)=2\Big\{E_{b,1}t_r\left(h_1/2\right)\Big[\psi_{bt,1}\left(z-h_1/4\right)+\psi_{bt,2}\left((z-3h_1)/4\right)\Big]+$$
$$+E_{b,2}(t_r/8)(z-h_1)^2(3\psi_{bt,3}-\psi_{bt,4})-E_{b,2}(t_r/2)\nu_{bm1}\left((\bar{h}-z-t_p)/2\right)-$$
$$-E_{b,2}t_b\nu_{b2}\Big[(t_p/2)\left((\bar{h}-z-t_p)/4\right)+b(\bar{h}-z)\Big]+E_xA_s(z-a)\Big\} \quad (14)$$

The group of $\alpha_{ji}(x,s)$, $S_{ji}(x,s)$ coefficients represents the longitudinal sectional flexural stiffnesses of the shell panel. Their values are determined by the reduced stiffnesses of longitudinal strips of unit width, which are cut from the shell panel by sections *x* and *x*+1. These stiffnesses are related to the formation of longitudinal cracks. The calculation of this group of coefficients is performed by multiplying the $f_1(s)$ diagram by its second-order derivative $f_1''(s)$.

$$\alpha_{11}(x,s)=2\nu E_{b,2}\Big/\left(12(1-\nu^2)\right)\Big\{0,035b\left(t^3_{p,red.1}\right)^3\times$$
$$\times\Big[f_1(0,787b)\left(4f_1''(0,787b)+f_1''(b)\right)+f_1''(0,787b)+f_1(0,578b)\Big]-$$
$$-0,048b\left(t^3_{p,red.1}\right)^3\big[f_1''(0,289b)(3f_1(0,578b)+4f_1(0,289b)+$$
$$+f_1(0))+f_1''(0,289b)+2f_1(0))\big]\Big\} \quad (15)$$

$$S_{11}(x,s)=2E_{b,2}\Big/\left(12(1-\nu^2)\right)\Big\{0,096b\left(t^3_{p,red.1}\right)^3\times$$
$$\times\Big[2\left(f_1''(0,289b)\right)+\left(f_1''(0)\right)^2+f_1''(0,289b)f''(0)\Big]+$$
$$+0,08b\left(t^3_{p,red.2}\right)^3\Big[2(f_1''(0,787b))^2+\left(f_1''(b)\right)^2+f_1''(0,787b)f_1''(b)\Big]\Big\} \quad (16)$$

Here $t^3_{p,red.j}$ is the reduced equivalent thickness of the flange in the *j* -th section within the zone of action of a transverse bending moment of a single sign, with width *dj*(*j* = 1,2,..,) which is determined by the equivalent flexural stiffness.

$$t^3_{p,red.j}=\sqrt[3]{12B^3_{red,j}} \quad (17)$$

Where $B^3_{red,j}$ is the equivalent reduced stiffness of the longitudinal sections of the shell within the boundaries of the *j*-th segment. When determining the stiffness of the longitudinal sections and, consequently, the reduced sections of the shell $\left(t_{p,red}(s)\right)$ the reduction in the area of the concrete in tension due to cracking within each segment is the same as that used for calculating the first group coefficients—i.e., it is determined using the y_{bt} coefficient.

Conclusion: The study presents slabs with a freely supported contour and a crack located at the center. There are certain slabs whose geometry, loading, and yield-line patterns approximate cyclic symmetry; in such cases, calculations based on the theory of elasticity yield identical bending moments in both directions. In addition to circular and square slabs, this category may include regular polygonal slabs, slightly elongated rectangular slabs, etc., when subjected to uniform loading.

To determine the ultimate load-bearing capacity (intensity) of such slabs, an equation must be formulated equating the internal and external work done during a virtual displacement. The values for the work of external and internal forces within the formula are calculated by assigning a unit translational velocity to the instantaneous center of intersection of the plastic hinges.

When extending the yield lines, they intersect at the center of the crack. The diagram of angular velocities is constructed according to the principle of Cremona diagrams. Additionally, the study covers the investigation of cracks caused by non-linear deformations in reinforced concrete slabs, specifically cases where the crack is situated between the diagonals of the slab.

References

[1]. Machaidze, E., Kipiani, G. Theory of Calculation of Composite Thin-Walled *Spatial Systems*. Edited by Professor G. Kipiani. Publishing House "Technical University", Tbilisi, 2006. 369 pages. (In Georgian).

[2]. Mikhailov, B. K., Kipiani, G. O., & Moskaleva, V. G. (1991). Fundamentals of the theory and methods of calculating the stability of three-layer plates with cuts. "Metsniereba", Tbilisi. – 189 p. M 607(106)-91.

[3]. Mikhailov, B. K., Kipiani, G. O., & Busorgina, O. V. (1993). Some problems of geometrically non-deformable shallow shells with discontinuous parameters. Tbilisi: Eureka. – 140 p.

[4].I.Katchiuri, G.kipiani, M.Rajczyk ,,Rigidity of three-layer plate with discrete parameters" AKJournals-DOI:https://doi.org/10.1556/606.2025.01280, 2025 https://akjournals.com/view/journals/606/aop/article-10.1556-606.2025.01280/article-10.1556-606.2025.01280.xml

[5] I. Kachiuri, M. Barbakadze, G. Kipiani. "Dynamic study of crane vehicles," Georgian Academy of Business Sciences "Moambe", vol. 50, pp. 30–39, 2024.

[6] I. Katchiuri, M. Barbakadze, G. Kipiani, and N. Nakvetauri, "Dynamic study of overhead crane," in Tashkent International Congress on Modern Sciences, vol. III, Tashkent, Uzbekistan, April 22–23, 2024, pp. 604–619.

[7] A. Tabatadze, I. Katchirui, and G. Kipiani, "Study of transverse oscillations of the building as a discrete-continuous system taking into account the shock effect caused by impulse impact," in Proceeding of the 5th International Scientific Conference, Brussel, Belgium, Feb. 22-23, 2024, pp. 62–72.

[8] M. Rajczyk, D. Jończyk, and B. Stachecki, "Innovative methods of strengthening the timber constructions, ïn Procedings of 9th International Conference Contemporary Problems of Architecture and Construction, Batumi, Georgia, September 13-18, 2017. pp. 25–28.

[9] G. Kipiani and N. Botchorishvili, "Analysis of lamellar structures with application of generalized functions", Transactions of the VSB -Technical University of Ostrova, Civil Engineering Series, vol. 16, no. 2, pp. 49–60, 2016.

[10] G. Kipiani, E. Qristesiashvilina, A. Tabatadze, and Z. Jangidze, "Study of non-linear environmental safety and natural resources, oscillations of the high-rise buildings," References // Environmental safety and natural resources. Academie Jurnal issue 2(46) April-June 2023 Kyev 2023 pp.194-201. language-English. www. https://es-journal.in.ua

Algorithms for Investigating the Strength, Stability, and Vibrations of Assembled Structures and Their Individual Elements

Gela, Kipiani, Nikoloz Kachkachishvili, Giorgi Gogoladze
Technical University of Georgia, M.Kostava st 77, Tbilisi 0159, Georgia.
Tbilisi, Akaki Tsereteli State University, Kutaisi
Gogoladze.giorgi24@gtu.ge
DOI: https://doi.org/10.52340/building.2025.72.02.22

Abstract This paper presents a comprehensive study of algorithms for analyzing the strength, stability, and vibration behavior of assembled structural systems and their individual elements. The information required for static strength analysis is formulated and processed using dedicated computational programs, transforming initial data into standardized forms suitable for algorithmic implementation. Numerical examples are presented, and the obtained results are critically analyzed, demonstrating the efficiency and reliability of the proposed approaches.
Keywords: algorithm; structural systems; strength; stability; vibrations.

1. Introduction

The proposed algorithms determine nodal displacements of structures in plane problems under asymmetric loading and in spatially symmetric problems with consideration of geometric nonlinearity. The obtained results have both independent significance and the role of initial input data for subsequent computational procedures. Algorithms for analyzing the strength of individual structural elements may be applied independently or as part of an integrated algorithmic framework addressing complex strength problems.

Algorithms intended for the investigation of stability and vibration behavior of symmetrically loaded structures (spatially symmetric systems) employ the results of nodal displacement determination obtained under symmetric loading. These results are used to define the critical stress–strain state. All presented algorithms may be applied to structures whose element properties can be described using geometric modeling and mesh-based procedures.

For the efficient solution of complex optimization problems, thorough analysis of available information on design projects and possible structural modifications is essential. Particular importance is assigned to incomplete input data and internal effects caused by various factors that may possess deterministic characteristics. However, for real structural systems, obtaining such information is closely associated with the application of efficient numerical methods.

One effective approach is design sensitivity analysis. This method forms the basis of techniques relying on structural optimality and iterative solution procedures. The most general design methodology includes decisions made by the engineer during the design process. This widely accepted approach can be significantly improved when information on structural sensitivity is available.

In such cases, systematic structural analysis and rational design improvement become possible. This information can be obtained using methods based on finite element formulations. The computational efficiency of sensitivity analysis in design depends on the representation of elements (in the present case, beam and bending elements). The availability of interactive graphical methods and modern operating systems enables computer-aided interactive design. Based on these considerations, the relevance of the present study is evident.

2. Main Part

Typically, design variables are represented by cross-sectional characteristics of beam elements, geometric parameters of shell elements, as well as their mechanical and elastic properties. Consequently, the global stiffness matrix K and the generalized load vector F are functions of the design variables, namely:

The research AR-25 23 99 has been supported by Shota Rustaveli National Science Foundation of Georgia.

$$K = K(b), \quad F = F(b)$$

where b denotes the vector of design variables characterizing the dimensions, mechanical properties, and nodal parameters of structural elements. In this study, the case in which boundary conditions do not explicitly depend on design variables is considered. Under this assumption, optimization procedures based on sensitivity analysis may be successfully applied.

The essence of the method is as follows: since the global stiffness matrix and load vector depend on the design variables, both linear and nonlinear forms of the governing equations are also dependent on them. Consequently, the displacement vector z becomes a function of the design variables, i.e.,

$$z = z(b).$$

In optimal structural design problems, either minimization or maximization of an objective function is required, subject to constraints on stresses, displacements, and design variables. The objective function may represent any criterion of optimal design. After solving the equilibrium equations, the dependence of the objective function on the design variables may be explicit or implicit. The purpose of sensitivity analysis is to determine the complete dependence of such functions on the design variables.

By applying differentiation rules for composite functions and matrix calculus, derivatives of the governing equations are obtained. Since the stiffness matrix is non-singular, the derivatives of nodal displacements with respect to design variables can be efficiently computed, enabling the effective application of gradient-based optimization techniques.

The application of this method to specific optimization procedures is not discussed in detail, as it lies beyond the scope of the present paper.

Any computational process performed on a computer is characterized by parameters such as static and dynamic memory requirements. In the present study, comparison is conducted not only for the complete structural analysis process but also for the stage involving determination of the stiffness matrix of bending elements. Exact methods based on numerical integration of systems of first-order differential equations are compared with approximate methods employing elementary functions that provide explicit expressions for stiffness matrix coefficients.

In the first case, in addition to static memory, dynamic memory is required, depending on the number of orthogonalization points along the entire length of the element. In contrast, approximate methods require only static memory. The performed comparisons demonstrate that the ratio of required memory volumes can be expressed as:

$$W_{exact} / W_{approx} = 1.07m - 0.035$$

where W_{exact} denotes the total memory required for numerical integration, W_{approx} is the memory required for the approximate method, and m is the number of orthogonalization points.

It follows from this relation that for elements of medium length, the required memory is practically independent of the applied method. For long elements ($m > 40$), the required memory for exact methods increases by approximately 2.5 times and reaches about 2.5 kB. Although this volume is not critical for modern computing systems, in complex software packages it may influence overall computational efficiency.

An analysis of computational time required for determining stiffness matrices using exact and approximate methods is performed over a wide range of parameters. The obtained results indicate that approximate methods provide significant time savings—up to two orders of magnitude for long elements—making them particularly advantageous for multi-variant optimal structural design.

Thus, the use of approximate methods for determining stiffness matrices of bending elements ensures acceptable accuracy while being substantially more

efficient than exact methods in terms of both memory consumption and computational speed. This clearly demonstrates the superiority of the approximate approach.

Conclusions

- A new approach to the optimal design of multilayer plates has been developed.
- Programs for processing initial stress–strain state information have been created.
- Information required for static strength analysis of assembled structures has been formulated and standardized for use in the proposed algorithms.
- Examples of structural calculations have been examined and the obtained results have been analyzed.

- ***Assembled / Frame Structures (Beam–Column Systems***

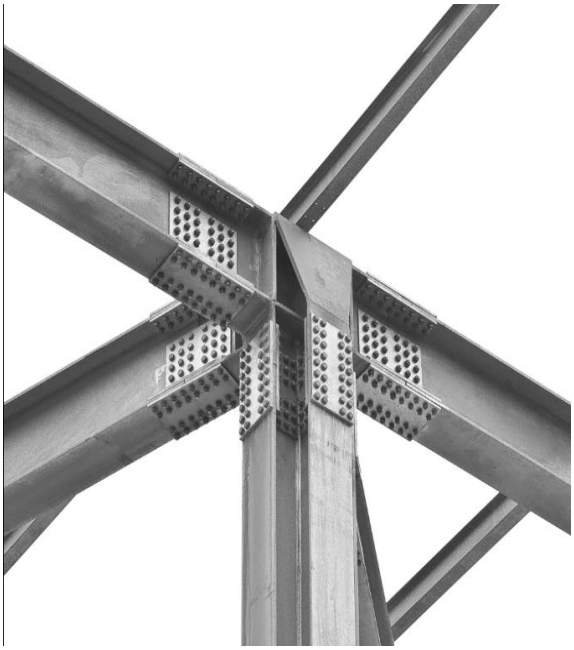

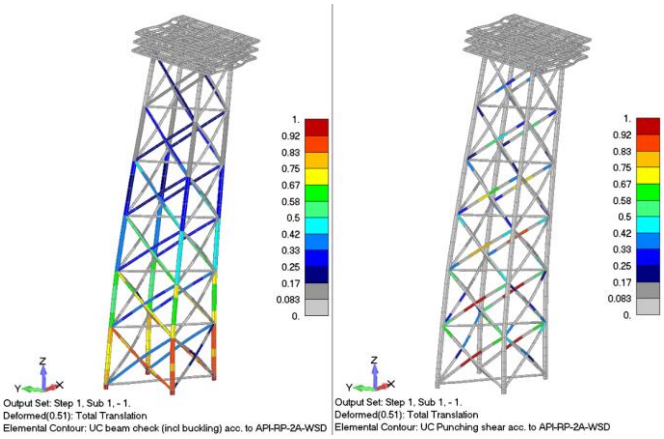

- ***inite Element Method (FEM) – Mesh & Structural Model***

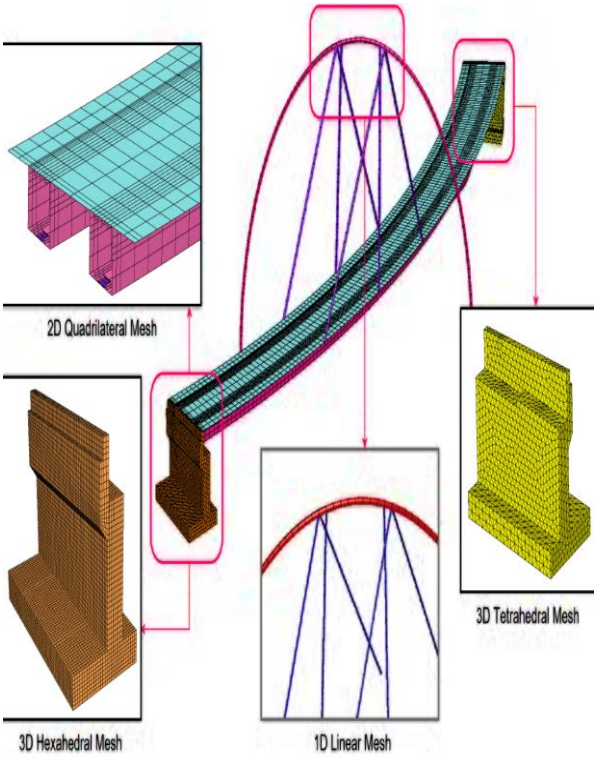

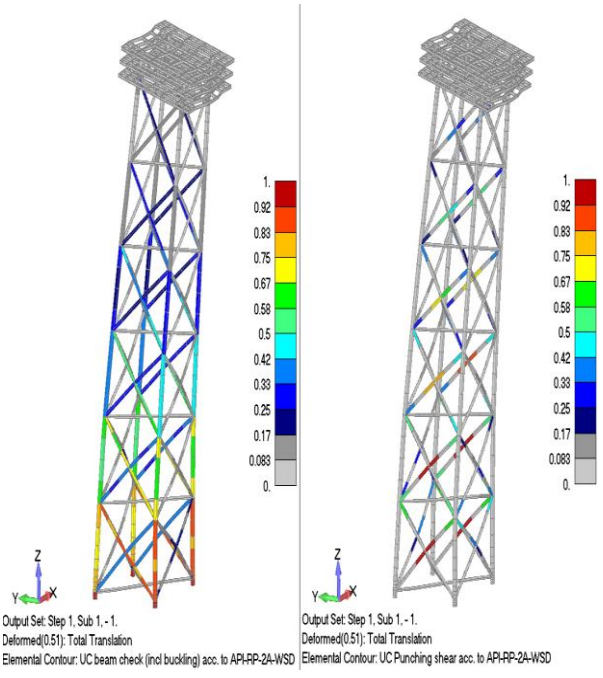

- ***Vibration / Modal Analysis***

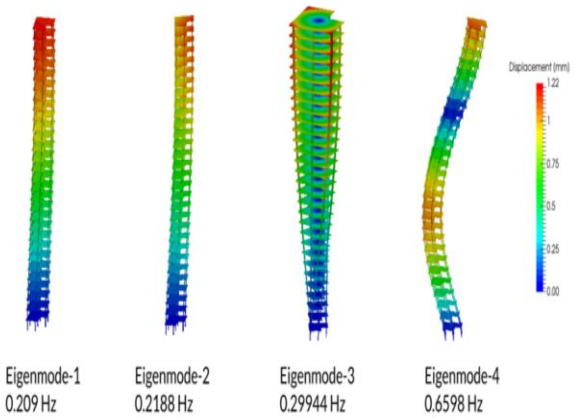

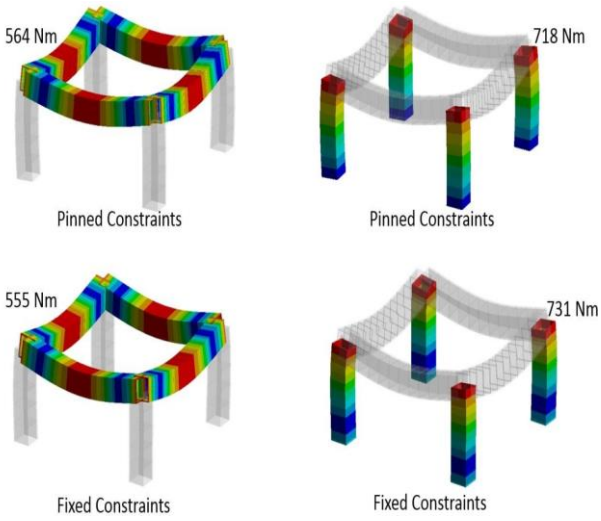

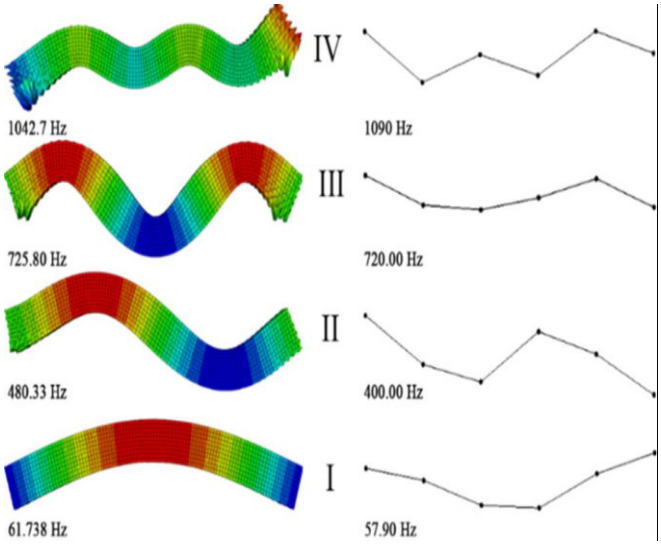

- ***Multilayer Plates / Shell Structures***

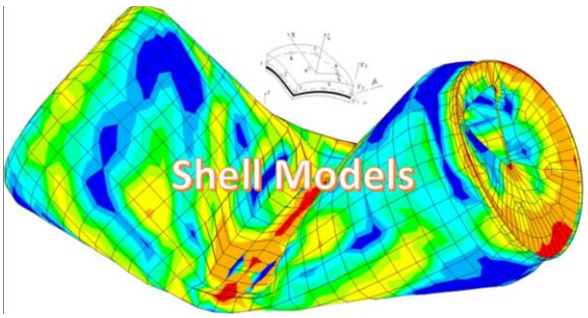

- ***uckling / Stability Mode Shape***

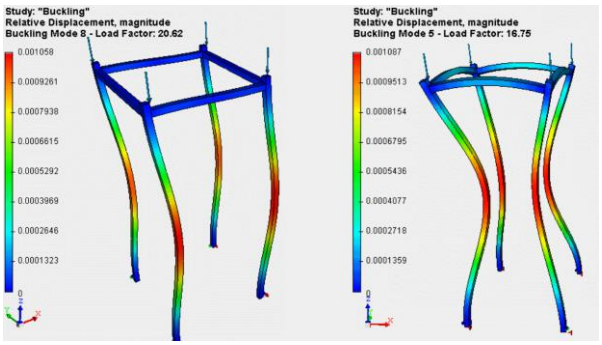

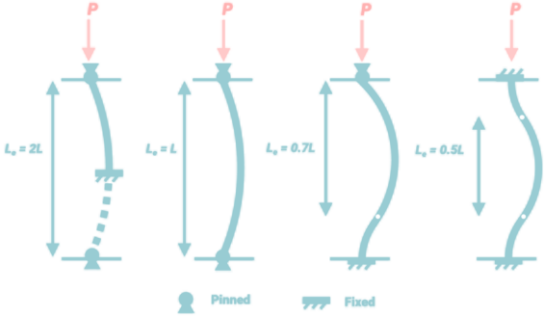

- ***Sensitivity Analysis / Optimization Flow***

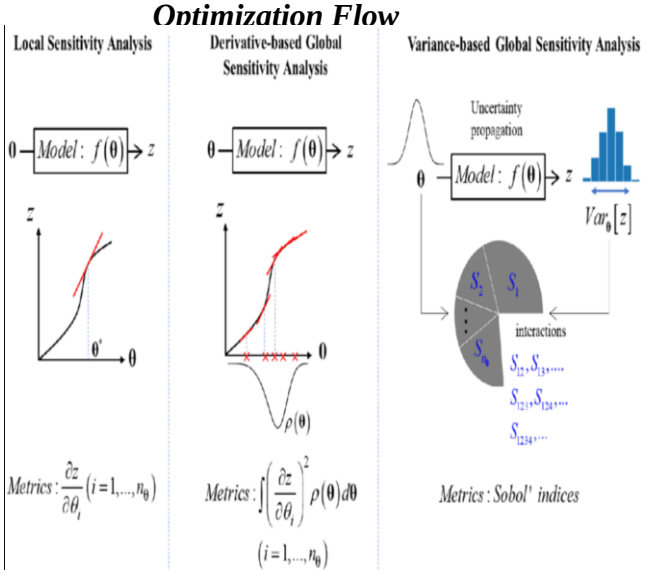

- ***Modern Structural Frame Buildings***

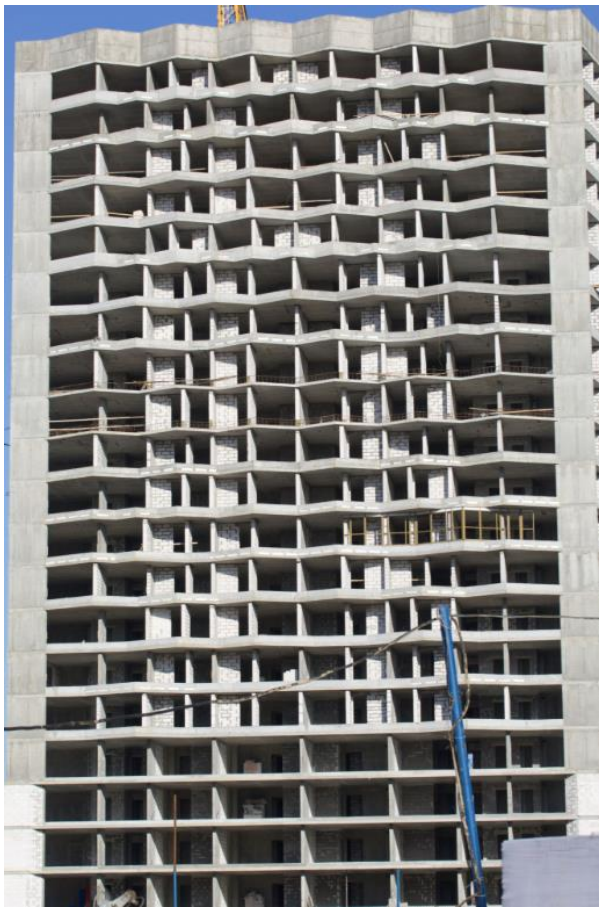

References

1. Mikhailov, B.K., Kipiani, G.O., Moskaleva, V.G. Fundamentals of Theory and Methods for Stability Analysis of Three-Layer Plates with Cuts. Metsniereba, Tbilisi, 1991.
2. Mikhailov, B.K., Kipiani, G.O. Deformation and Stability of Spatial Plate Systems with Discontinuous Parameters. Stroyizdat, St. Petersburg, 1996.
3. Kipiani, G., Kachkachishvili, N. Investigation of the Stress–Strain State of Machine Housing Structures. Universali Publishing House, Tbilisi, 2025.
4. Kipiani, G., Badzgaradze, G. Stability Analysis of Thin-Walled Spatial Systems with Discontinuous Parameters. Universali Publishing House, Tbilisi, 2025.
5. Kipiani, G., Sulashvili, V. Elastic–Plastic State of Seismically Resistant Thin-Walled Spatial Systems with Discontinuous Parameters. Universali Publishing House, Tbilisi, 2025.
6. Kipiani, G. Application of Elasticity Theory Methods in the Analysis of Building Structures and Foundations. Technical University Press, Tbilisi, 2009.
7. Kipiani, G. Fundamentals of Applied Vibration Theory. Universali Publishing House, Tbilisi, 2023.

Application of Hydrocyclone for Wastewater Treatment in Wine Industry

Alexander Bagration-Davitashvili, Zaal Tsinadze, Ketevan Gordeziani, Maka Mzhavanadze
Georgian Technical University, M. Kostava 77, Tbilisi 0159, Georgia.
adavitashvili@gtu.ge

DOI: https://doi.org/10.52340/building.2025.72.02.23

bstract Global water scarcity is increasing in many regions causing a deficiency in agricultural, human and industrial needs. Industrial activities produce wastewater and solid waste streams needed management. These waste streams have a negative environmental impact. Therefore, wastewater treatment will be important to solve the problem.

The varying amounts of generated winery wastewater, together with their composition during the winemaking process, pose a challenge for wineries when selecting suitable treatment methods. A general trend in winery wastewater treatment, where the shortcomings of many techniques are related to the variations in the organic content and volume of the wastewater.

A single operation is generally not sufficient to improve the quality of wastewater treatment for discharge into the environment. However, hydrocyclone treatment is a promising technology. Hydrocyclone treatment technology has become more popular and accepted in recent years for the treatment of many types of wastewaters, while conventionally activated sludge processes cannot. handle the composition of wastewater or fluctuations in the wastewater flow. According to our research, hydrocyclone treatment makes it easier to treat winery wastewater at lower costs.

Key words: Hydrocyclone, Winery Wastewater, Wastewater Treatment

Introduction

A hydrocyclone is a device used in water purification processes for the efficient separation and classification of particles in suspensions [1,2]. It is a cylindrical device whose operating principle is based on centrifugal force. This technology converts water flows containing mixed particles of varying sizes and densities into a clean product ready for further use.

A hydrocyclone allows for the highly accurate separation of solid particles from liquids, making it widely used in wastewater treatment plants. The design includes a slurry feed port through which the material is injected under pressure into the device.

A rotating flow is created within the device, where centrifugal force separates the particles by size and density. Heavy and large particles are forced to the periphery and removed through the lower outlet, while lighter and smaller particles, along with water, are carried away through the upper outlet. The hydrocyclone's operating principle is based on using water as a medium to create a centrifugal field, ensuring high separation efficiency with minimal loss of useful material. Hydrocyclones employ a unique separation method based on the principle of centrifugal classification. This process is key to the device's operation and occurs in an aqueous environment. A key feature is its ability to separate solid particles from suspension, making it effective in wastewater treatment.

During operation, wastewater is fed under pressure into the cylindrical section of the device, where a rotating flow is created. Under the influence of centrifugal force, heavier and larger particles are displaced toward the periphery and settle at the bottom of the hydrocyclone, where they are then removed. Meanwhile, lighter and smaller particles, along with water, rise to the center of the vortex and are removed through the upper outlet.

In wastewater treatment plants a hydrocyclone plays a vital role, ensuring high efficiency at minimal cost. When the slurry, a mixture of liquid and solid particles, is fed into the hydrocyclone, it enters a vortex. Under the influence of centrifugal force, heavier and larger particles are moved toward the outer wall of the apparatus and removed through the lower discharge pipe. Meanwhile, lighter particles and water are carried by the central part of the vortex toward the upper outlet.

Hydrocyclones are ideal for cleaning applications requiring a high degree of material separation. The hydrocyclone's effectiveness in cleaning stems from its ability to process large volumes of suspension while maintaining high separation accuracy and minimizing loss of valuable raw materials.

Hydrocyclone Design

The hydrocyclone design is a unique combination of simplicity and engineering sophistication, ensuring its high efficiency. Its main elements are a cylindrical upper section, a conical extension, and material inlet and outlet ports (Fig. 1).

The cylindrical section serves to introduce the slurry, which is introduced through a side port under pressure. The conical lower section collects and removes heavier particles that settle under centrifugal force.

The upper section houses the discharge port (upper), through which the clarified liquid is removed along with smaller, lighter particles. The lower discharge port is used to remove heavy particles that have settled in the conical section.

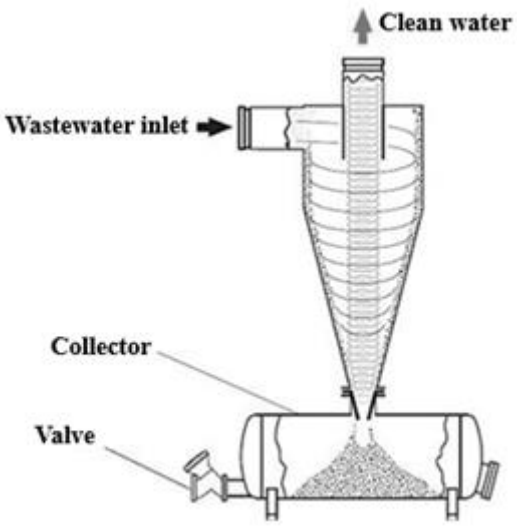

Fig. 1. Hydrocyclone design diagram

One of the most common types is the classic hydrocyclone, a cylindrical-conical shape. It is effective at separating heavy particles from lighter, smaller ones. They are widely used in wastewater treatment.

Characterisation of wine industry wastewater

Wine industry enterprises include grape juice distilleries, primary wineries, champagne distilleries, cognac distilleries, and municipal wineries.

Winery wastewater is a major waste stream generated by the many cleaning operations that occur during each phase of production. The wastewater produced contains a variety of pollutants. The volume and pollution vary significantly depending on the operating period (harvest, storage, bottling) and the winemaking technologies used (e.g. red, white and specialty wines).

Wastewater at grape juice distilleries is generated because of the following technological processes: juice cooling in coolers, separation in separators and refrigeration compressor stations, and cleaning equipment, pipelines, and floors. In addition, there is also domestic wastewater.

Processing 1 ton of grapes generates 1.08 m^3 of wastewater (including the recycling water supply system and consistent water use). Of this amount, 0.28 m^3 is produced by industrial wastewater, 0.02 m^3 by domestic wastewater, and 0.78 m^3 by relatively clean water. During the winemaking period, 0.19 m^3 of wastewater is discharged to produce 1 dl of grape juice. Primary wineries produce wine from fruit raw materials. The wastewater generated here consists of rinsing and flushing water, which contains contaminants such as stems, leaf debris, and small particles of damaged fruit.

Wine production faces many serious environmental challenges. The main potential environmental impacts of wineries are:

• Groundwater and surface water pollution, soil degradation and vegetation damage resulting from the reuse and disposal of liquid and solid waste

• Odors and air emissions resulting from the management of raw materials, wastewater, solid and semi-solid by-products of the winemaking process; noise from pumps, chillers, crushers and other winemaking equipment, as well as noise from machinery, especially during the harvest.

The main environmental problems associated with the operation of wineries fall into six categories: wastewater, water and energy consumption, solid waste, chemical use, and air emissions.

Wastewater from urban wineries and primary winemaking plants is similar in quantity and

pollution levels. During grape processing, wastewater discharge, considering the recirculating water supply system, is 1.14 m³ per 1 g of grapes; of this, 0.74 m³ is production wastewater, 0.02 m³ is domestic wastewater, and 0.38 m³ is conditionally clean wastewater. During the winemaking period, the production of 1 dl of wine generates wastewater of 0.05 m³, 0.04-0.001 m³, and 0.009 m³, respectively. At cognac distilleries with a water supply system with sequential use of water, the discharge is 1.47 m^3 to produce 1 dl of cognac spirit, of which 0.29 m^3 is production waste, 0.01 m^3 is household waste, and 1.17 m^3 is relatively clean waste. The coefficient of unevenness of wastewater inflow at both plants in summer and winter is equal to one.

The content of organic matter, salts, macro- and microelements in the sludge from winery treatment facilities is:

Organic matter, % - 37.7
Mineral matter, % - 53.7
Total nitrogen, % - 2.58
Total phosphorus, % -1.3
Hygroscopic wet, % - 8.6
Potassium, mg/100 g soil - 62.3
Phosphorus, mg/100 g soil - 9.9
Titanium, mg/1 kg soil - 1701
Copper, mg/1 kg soil - 459
Manganese, mg/1 kg soil - 360
Chromium, mg/1 kg of soil - 296
Boron, mg/1 kg of soil - 196
Nickel, mg/1 kg of soil - 106
Cobalt, mg/1 kg of soil -135
Molybdenum, mg/1 kg of soil - 178
Zinc, mg/1 kg of soil - 2800-3400
Lead, mg/1 kg of soil - 160-230
Strontium, mg/1 kg of soil - 160-230

Application of Hydrocyclone for Wastewater Treatment in Wine Industry

Winery wastewater is typically described as a mixture of fresh water, readily soluble and biodegradable organic material such as proteins, polypeptides and polysaccharides, dissolved salts, minerals and low concentrations of heavy metal ions and other phytotoxic and persistent compounds. Raw wastewater must undergo treatment to meet wastewater quality requirements.

In most cases, wineries use a combination of treatment phases, including pre-treatment, primary, secondary and tertiary treatment phases. A final treatment stage is also often used to disinfect the treated wastewater, which largely depends on its destination.

Three main variations of treatment are mainly used: physicochemical treatment, biological treatment, and advanced oxidative treatment.

In most cases, wineries use a combination of processing phases, which include pre-, primary, secondary, and tertiary processing phases [4,5,6].

We propose the treatment of winery wastewater using hydrocyclone.

The advantages of hydrocyclone are:

- Reduced processing time: The processing time is very low (approximately 2-3 seconds) compared to other traditional gravity systems.
- No moving parts: The separation is carried out entirely by gravity, so there are no moving parts in the system, which results in less maintenance and operating costs.
- No chemicals are required: The system is self-cleaning due to the effect of gravity; therefore, no chemicals are required during operation.
- Continuous process: Since the system does not need to be backwashed, the service life is very high.
- Modularity: Ability to operate at a wide range of flow rates, in the case of low flow rates, by changing the working elements.
- Energy consumption: They do not require energy to operate and are relatively inexpensive.
- The maintenance of hydrocyclone does not require complex equipment or qualified personnel. In terms of technical capabilities, hydrocyclones can compete with other water treatment methods, offering undeniable advantages over some of them.

For example, compared to sedimentation tanks, hydrocyclones require minimal installation space.

The results of laboratory data processing clearly show the high degree of removal of

organic substances from liquids at different concentrations using a small diameter hydrocyclone. When increasing the concentration from 1 to 10 g/l, the degree of removal decreases from 98.95% to 93.50%, based on the dry residue of treated wastewater and winery wastewater.

In the case of a nozzle diameter of 7 mm, a better removal rate was obtained than in the case of a diameter of 6 mm, which demonstrates the possibility of controlling the quality of removal by this method.

With an increase in the concentration of organic substances to 10 g/l, the proportion of large particles increases. These particles settle out during water circulation in the tank, thereby affecting the analysis results, since the pump takes up the suspension from the bottom of the tank. Therefore, the removal results were calculated based on the ratio of the mass of particles in the treated wastewater to the mass of particles in the sand wastewater.

The object of the study was a laboratory analogue of wine production wastewater, which contains suspended particles of organic compounds at a concentration of 1–10 g/L, which corresponds to the size of particles present in winemaking wastewater. The results of laboratory tests showed a high removal rate of organic matter particles from the recirculated water model samples from the liquid ring pump cycle. Hydrocyclonic treatment at low particle concentrations (1 g/l) is effective even without the use of post-treatment filters. However, to achieve consistent treatment results at all possible concentrations of organic compounds (from 5 to 40 g/l), it is necessary to treat the recirculated water using two volumetric filters. This allows for rapid treatment of the recirculated water during alternating operations of the recirculation and regeneration.

The collected samples were filtered through filter paper and dried in an oven at 110°C for 40 minutes to remove free water. The difference in the weight of the filter paper before and after filtration was used to calculate the dry residue separated in the waste stream and the weight of the particles in the hydrocyclone. The degree of purification was calculated using the following ratios:

$$X = \frac{m_{oc}}{m_{dw}} \times 100\%$$

X – Degree of suspension purification to initial concentration, $\%M_{oc}$-Mass of the organic compound sample, gM_{dw} – Mass of dry waste resulting from the hydrocyclone discharge, g

$$X_1 = \frac{m_{\mathrm{d}}}{m_{\mathrm{d.d}}} \times 100\%$$

where X_1 - is the rate of purification of the solution of discharged organic substances, %;m_d. - is the weight of dry residues of discharged organic substances, g;$m_{d.d}$. is the weight of dry residues discharged from the hydrocyclone.

The rate of solution purification in relation to the discharge of organic substances considers the uneven mixing during the operation of the hydrocyclone cycle under laboratory conditions. Under industrial conditions, coarsely weighed substances do not have time to settle in the supply pipeline and remain stable.

Based on the research conducted, the following optimal dimensions of a D_{50} hydrocyclone are recommended for removing organic matter from recirculated water at a pressure of P = 2.0 kg/cm^2:

Height of hydrocyclone h	250 mm
Hydrocyclone diameter dc	50 mm
Height of cylindrical part h_c	50 mm
Cone angle θ°	8–10°
Capacity	4.3 m^3/h
Drainage pipe diameter d_{dpd}	17.0 mm
Inlet diameter d_{id}	13.6 mm
Solution filler diameter d_s	9.3 mm
Length of drainage pipe inside hydrocyclone l	57 mm

Laboratory and calculated values for the performance of the hydrocyclone show that this type of device can be used as a primary unit for cleaning recirculating water from liquid-ring pumps. The use of a sedimentation tank with a thin-film module requires a longer retention time of the organic matter suspension in the device,

higher costs of equipment and instruments, and a greater load on the equipment.

Conclusion

It should be noted that the treatment of winery wastewater by the traditional convection method, which includes mechanical cleaning, coagulation-flocculation, sedimentation and disinfection, is not sufficient for sufficient treatment of winery wastewater.

At the same time, the impact of wineries on the environment leads to pollution of groundwater and surface waters, soil degradation and damage to vegetation cover, which occurs due to the impact of liquid and solid waste.

The treatment of winery wastewater by means of a hydrocyclone is discussed and its parameters are proposed based on the analysis of the obtained laboratory results.

References

1. K. Tsamoutsoglou, A. Kechagias, V. E. Katzourakis, C. V. Chrysikopoulos, P. Gikas. Investigation and efficiency estimation of a hydrocyclone for the treatment of primary municipal wastewater. Journal of Environmental Management, V. 380. 2025.

2, Z. Kassymbekov, K. Akmalaiuly, G. Kassymbekov. Application of Hydrocyclones to Improve Membrane Technologies for Urban Wastewater Treatment. Journal of Ecological Engineering 22(4). 2021

Congratulations

Gela Kipiani 70

Gela Kipiani graduated from the Faculty of Mechanics and Mathematics of Tbilisi State University, specializing in Mechanics. In 1986, he was enrolled in the postgraduate program at the Department of Theoretical Mechanics at the Leningrad Institute of Civil Engineering, specializing in Construction Mechanics, code 05.23.17. There, he defended his candidate dissertation on the topic "Stability of a Three-Layer Plate with a Rectangular Cut" ahead of schedule and was awarded the degree of Candidate of Technical Sciences in Construction Mechanics. From 1993 to 1996, he was a doctoral student at the Department of Timber and Plastic Structures at the Saint Petersburg State Architectural and Civil Engineering University, specializing in Construction Mechanics, code 05.23.17. In 1997, he defended his doctoral dissertation on the topic "Deformation and Stability of Thin-Walled Parametric Spatial Systems" and was awarded the degree of Doctor of Technical Sciences.

In 1999, he was awarded the title of Professor in Construction Mechanics. In the same time, he lectured at the Department of Theoretical Mechanics at the Georgian Technical University (serving as Assistant, Associate Professor, and Professor). From 2006 to 2013, he was a full professor at the Department of Engineering Mechanics at the Georgian Technical University. From 1997 to 2005, he served as the head of the Scientific Research Department at the Georgian Technical University. From 2005 to 2007, he was the head of the Scientific Service.

From 2014 to 2018, he was the Vice-Rector for Scientific Affairs at the Georgian Aviation University and Professor at the Faculty of Engineering, where he delivered lectures in Theoretical Mechanics. He was also the head of the Master's and Doctoral educational programs.

From 2019 to 2020, he was a Professor at the Department of Civil and Industrial Construction named A. Sokhadeze , on Faculty of Civil Engineering of Georgian Technical University, and head of the Scientific-Research Development Group. In 2021, following a competitive selection, he was appointed Professor at the Department of Construction Machinery of the Georgian Technical University. He is the laureate of the State Prize in the field of Science and Technology of Georgia, the Meskheti Publishing Prize laureate, and a Distinguished Builder of Georgia. He is a member of several Georgian and international professional academies and has been involved in public activities.

Since 2001, G. Kipiani has been one of the founders and the first Secretary General of the National Committee on Theoretical and Applied Mechanics of Georgia. Since 2011, he has been one of the founders and Executive Secretary of the Union of Mechanics of Georgia and a member of the Board of Governors of the Society of Engineers. He is the author and co-author of over 400 scientific papers, including 10 patents, 18 monographs, 26 textbooks, teaching aids, and methodological guidelines. He is also the Deputy Chief Editor of the scientific-technical journal "Construction."

Professor Gela Kipiani celebrates his 70th birthday, we extend our congratulations and best wishes. May he continue to exhibit courage, inexhaustible energy, and contribute to the longevity, professional success, and happiness of his family. We express gratitude for his dedication to the Georgian Technical University and our country. May he steadfastly uphold scales of truth, exemplifying nobility in all endeavors.

Georgian Technical University, Faculty of Civil Engineering, The Editorial Board of the Magazine "Building", "Theoritical and Applied Mechanics National Committee of Georgia," " Union of Mechanics of Georgia"

Is published in the prepared by authorsformat